Title: A converged ubiquitin-proteasome pathway for the degradation of TOC and TOM tail-anchored receptors

Authors: Meijing Yang[1,3,*], Shuai Chen[2,*,&], Shey-Li Lim[1], Lang Yang[1,3], Jia Yi Zhong[1], Koon Chuen Chan[1], Zhizhu Zhao[1], Kam-Bo Wong[2,5], Junqi Wang[3,] and Boon Leong Lim[1,4,5,†]

Affiliations:

[1]School of Biological Sciences, University of Hong Kong; Pokfulam, Hong Kong, China.

[2]School of Life Sciences, the Chinese University of Hong Kong; Shatin, Hong Kong, China.

[3]Department of Biology, Southern University of Science and Technology; Shenzhen, China.

[4]HKU Shenzhen Institute of Research and Innovation; Shenzhen, China.

[5]State Key Laboratory of Agrobiotechnology; The Chinese University of Hong Kong, Hong Kong, China.

*These authors contributed equally to this work.

[†]Correspondence to: Boon Leong Lim (bllim@hku.hk)

[&]Present address: Department of Biology, Southern University of Science and Technology, Shenzhen, Guangdong, China.

Running title: Degradation of TOC/TOM translocons

Abstract

In plants, thousands of nucleus-encoded proteins translated in the cytosol are sorted to chloroplasts and mitochondria by binding to specific receptors of the TOC (translocon at the outer membranes of chloroplasts) and TOM (translocon at the outer membranes of mitochondria) complexes for import into those organelles. The degradation pathways for these receptors are unclear. Here, we discovered a converged ubiquitin-proteasome pathway for the degradation of *Arabidopsis thaliana* TOC and TOM tail-anchored receptors. The receptors are ubiquitinated by E3 ligase(s) and pulled from the outer membranes by the AAA^+ ATPase CDC48, after which a previously characterized cytosolic protein, TTOP, binds to the exposed transmembrane domains (TMDs) at the C termini of the receptors and CDC48, and delivers the complexes to the 26S proteasome.

Keywords

E3 ligase, CDC48, SP1, TOC, TOM, 26S Proteosome, Ubiquitination

Introduction

The plant organelles chloroplasts and mitochondria are derived from two ancient endosymbiotic events, whereby a photosynthetic cyanobacterium and an aerobic prokaryote were separately engulfed by a eukaryotic cell. Over the intervening billion years of evolution, most genes from the endosymbiont genomes have been transferred to the host nucleus. Hence, most chloroplasts and mitochondrial proteins are encoded in the nucleus, synthesized in the cytosol, and imported into the organelles through the TOC (translocon at the outer membranes of chloroplasts) and TOM (translocon at the outer membranes of mitochondria) complexes, respectively (Duncan, Murcha, & Whelan, 2013; Nakai, 2018; L.-X. Shi & Theg, 2013). Components of the TOC complex, including Toc33 and Toc159, are directed to the 26S proteasome by the ubiquitin-dependent chloroplast-associated protein degradation (CHLORAD) system (Ling, Huang, Baldwin, & Jarvis, 2012; Q. H. Ling et al., 2019). These TOC proteins are first ubiquitinated by SUPPRESSOR OF PPI1 LOCUS1 (SP1), an E3 RING ubiquitin ligase embedded in the chloroplast outer membrane (OM) (Ling et al., 2012). SP1 forms a complex with SP2, an Omp85-type β-barrel channel embedded in the OM, and CDC48A, a cytosolic AAA^+ protein, at the chloroplast surface (Q. Ling et al., 2019). Both SP2 and CDC48A are essential for the re-translocation of TOC components from the OM to the cytosol. SP2 is believed to play a conductance role, while CDC48A pulls the TOC proteins out of the membrane via ATP hydrolysis, after which ubiquitinated TOC proteins are targeted to the 26S proteasome for degradation (Q. Ling et al., 2019). Yet, how ubiquitinated TOC proteins and the SP1/SP2/CDC48A complex are targeted to the 26S proteasome has been unclear. The CHLORAD system is critically important for chloroplast biogenesis, plant development, and stress responses (Q. Ling et al., 2019; Ling et al., 2012; Ling & Jarvis, 2015). Overexpression of *SP1* reduces the abundance of TOC complexes (Ling et al., 2012) and confers transgenic plants with higher resistance to salt, osmotic, and reactive oxygen species (ROS) stresses (Ling & Jarvis, 2015). A reduction in the import of photosynthesis-related proteins can decrease the amount of ROS generated from chloroplasts during photosynthesis. Although SP1 is also present in mitochondria, whether it is involved in the ubiquitination of the TOM complex is unknown (R. H. Pan & Hu, 2018). In addition, while the mitochondria-associated protein degradation (MAD) pathways of mitochondrial outer membrane (MOM) proteins are well characterized in yeast and mammalian cells (T. Zhang & Ye, 2016; Zheng, Li, & Jiang, 2019), the equivalent plant pathway(s) remain obscure. Here, we discovered a novel plant protein, which participates in ubiquitin-proteasome pathways for the degradation of Arabidopsis thaliana TOC and TOM tail-anchored receptors

Results

A novel cytosolic protein interacts with the C-terminal transmembrane domains of tail-anchored TOC and TOM receptors

We previously showed that Arabidopsis PURPLE ACID PHOSPHATASE2

(PAP2) plays a role in protein import into chloroplasts and mitochondria (Law et al., 2015; Sun et al., 2012; Voon et al., 2021; R. Zhang et al., 2016). Similar to Toc33 and Toc34 and to Tom20-2, Tom20-3, and Tom20-4, PAP2 is a tail-anchored (TA) protein anchored on the outer membranes of these two organelles via its hydrophobic C-terminal motif (Sun et al., 2012). PAP2 interacts with the precursor of the small subunit of Rubisco (pSSU) (R. Zhang et al., 2016) as well as the presequences of several MULTIPLE ORGANELLAR RNA EDITING FACTOR (pMORF) proteins (Law et al., 2015) and plays a role in their import into chloroplasts (R. Zhang et al., 2016) and mitochondria (Law et al., 2015), respectively. To further elucidate these processes, we first performed a yeast two-hybrid (Y2H) screen to identify PAP2-interacting proteins (Voon et al., 2021). One novel protein encoded by the gene At5g42220 drew our attention, as multiple clones were isolated during screening. The C-terminal transmembrane domain (TMD) of PAP2 was required for its interaction with At5g42220.1 (Figure1A). We named the protein encoded by At5g42220.1 TMD-binding protein for tail-anchored outer membrane proteins (TTOP). TTOP is an 879-amino-acid (aa) protein containing a ubiquitin-like (Ubl) domain at its N terminus (aa 24–95), while the rest of the protein lacks known conserved domains.

Y2H analysis of the interaction of TTOP with other tail-anchored (TA) proteins on the outer membranes of chloroplasts and mitochondria revealed an interaction with Tom20-2, Tom20-3, and Tom20-4 (hereafter referred to together as Tom20-2/3/4) (Figure 1A). The TMDs of the mitochondrial proteins were essential for their interactions with TTOP, as we observed no interaction between TTOP and TMD-truncated versions of Tom20-2/3/4 (Figure 1A). We did not detect an interaction of TTOP with Toc33 and Toc34 (hereafter Toc33/34) by Y2H (fig. S1), possibly because the BD-Toc33/34 fusion proteins could not enter the yeast nucleus, as the TA motifs from Toc33/34 and Tom20-2/3/4 have different properties (Sun et al., 2012). We then turned to bimolecular fluorescence complementation (BiFC) to confirm these interactions: TTOP fused to the C-terminal half of yellow fluorescent protein (cY) interacted with fusion proteins between the N-terminal half of YFP (nY) and Toc33/34, Tom20-2/3/4 and PAP2 (Figure 1B), as determined by the reconstitution of YFP fluorescence. This interaction was dependent on their TMDs (fig. S2), as we saw no interaction between TTOP and TMD-truncated TA proteins (fig. S3A). Notably, we did not detect interaction between the above TA proteins and TTOP fused to cY at its C terminus (fig. S3B), indicating that a free TTOP C terminus is essential for these interactions. In the BiFC analysis conducted in protoplasts, we noticed that TTOP did not interact with these TA proteins on the organellar outer membranes, but rather formed patches in the cytosol. This observation was not due to a failure of targeting to the outer membranes, as GFP-TA fusions between the green fluorescent protein (GFP) and the TA proteins were successfully targeted to the organellar outer membrane (fig. S4). This result suggested that TTOP interacts only with cytosolic TA proteins carrying free TMDs but not with TA proteins whose TMDs are embedded in the outer membranes. In agreement with the BiFC results, co-immunoprecipitation (co-IP) assays from protein extracts of transiently co-transfected protoplasts confirmed the

physical associations between TTOP and the above TA proteins (Figure 1C).

TTOP is essential for chloroplast biogenesis

To characterize the role of TTOP in organelle biogenesis and plant development, we first obtained two *ttop* mutants, SALK_128909 and SALK_151742, but these lines did not harbor a T-DNA insertion in *TTOP*, as determined by genotyping PCR. We therefore generated our own *TTOP* knock-out mutants using a highly efficient CRISPR/Cas9 system (Tsutsui & Higashiyama, 2017), leading to the isolation of the *ttop-1* and *ttop-5* mutant alleles, with a single-base insertion of an A or T in the 43 bp of the first *TTOP* exon, respectively (fig. S5A). Both alleles were predicted to introduce a premature stop codon 78 bp into the first exon. We selected Cas9-free *ttop-1* and *ttop-5* mutant lines and confirmed the absence of TTOP accumulation by immunoblotting with anti-TTOP antibodies (fig. S5B). Both *ttop-1* and *ttop-5* mutants grew normally under standard growth conditions (fig. S5C). We then attempted to generate transgenic lines overexpressing a construct encoding N-terminal GFP-tagged TTOP (GFP-TTOP), as adding a tag to the C terminus of TTOP affected its interaction with TA proteins in the BiFC assay. However, we failed to obtain lines that overexpressed *GFP-TTOP* when driven by either *UBIQUITIN10* (*UBQ10*) or the cauliflower mosaic virus *35S* promoter, suggesting that constitutive expression of *TTOP* might lead to lethality. Accordingly, we generated stable Arabidopsis transgenic lines expressing *GFP-TTOP* under the control of a dexamethasone (DEX)-inducible promoter (pTA7002-*GFP-TTOP*) (Aoyama & Chua, 1997). These pTA7002-*GFP-TTOP* lines grew normally when sown on unadulterated MS medium but not on MS medium containing 10 μM DEX (Figure 2A, B), confirming that constitutive overexpression of *GFP-TTOP* is early seedling-lethal, possibly due to an influence on chloroplast biogenesis, as indicated by the impairment of chloroplast development in cotyledons (Figure 2C, D). When 5-day-old pTA7002-*GFP-TTOP* seedlings germinated on MS medium were transferred to MS medium containing 10 μM DEX for 3 days, their cotyledons turned yellow (Figure 3A) and their chloroplasts degenerated, as evidenced by a decline in chloroplast and thylakoid size (Figure 3B) observed during transmission electron microscopy (TEM) analysis. We confirmed the high accumulation of GFP-TTOP in pTA7002-*GFP-TTOP* lines by immunoblotting with anti-TTOP antibodies (Figure 3B). Immunoblotting showed that higher TTOP protein accumulation reduced the abundance of outer envelope proteins in chloroplasts, without affecting the level of Tic40 (Figure 3C). We failed to analyze mitochondrial proteins by immunoblotting, possible due to the low abundance of mitochondrial proteins in total protein extract and the lack of highly sensitive antibodies. We also tested the response of etiolated *ttop* seedlings to illumination, which induces chlorophyll biosynthesis and cotyledon opening in the wild type: Both *ttop* mutants also showed defects in cotyledon development and lower survival rates (Figure 3D), as a consequence of impaired chloroplast biogenesis (Figure 3E), upon exposure to light.

TTOP is expressed in actively dividing tissues

To determine the cellular localization of TTOP, we generated *ttop-5 pTTOP*:*GFP-TTOP* transgenic plants by transforming the construct *pTTOP*:*GFP-TTOP*, driving *TTOP* expression from the *TTOP* promoter, into *ttop-5* plants. The transgene complemented the *ttop-5* mutant, as evidenced by the rescue of the cotyledon phenotypes (Figure 3D) upon de-etiolation. These results hinted that *TTOP* expression is strictly controlled. Confocal laser scanning microscopy (CLSM) analysis of stable Arabidopsis *ttop-5 pTTOP*:*GFP-TTOP* seedlings showed that GFP-TTOP accumulated in the cytosol of all tissues tested, including mesophyll cells, the epidermis, the hypocotyl, and the roots, and was highly abundant in the root and shoot meristems and the first true leaves of 6-day-old seedlings (Figure 4A). The cytosolic location of TTOP is also confirmed in protoplasts (fig. S4). To independently confirm the expression pattern of *TTOP*, we generated transgenic lines harboring a transgene driving the expression of the *β-GLUCURONIDASE* (*GUS*) reporter gene under the control of the *TTOP* promoter (*pTTOP*:*GUS*) (Figure 5). Consistent with the GFP-TTOP accumulation pattern in *ttop-5 pTTOP*:*GFP-TTOP* seedlings, GUS staining was strong in root and shoot meristems (Figure 5A–D), which are characterized by actively dividing cells with high energy demand. The *TTOP* promoter was active in young leaves but not in mature leaves (Figure 5E) and was also active in trichomes, flowers, and pollen (Figure 5F–I).

TTOP participates in the CHLORAD pathway

As TTOP interacted with TA proteins targeted to chloroplasts and mitochondria, we generated *p35S:mCherry-Toc33* and *p35S:mCherry-Tom20-2* transgenic plants in the *ttop-5* mutant background. We then crossed these transgenic lines with wild-type (WT) plants and selected homozygous *p35S:mCherry-Toc33* and *p35S:mCherry-Tom20-2* transgenic plants in the WT background from their progeny. With this crossing strategy, we thus obtained *p35S:mCherry-Toc33* and *p35S:mCherry-Tom20-2* transgenic plants in the WT and *ttop-5* backgrounds carrying the same T-DNA insertion events, allowing us to compare mCherry-Toc33 and mCherry-Tom20-2 protein abundance. The initial abundance of mCherry-Toc33 and mCherry-Tom20-2 was the same in the two WT lines (Figure 4B). Importantly, mCherry-Toc33 and mCherry-Tom20-2 abundance was much higher in *ttop-5* relative to the WT lines, as evidenced by immunoblotting with anti-mCherry antibodies (Figure 4B). We thus concluded that TTOP may contribute to the degradation of Toc33 and Tom20-2, which prompted us to explore whether TTOP participates in the CHLORAD pathway. BiFC analysis showed that TTOP interacts with SP1, CDC48A, and the 26S proteasome subunits REGULATORY PARTICLE NON-ATPASE6 (RPN6), RPN10, RPN12, and RPN13a (Figure 6A), but not with SP2. In agreement with this, co-IP assays from transiently transfected protoplast extracts showed that TTOP can pull down SP1, CDC48, RPN6, RPN10, RPN12 and RPN13 (Figure 6B). Co-transfection of *mCherry-TTOP*, *cY-CDC48A*, and *nY-Toc33/Toc34* constructs in Arabidopsis protoplasts resulted in the reconstitution of YFP fluorescence and co-localization of YFP with mCherry fluorescence in the cytosol, indicating that these

proteins co-localize (fig. S6). Likewise, co-transfection of *mCherry-TTOP*, *cY-CDC48A*, and *nY-Tom20-2/Tom20-3/Tom20-4* constructs in protoplasts also demonstrated their co-localization in the cytosol and exhibited a network appearance (fig. S7), which disappeared when TTOP was co-expressed (fig. S6). CDC48A interacted with Toc33/34 and Tom20-2/3/4 at the periphery of chloroplasts and mitochondria, as indicated by BiFC assays (fig. S7). We repeated the BiFC assays in protoplasts prepared from *ttop-5* plants and observed the same results (fig. S8), indicating that TTOP is not essential for the interaction of CDC48A with Toc33/34 or Tom20-2/3/4.

TTOP participates in a ubiquitin-dependent MAD pathway

Next, we tested whether SP1 can ubiquitinate Toc33 and Tom20-3 by *in vitro* ubiquitination assays. Recombinant Arabidopsis UBIQUITIN-ACTIVATING ENZYME1 (UBA1), UBIQUITIN CONJUGATING ENZYME8 (UBC8), and ubiquitin (fig. S9), recombinant SP1flex, TTOP (fig. S10) and Toc33 and Tom20-3 (fig. S11) were purified in *E. coli*. SP1flex and GST-SP1RING, but not SP1flex, self-ubiquitinated (Figure 7A). These data showed that the SP1RING domain is able to ubiquitinate its GST fusion partner, whereas SP1flex which contains SP1RING domain cannot self-ubiquitinated itself. SP1flex also ubiquitinated full length Toc 33 (Toc33FL, a.a. 1-297) and Toc33 without the C-terminus (Toc33NC, a.a. 1-251) (Figure 7B). GST-TTOP, but not GST alone, pulled down both non-ubiquitinated (Figure 7C) and ubiquitinated Toc33FL (Figure 7D), but not Toc33NC in either form (Figure 7E), indicating that SP1 ubiquitinates the receptor domain of Toc33, whereas TTOP binds to the TMD motif of Toc33, independent of its ubiquitination status. SP1flex/UBC8 did not ubiquitinate Tom20-3 without the C-terminus (Tom20-3NC, a.a. 1-174) or TTOP (Figure 7F). Unidentified E2/E3 ligase(s) in seedling extracts appeared to ubiquitinate His-Tom20-3NC, which was not pulled down by GST-TTOP due to the lack of the TMD motif of Tom20-3 (Figure 7G). We could not test the ubiquitination of full length Tom20-3 as we failed to express it in *E. coli*. Unknown E3 ligase(s) in the plant extracts may therefore ubiquitinate Tom20-3, or SP1 at the mitochondrial OM may still act as the cognate E3 ligase of Tom20-3, as our *in vitro* experiments did not test all 37 Arabidopsis E2 ligases.

TTOP binds to RPN13 of the 26S Proteosome via its N-terminal UBL domain.

Using the TTOP protein sequence to PBLAST the proteins in the human genome, the protein with the highest protein sequence identity was human BAG6 (Chio, Cho, & Shan, 2017; Shao, Rodrigo-Brenni, Kivlen, & Hegde, 2017). The length of BAG6 (1132 a.a.) is much longer than TTOP (879 a.a.) and they only share 23% protein sequence identity, mainly at their N-terminal UBL domains and their C-terminal BAG domain (Mock et al., 2015). In mammalian system, the Bag6/Ubl4A/Trc35 complex directs mislocated polypeptides on the ER membrane toward 26S proteasome for degradation to avoid protein aggregations in the cytosol (Hessa et al., 2011; Q. Wang et al., 2011). Besides BAG6, many UBL-containing proteins are involved in shuttling

ubiquitinated substrates to 26S proteasomes and some UBL domains were shown to bind to RPN subunits (Chen et al., 2016; Y. Shi et al., 2016). Here, we employed AlphaFold2 (Jumper et al., 2021; Mirdita, Ovchinnikov, & Steinegger, 2021) to predict the interaction between the UBL domain of TTOP with the RPN proteins we identified by BiFC. As predicted by AlphaFold2, the UBL domain of TTOP could interact with the pleckstrin-like receptor for ubiquitin (PRU) domain of RPN13 (Figure 8 and fig. S12). The interaction between these two domains was confirmed by ITC experiment and the affinity was determined to be 29 μM (Figure 8D). In addition, sequence alignment with the UBL domain of BAG6 showed that TTOP UBL contains the RNF126_NZF interacting residues (Krysztofinska et al., 2016), suggesting that TTOP UBL may have a zinc finger (ZF) binding ability (fig. S13A). SP1 RING is a ZF protein with the E3 ligase function (Q. H. Ling et al., 2019; R. H. Pan & Hu, 2018) and Alphafold2 predicted that the UBL domain of TTOP could bind to SP1 RING, too (fig. S13B). By contrast, the C-terminus of TTOP contains a BAG domain that contains conserved Ubl4A interaction residues (Mock et al., 2015) and this domain was predicted to be able to bind human Ubl4A by AlphaFold2 (fig. S14).

Heat treatment induces TTOP-dependent clearance of mCherry-Toc and mCherry-Tom20-2 in planta

The homozygous DEX-GFP-TTOP line was transformed with the *p35S:mCherry-Toc33* and *p35S:mCherry-Tom20-2* constructs to generate double expression lines. These lines expressed mCherry-Toc33 and mCherry-Tom20-2 constitutively at high levels. GFP-TTOP was induced by 24h Dex treatment in some 8-day-old seedlings and then subject to 30 min heat treatment at 45°C. The signals of mCherry-Toc33 and mCherry-Tom20-2 disappeared when GFP-TTOP was present, but remained when GFP-TTOP was absence (Figure 9). These in planta data showed that GFP-TTOP is required for the degradation of mCherry-Toc33 and mCherry-Tom20-2. Heat treatment was also shown to induce mRNA expression of TTOP (fig. S15).

Discussion

In this study, we discovered a converged pathway for the delivery of ubiquitinated tail-anchored receptors of the TOC and TOM complexes to the 26S proteasome for degradation (Figure 10). In CHLORAD, a system for the clearance of the TOC complex by the ubiquitin-proteasome system, the E3 ligase SP1 mediates the ubiquitination of the TOC complex, while SP2 and the AAA^+ ATPase CDC48A act as a conduit and a motor, respectively, to retrotranslocate the ubiquitinated TOC complex out of the chloroplast OM (Q. Ling et al., 2019). However, how the retrotranslocated, ubiquitinated TOC proteins are delivered to the 26S proteasome was not clear. Here, we showed that TTOP is the cytosolic shuttling factor responsible for the delivery of the ubiquitinated TOC proteins to the 26S proteasome. In addition, we discovered a similar MAD pathway for the removal of Tom20 from the mitochondrial OM, which involves uncharacterized E2/E3 ligases, CDC48A, and TTOP. In this pathway, after

Tom20 receptors in the TOM complexes are ubiquitinated, they are retrotranslocated from the OM to the cytosol, followed by the delivery of the complex to the 26S proteasome by TTOP. Ubiquitination of the TOC and TOM receptors is not required for TTOP binding; hence, the binding takes place after these receptors are retrotranslocated from the OMs to the cytosol. During TOC biogenesis, cytosolic Arabidopsis ankyrin repeat protein 2A (AKR2A) binds to the TMDs of newly synthesized Toc33 and Toc34, but not that of Tom20-2, when they are released from ribosomes to maintain the nascent TOC receptors from forming aggregates or binding to non-specific hydrophobic proteins before their insertion into the chloroplast OM (Bae et al., 2008; Kim, Na, Park, Baek, & Kim, 2019). Thus, although both AKR2A and TTOP can bind to the TMDs of Toc33 and Toc34, they may bind to the receptors at different processes: the biogenesis and degradation stages of the TOC complex, respectively.

Besides the UBL domain at its N-terminus and the BAG domain at its C-terminus, the other region of TTOP does not show any sequence homology to any known structures. In the mammalian Bag6/Ubl4A/Trc35 complex, the C-terminal BAG domain of BAG6 interacts with UblA4 (Mock et al., 2015), which in turn interacts with the small glutamine-rich tetratricopeptide repeat-containing protein alpha (SGTA), and the latter binds TMD directly (Guna & Hegde, 2018; Shao et al., 2017). Different from the BAG6 in the mammalian system, TTOP can bind to TMDs of the TOC/TOM TA receptors directly. Although the BAG domain at the C-terminus of TTOP was predicted to be able to interact with human UblA4 by Alphafold2 (fig. S14), PBLAST search could not find any homolog of UblA4 in Arabidopsis and the closet homolog of SGTA are proteins containing the tetratricopeptide repeat (TPR) domains, including HOP1(Fellerer, Schweiger, Schongruber, Soll, & Schwenkert, 2011), HOP2, HOP3 (Fernández-Bautista, Fernández-Calvino, Muñoz, & Castellano, 2017), OM64 (Panigrahi, Whelan, & Vrielink, 2014) and Toc64 (Sommer et al., 2013), of which they only share homology with SGTA at their TPR domains. It might be interesting to investigate whether these proteins could bind to TMDs and play a role similar to SGTA in the plant system.

Although BiFC data showed that TTOP interacted with RPN6/10/12/13, Alphafold2 only predicted that TTOP could interact with the pru domain of RPN13 via its UBL domain (fig. S12). This interaction was experimental confirmed by ITC experiment (Figure 8). The interaction affinity (29 μM) is comparable to the affinity between human $RPN13^{PRU}$ domain with the UBL domain of hPLC2 (9.5 μM) (Chen et al., 2016; VanderLinden, Hemmis, Yao, Robinson, & Hill, 2017) and the affinity between human $RPN13^{PRU}$ domain with the UBL domain of human HR23a (26 μM) (Chen et al., 2016; Husnjak et al., 2008), and is stronger than the affinity between human $RPN13^{PRU}$ domain with ubiquitin (91 μM) (VanderLinden et al., 2017). This mean that TTOP could have the similar 26S interaction ability like that of hPLC2 and HR23a. While Alphafold2 may not be able to predict all interactions precisely, it is also possible that not all BiFC signals were generated from direct interaction between

TTOP and these RPN subunits (Figure 6). It is also possible that the binding of TTOP and RPN13 may indirectly enhance the formation of complex between TTOP and the other RPN subunits. The interaction between TTOP and 26S proteosome could become stronger when more than one interacting partners are involved. Without binding to ubiquitinated substrates, 26S proteosome is inactive (Eisele et al., 2018). All seven tested UBL-containing proteins were able to stimulate peptide hydrolysis of 26S proteosome, and all three tested UBL-containing proteins were able to stimulate ATPase activities of 26S proteosome (Collins & Goldberg, 2020). It will be interesting to investigate whether plant UBL-containing proteins, such as TTOP, could also activate plant 26S proteosomes.

The E1/E2/E3 ligase-CDC48A-TTOP-26S proteasome degradation pathway also applies to the plant Tom20 receptors. In yeast, a ubiquitin-proteasome pathway for the degradation of Tom70, a TOM receptor lacking a plant ortholog (Ghifari, Gill-Hille, & Murcha, 2018), has been characterized (Wu, Li, & Jiang, 2016). Tom70 is ubiquitinated by the cytosolic E3 ligase RSP5 (Reverses Spt-Phenotype 5) and binds to the ubiquitin binding domain of Doa1 (Degradation Of Alpha 1), which in turn binds to Cdc48 of the Cdc48/Ufd1/Npl4 complex via its C-terminal PUL domain (Mullally, Chernova, & Wilkinson, 2006). Surprisingly, this ubiquitin-proteasome pathway is specific to Tom70, as it does not target the other yeast TOM receptor, Tom22, for degradation (Wu et al., 2016). In addition to this pathway for mitochondrial OM proteins, yeast also possesses a mitochondrial protein translocation-associated degradation (mitoTAD) pathway. The transmembrane protein Ubx2 (Ubiquitin regulatory X 2), which associates with the TOM complexes, can recruit the Cdc48/Ufd1/Npl4 complex (Schuberth & Buchberger, 2005) to remove clogged precursor proteins from the TOM channel (Martensson et al., 2019). Our results revealed that there is a converged ubiquitin-proteasome degradation pathway, mediated by specific E3 ligases, CDC48 and TTOP, for tail-anchored receptors of TOC and TOM in Arabidopsis. This pathway is important for chloroplast biogenesis, plant development (Figure 3D) and heat stress (Figure 9). *TTOP* is also highly expressed in active sites of cell division (Figure 4A and Figure 5), where mitochondria are abundant and active to meet the high energy demand of cell division. Nonetheless, loss of *TTOP* function did not affect plant growth under normal growth conditions. Perhaps TTOP is required only when the turnover of TOC and TOM receptors is extremely high (e.g., during etiolation) and under stresses (e.g. heat). When their turnover is low, the absence of TTOP may not cause significant phenotypes, possibly because of a lower chance of protein aggregation of TOC and TOM receptors. There is only one *TTOP* gene in the Arabidopsis genome, and no homologous protein has been identified in any non-plant species (fig. S16). Hence, this converged ubiquitin-proteasome pathway for the degradation of tail-anchored receptors may have co-evolved with the TOC/TOM receptors during the endosymbiosis processes in plant species. While the general steps (ubiquitination by E3 ligases, retrotranslocation by CDC48, shuttling to 26S proteosomes by UBL-containing proteins, and 26S proteosome degradation) are in common, there are

mechanistic differences between the animal and plant systems. In term of masking the TMD motifs of TA receptors to prevent protein aggregation during their cytosolic shuttling to 26S proteosome, plant TTOP can bind to TMDs directly, whereas animal BAG6 requires bridging to SGTA via Ubl4A for TMD binding. TTOP may evolve for direct binding to the TMDs of both TOC/TOM TA receptors to simplify the process.

Materials and Methods

Plant Growth Conditions and Generation of Mutants and Transgenic Lines

All wild-type, mutant, and transgenic Arabidopsis (*Arabidopsis thaliana*) plants used in this study were from the Columbia-0 accession (Col-0). Plants were grown on soil or on Murashige-Skoog (MS) agar medium in petri plates at 22°C under a 16-h-light/8-h-dark cycle using cool white fluorescent light bulbs (100 μmol m^{-2} s^{-1}). Seeds were surface sterilized, sown on half-strength MS medium with 1% (w/v) sucrose (pH 5.8-6.2), stratified at 4°C in the dark for 3 days, and then released in a growth chamber.

To generate transgenic plants, all constructs were introduced into Agrobacterium (*Agrobacterium tumefaciens* GV3101 strain) and transformed into plants by the floral dip method (Clough & Bent, 1998). The transgenic plants were selected based on resistance to the appropriate antibiotic, and then protein accumulation in the plants was confirmed by confocal microscopy or immunoblotting. Homozygous lines were obtained after propagation and selection for several generations and used for experiments. To induce the expression of *TTOP* in pTA7002-*GFP-TTOP* plants, 10 μM DEX (10 mM stock dissolved in DMSO) was added to the culture medium or 25 μM DEX was dissolved in ddH_2O and sprayed on the plants. The equivalent volume of DMSO was added to the culture medium or ddH_2O as negative control. The *ttop* knock-out mutants were generated using a CRISPR/Cas9 system (R. Pan, Satkovich, & Hu, 2016). The designed single guide RNA (sgRNA) sequence CTCTAGTAGCACCAATGCGT was cloned into plasmid pKI1.0R and the plasmid transformed into Col-0 (WT) plants. The transformants were selected by antibiotic resistance. The *ttop* mutants were identified from the above selected transformants by genomic PCR and sequencing. To ensure genetic stability, Cas9-free *ttop* mutants that did not carry the CRISPR/Cas9 cassette were obtained by selecting only those seeds showing no red fluorescence under a stereomicroscope (model SZX16, Olympus). The Cas9-free seedlings were grown to maturity and their progeny used for experiments.

The *ttop-5 p35S:mCherry-Toc33* transgenic plants were generated by transforming the plasmid *p35S::mCherry-Toc33* into the *ttop-5* mutant. Homozygous *ttop-5 p35S:mCherry-Toc33* plants were obtained and crossed to WT plants, and WT transgenic plants harboring the *p35S:mCherry-Toc33* transgene were selected from the second generation of the crossed plants by sequencing of the respective PCR-amplified genomic sequences. Two individual homozygous transgenic lines expressing mCherry-Toc33 in the *ttop-5* and WT backgrounds were obtained: *ttop-5 p35S:mCherry-Toc33* #1, *ttop-5 p35S:mCherry-Toc33* #2,

p35S:mCherry-Toc33 #1, and *p35S:mCherry-Toc33* #2. Similarly, *ttop-5 p35S:mCherry-Tom20-2* transgenic plants were generated by transforming the construct *p35S:mCherry-Tom20-2* into the *ttop-5* mutant background. Homozygous *ttop-5 p35S:mCherry-Tom20-2* plants were then crossed to WT plants, and WT plants harboring the *p35S::mCherry-Tom20-2* transgene were identified. Two individual transgenic lines each in the *ttop-5* and WT background were obtained: *ttop-5 p35S:mCherry-Tom20-2* #1 and *ttop-5 p35S:mCherry-Tom20-2* #2, and *p35S:mCherry-Tom20-2* #1 and *p35S:mCherry-Tom20-2* #2.

De-etiolation experiments were performed as reported previously (Ling et al., 2012). Seeds harvested from the same growth batch were sown on MS medium, stratified at 4°C in the dark for 3 days, and then exposed to light for 6 h to induce germination. Next, the seedlings were grown in the dark for 6 days and transferred to continuous light for different periods, and their survival rates and seedling growth phenotypes were recorded. Organellar morphology in cotyledons was examined by transmission electron microscopy (TEM). Each experiment was performed independently four times, and more than 100 seedlings per genotype were used in each experiment for survival rate analysis.

To mark mitochondria in plant cells, seedlings were incubated in half-strength MS liquid culture medium containing 1 mM MitoTracker (Thermo Fisher Scientific, USA) for 30 min, and the dye was removed by washing with culture medium twice. To induce the expression of *TTOP* in pTA7002-*GFP-TTOP* transgenic plants, seedlings were grown on MS medium containing 10 μM dexamethasone (DEX) or sprayed with 25 μM DEX dissolved in ddH_2O.

Construction of Plasmids

Most plasmids used in this study were generated using the One Step Cloning Kit (Vazyme) according to the manufacturer's instructions. All primers are listed in Table S1. All Arabidopsis coding sequences (CDSs) were PCR amplified from Col-0 cDNA. To generate constructs for yeast two-hybrid assays, full-length or truncated CDSs were amplified and inserted into the pGADT7 and pGBKT7 vectors (Clontech, USA). The constructs used for transient expression in Arabidopsis protoplasts were generated by cloning the PCR-amplified CDSs into a version of the pBI221 plasmid that was modified to contain the coding sequence of either *green fluorescence protein* (*GFP*), *yellow fluorescence protein* (*YFP*), or *mCherry* under the control of the cauliflower mosaic virus (CaMV) *35S* promoter. To generate constructs for protoplast transfection for co-immunoprecipitation (co-IP), CDSs were amplified with specific primers harboring the sequence encoding the Myc, 6xHistidine (His), or Hemagglutinin (HA) epitope tags and then cloned into the pBI221 or HBT vector. For BiFC assays, the full-length or truncated CDSs were cloned into the pBI221 vector containing either the sequence encoding the N-terminal half or the C-terminal half of YFP (nY or cY) as described previously (Waadt et al., 2008).

To generate the pBI121-*pTTOP:GFP-TTOP* construct to drive *TTOP* expression under the control of its own promoter, 1,983 bp of sequence upstream of the *TTOP* translation start was amplified and used to replace the original *35S* promoter in the

pBI121 plasmid. The *GFP-TTOP* fragment was amplified from the plasmid pBI221-*p35S:GFP-TTOP* and cloned into the pBI121 plasmid containing the *TTOP* promoter.

To generate the pTA7002-*GFP-TTOP* construct for inducible transcription of *GFP-TTOP* by dexamethasone (DEX) treatment (Park, Canlas, & Ronald, 2012), the *GFP-TTOP* fragment was amplified from pBI221-*p35S:GFP-TTOP* and cloned into the plasmid pTA7002. The same *TTOP* promoter fragment used above was cloned into pBI121 in place of the *35S* promoter to generate the pBI221-*pTTOP:GUS* construct. To generate the construct for generation of *ttop* mutants by genome editing using the CRISPR/Cas9 (clustered regularly interspaced short palindromic repeats/CRISPR-associated 9) system, a single guide RNA (sgRNA) with the sequence CTCTAGTAGCACCAATGCGT was cloned into the pKI1.1R vector, harboring the *RIBOSOMAL PROTEIN S5 A* (*RPS5A*) promoter, the *OLE1–TagRFP* (*red fluorescent protein*) cassette, and the *Cas9* endonuclease gene, as described previously (R. Pan et al., 2016). To generate the *p35S:mCherry-Toc33* and *p35S:mCherry-Tom20-2* constructs for plant transformation, the *mCherry-Toc33/Tom20-2* fragments were individually amplified and cloned into the Gateway® pENTR vector (Invitrogen, USA). The gene cassettes were then transferred into the pEarleyGate100 vector using Gateway LR Clonase (Invitrogen, USA) (Earley et al., 2006).

To generate vectors for protein production in *Escherichia coli*, the codon-optimized coding sequence of *SP1flex* (Ling et al., 2012), *AtUba1* (72-1080), *AtUbc8*, *AtUb* were ordered from GenScript (http://www.genscript.com), as listed in Table S2, and cloned into the pGEX-6p-1 vector (for GST-tagged fusion proteins). SP1 is a transmembrane protein and its overexpression in *E. coli* is prone to insolubility. To remove the transmembrane domain and express a soluble and catalytically active enzyme, the intermembrane domain (*SP1ims*, a.a. 21-225 of SP1) and the cytoplasmic domain (*SP1cyt*, a.a. 244-343 of SP1) were connected with a flexible linker: -[Gly4-Ser]2-) to create SP1flex in a previous study (Ling et al., 2012). To generate vectors for the production of recombinant Toc33FL (a.a. 1–297), Toc33NC (a.a. 1–251), TTOP (a.a. 1–879), Tom20-3NC (a.a. 1–174) and GST-SP1RING, which carry the RING motif of E3 ligase (a.a. 254-343 of SP1) (Ling et al., 2012), in *E. coli*, all CDSs were PCR amplified from Arabidopsis Col-0 cDNA and were cloned into the pGEX-6p-1 vector (for GST-tagged fusion proteins) or the pET507a vector (for His-tagged fusion proteins) as listed in Table S1.

Protein Production and Purification

The expression vectors pGEX-6p-1-GST-SP1flex, pGEX-6p-1AtUba1, pGEX-6p-1-AtUbc8, pGEX-6p-1-AtUb, pGEX-6p-1-GST-SP1RING, pGEX-6p-1-GST-TTOP, pGEX-6p-1-GST-UBL, pGEX-6p-1-GST-RPN13pru, pET507a-His-Toc33NC, pET507a-His-Toc33FL, and pET507a-His-Tom20-3NC were transformed into *E. coli* BL21 cells (Sangon Biotech) for production of recombinant protein, which was induced by the addition of 0.4 mM isopropyl β-D-1-thiogalactopyranoside (IPTG) when the cultures reached OD_{600} of 0.8. After

incubation at 16□ for 18 h in the presence of IPTG, the cells were harvested by centrifugation at 14,160*g* for 12 min at 16□. The pellets of cells carrying pGEX-6p-1 vector derivatives were resuspended in lysis buffer consisting of 30 mM Tris buffer pH 7.6, 500 mM NaCl, and 5 mM dithiothreitol (DTT) and sonicated on ice (Qsonica Q500 sonicator, 300 W, 10 s/10 s, 30 min on ice). After centrifugation at 29,000*g* for 36 min, the supernatant was filtered (0.22-μm Millipore filter) and then incubated with GSTrap Sepharose (GE Healthcare) for 2 h at 4□. After extensive washing with wash buffer (30 mM Tris buffer, pH 7.6, 150 mM NaCl, and 5 mM DTT), the bound GST-tagged proteins were incubated with GST-tagged PreScission protease (GE Healthcare) at 4□ overnight to cleave the GST tag, and the target proteins without the GST tag were then collected in the eluted fractions. The pellets of cells harboring pET507a derivatives were resuspended in nickel binding buffer (30 mM Tris buffer, pH 7.6, 500 mM NaCl, and 1 mM Tris(2-carboxyethyl)phosphine [TCEP]) and sonicated on ice (Qsonica Q500 sonicator, 300 W, 10 s/10 s, 30 min on ice). After centrifugation at 29,000*g* for 36 min at 4□, the supernatants were filtered (0.22-μm Millipore filter) and individually loaded onto a 5-mL HisTrap Ni-Chelating HP column (GE Healthcare). After extensive washing of the HisTrap column with 40 mM imidazole in nickel binding buffer, the His-tag proteins were eluted with 300 mM imidazole in nickel binding buffer.

For purification of His-Toc33FL, the cell pellet was resuspended in denaturing nickel binding buffer (30 mM Tris buffer, pH 7.6, 500 mM NaCl, 1 mM TCEP, 1% (v/v) TritonX-100 and 8 M urea) and sonicated on ice. After centrifugation at 29,000*g* for 36 min at 4□, the supernatant was filtered (0.22-μm Millipore filter) and loaded onto a 5-mL HisTrap Ni-Chelating HP column (GE Healthcare). After extensive washing of the HisTrap column with 60 mM imidazole in denaturing nickel binding buffer, the fusion protein was eluted with 300 mM imidazole in denaturing nickel binding buffer. The solubilized recombinant His-Toc33 protein was first dialyzed in 200-fold (v/v) volumes of dialysis buffer 1 (30 mM Tris buffer, pH 7.6, 500 mM NaCl, 1 mM TCEP, 0.1% (v/v) TritonX-100 and 2 M urea) and then in buffer without urea, each time for 18 h at 4□. After removal of precipitated proteins by centrifugation at 29,000*g* for 36 min at 4□, soluble His-Toc33 was further purified by gel filtration using a HiLoad 26/60 Superdex 75 column (GE Healthcare) pre-equilibrated with 30 mM Tris, pH 7.5, 150 mM NaCl, and 2 mM DTT.

In vitro Ubiquitination and Pull-down Assays

In vitro ubiquitination assays were performed in a 30-μL reaction mixture. For the SP1 auto-ubiquitination assay, 1 μg of recombinant GST, GST-SP1flex, GST-SP1RING, or SP1flex was incubated with 0.1 μg of AtUba1 E1, 0.3 μg of AtUbc8 E2, and 2.5 μg of AtUb in a 30-μL reaction containing 30 mM Tris-HCl, pH 7.5, 2 mM ATP, 5 mM $MgCl_2$, 2 mM DTT, and 0.5 U inorganic pyrophosphatase (Sigma). The mixture was incubated at 30°C for 2 h, and the reaction was stopped by adding an equal volume of 2× sodium dodecyl sulfate-polyacrylamide gel electrophoresis (SDS-PAGE) buffer. Immunoblotting analysis was conducted using anti-ubiquitin antibodies (FK2, MERCK). To test the ubiquitination of substrates by

SP1flex, the substrates His-Toc33NC, His-Toc33FL, and His-Tom20-3NC were individually added to the above reactions, and the reaction mixtures were subjected to immunoblotting analysis with anti-ubiquitin antibodies (FK2, MERCK). To test whether unknown E2/E3 ubiquitin conjugating enzymes or ligases in plant extracts can ubiquitinate His-Tom20-3NC, 20 μg of plant extract (PE) from 7-day-old seedlings was added to the *in vitro* ubiquitination assay.

In the pull-down analysis of ubiquitinated substrates by TTOP, 120 μL of ubiquitination reaction products was prepared using the above ubiquitination reaction system. The ubiquitination reaction products were incubated with equimolar amounts of GST or GST-TTOP in the presence of GSTrap Sepharose (GE Healthcare) in binding buffer (30 mM Tris, pH 7.5, 150 mM NaCl, and 2 mM DTT) for 1 h at 4□. After extensive washing with binding buffer, GST-bound proteins were eluted with 20 mM reduced glutathione in binding buffer and subjected to immunoblotting analysis with anti-ubiquitin antibodies (FK2, Merck).

Isothermal titration calorimetry (ITC) analysis

ITC experiments were carried out on a VP-ITC Microcal calorimeter (Malvern) at 25 °C. All proteins were dissolved in buffer containing 50 mM Tris-HCl pH 7.5, 100 mM NaCl, and 1 mM DTT. Each titration point typically is consisted of injecting 10 μl aliquots of the RPN13 pru domain, at a concentration of 500 μM into the solution of containing TTOP UBL domain at a concentration of 50 μM. A time interval of 150 or 180 s between two titration points was used to ensure the complete equilibrium of each titration reaction. The titration data were analyzed using the program Origin7.0 and fitted by a one-site binding model.

Yeast Two-Hybrid, Protoplast Transient Expression, and BiFC assays

Yeast two-hybrid analysis was performed using the MatchMaker GAL4 Two-Hybrid System 3 (Clontech, USA) according to the manufacturer's instructions. The different CDSs were cloned into the pGBKT7 or pGADT7 vector. Pairs of pGBKT7 and pGADT7 vectors carrying the appropriate CDSs were co-transformed into the Y2HGold yeast strain. Diploids were selected on synthetic defined (SD) medium lacking tryptophan (Trp) and leucine (Leu) (SD –Trp –Leu) to select transformants. The colonies growing on SD –Trp –Leu medium were then transferred to selective SD medium lacking histidine (His), Trp, and Leu (SD –His –Trp –Leu) or lacking adenine (Ade), His, Trp, and Leu (SD –His –Ade –Trp –Leu) and were incubated at 30°C for 3–6 days to investigate protein–protein interactions. The control vector pairs pGADT7-T and pGBKT7-lam, and pGADT7-T and pGBKT7-53 were co-transformed into yeast as negative and positive controls, respectively. Yeast colonies were grown on selective SD –His –Ade –Trp –Leu medium. The experiments were repeated three times independently with similar results.

Arabidopsis mesophyll protoplast preparation and transfection were performed according to a previously described method (Yoo, Cho, & Sheen, 2007). Protoplasts were isolated from rosettes of 4-week-old Col-0 plants grown on soil by incubating the rosettes with enzyme solution containing 1% (w/v) cellulose (Onozuk R-10, Yakult, Japan) and 0.2% (w/v) macerozyme (R-10, Yakult, Japan) for 2–4 h. The

isolated protoplasts were washed with W5 buffer three times to thoroughly remove the enzymes. PEG4000 was used to transfect plasmids into protoplasts; 0.1 mL (10^5) of protoplasts was transfected with 8 μg of DNA. The transfected protoplasts were cultured for 12 h in darkness to allow protein accumulation and were collected for fluorescence detection or protein extraction. To mark the mitochondria in the cells, protoplasts were incubated in W5 culture medium containing 100 nM MitoTracker for 20 min, and excess MitoTracker was removed by washing with W5 culture medium twice.

For the BiFC assay, Arabidopsis mesophyll protoplasts were co-transfected with the appropriate pairs of constructs carrying either *nY* or *cY*, fused to different CDSs, and cultured overnight (12 h) for protein expression. The reconstitution of YFP fluorescence, indicating protein–protein interaction, was detected by fluorescence microscopy using a confocal microscope. For each experiment, more than 40 individual cells were analyzed by confocal imaging that represented >90% of cells that showed similar protein expression levels and patterns. Images were captured using a Leica SP8 laser scanning confocal microscope (Leica Microsystems, German). To avoid possible cross-talk between the fluorescence channels, sequential scanning was used when necessary. Images were processed and assembled using Photoshop CS6 software (Adobe, USA).

Protein Extraction, Co-immunoprecipitation, Immunoblots, and Blue Native PAGE Assays

For extraction of proteins from seedlings and protoplasts, total proteins were extracted in ice-cooled protein extraction buffer, containing 25 mM Tris-HCl, pH 7.5, 150 mM NaCl, 1 mM EDTA, 1% (v/v) Triton X-100, and 1% (v/v) plant protease inhibitor cocktail (P9599, Sigma, Germany). After incubation in extraction buffer for 30 min on ice, the supernatants were collected by centrifugation at 16,000*g* at 4°C for 15 min. The protein concentration in the supernatants was determined using the Bradford Protein Assay Kit (5000201EDU, Bio-Rad, USA).

For co-IP analysis, the transfected protoplasts were incubated overnight to express the transgenes. Total protein was extracted as mentioned above, and 80 μL of the supernatants was kept as input. The remaining supernatants were diluted with an equal volume of buffer containing 25 mM Tris-HCl, pH 7.5, 150 mM NaCl, 1 mM EDTA, and 1% (v/v) plant protease inhibitor cocktail [P9599, Sigma, Germany]), mixed with 10 μL of GFP-Trap agarose (gta-20, Chromotek, Germany), and incubated on a rotary mixer overnight at 4°C. The GFP-Trap agarose was used according to the manufacturer's instructions. After six washes of the GFP-Trap agarose with washing buffer (25 mM Tris-HCl, pH 7.5, 150 mM NaCl, and 1 mM EDTA), bound proteins were eluted from the GFP-Trap agarose by boiling in 2× SDS-PAGE buffer (50 mM Tris-HCl, pH 6.8, 20% glycerol, 1% SDS, and 0.1 M DTT) for 5 min and analyzed by SDS-PAGE and immunoblotting with anti-GFP and anti-FLAG antibodies.

For immunoblotting, the protein extracts were denatured in 2× SDS-PAGE buffer, separated on SDS-PAGE gels, and transferred onto nitrocellulose membrane (GE10600002, Amersham™, Merck, Germany). SDS-PAGE and immunoblotting

were performed as described (R. Pan et al., 2016) with minor modifications. When necessary, the gels were stained with Coomassie Brilliant Blue G250 (6104-58-1, Sigma, Germany). For immunoblots, the membranes were probed with the following primary antibodies, which were used according to the manufacturer's instructions: anti-GFP (SAB43011338, Sigma, Germany), anti-mCherry (PA534974, Thermo Fisher, USA), anti-TTOP (residues 158–449; the antigen for the immunization of rabbits was bacterially-produced, GenScript China Inc.), anti-HA tag (A02040, Abbkine, China), anti-Myc tag (A02060, Abbkine, China), anti-FLAG tag (A02010, Abbkine, China), anti-His tag (A02050, Abbkine, China), anti-cFBPase (AS04043, Agrisera, Sweden), and anti-actin (A01050, Abbkine, China). To identify TOC and TIC proteins, the following antibodies were used according to the manufacturer's instructions: anti-atToc75-III (AS08-351, Agrisera, Sweden), anti-atToc159 (ASO7239, Agrisera, Sweden), anti-atToc34 (AS07238, Agrisera, Sweden), anti-atToc33 (AS07236, Agrisera, Sweden), and anti-atTic40 (AS10709, Agrisera, Sweden). The following secondary antibodies were used according to the manufacturer's instructions: anti-rabbit IgG conjugated to horseradish peroxidase (170-6515, Bio-Rad [Shanghai]), anti-mouse IgG conjugated to horseradish peroxidase (A25012, Abbkine, China), anti-guinea pig conjugated to peroxidase (A5545, Sigma, Germany), and anti-chicken conjugated to peroxidase (A9046, Sigma, Germany). Chemiluminescence was detected using the ECL Plus Western Blotting Detection Reagents (1705061, Bio-Rad [Shanghai]) and an Alliance Q9 chemiluminescence and spectral fluorescence imaging system (UVITEC, UK). Signal intensities were quantified using ImageJ software (version 64-bit Java 1.8.0_172, USA) (Schneider, Rasband, & Eliceiri, 2012).

The first-dimension BN-PAGE was performed as described previously (Eubel, Braun, & Millar, 2005) with minor modifications. Transfected protoplasts were cultured overnight to allow transgene expression and lysed in native protein extraction buffer (30 mM HEPES, pH 7.4, 150 mM potassium acetate, 10% (v/v) glycerol, 1% (v/v) digitonin and 1% (v/v) plant protease inhibitor cocktail [P9599, Sigma, Germany], added before use). After incubation in extraction buffer for 30 min on ice, the supernatants were collected by centrifugation at 16,000*g* at 4°C for 15 min. The solubilized proteins were separated on a native gradient gel and transferred onto a nitrocellulose membrane, in both cases using 0.5× Tris borate EDTA (TBE) buffer containing 0.5% (w/v) Tris base, 0.04% (w/v) EDTA, and 0.3% (w/v) boric acid; they were then immunoblotted with anti-His, anti-HA, anti-FLAG, and anti-Myc antibodies as described above.

GUS Staining and Transmission Electron Microscopy (TEM)

Plant tissues were submerged in 90% (v/v) acetone fixation solution and incubated at 4°C for 40 min. The fixation solution was discarded, and the plant tissues were washed three times in wash solution (100 mM sodium phosphate buffer, pH 7.0, 10 mM EDTA, 2 mM potassium ferrocyanide, and 2 mM potassium ferricyanide). For GUS staining, the plant tissues were submerged in standard X-GlcA solution (100 mM sodium phosphate buffer, pH 7.0, 10 mM EDTA, 2 mM potassium ferrocyanide,

2 mM potassium ferricyanide, and 0.5 mg/mL X-GlcA), vacuum infiltrated for 5 min, and then incubated at 37°C for 4–6 h to allow development of the blue color, as described previously (Jefferson, Kavanagh, & Bevan, 1987). The images of the GUS-stained specimens were captured using a stereomicroscope (model SZX16, Olympus, Japan). A minimum of five different samples were analyzed for each treatment, and typical images are shown.

The general procedures for transmission electron microscopy, sample preparation, and ultrathin sectioning were performed as described previously (Gao et al., 2012; J. Wang, Tse, Hinz, Robinson, & Jiang, 2012). The tissues from at least 10 plants per genotype were used for the TEM. Measurements of chloroplast cross-sectional areas were estimated using ImageJ software (version 64-bit Java 1.8.0_172, USA). At least 30 different plastids/chloroplasts per genotype were analyzed. The plastids were classified into three developmental stages: I, plastids with large rudimentary prothylakoids and prolamellar bodies (PLBs); II, plastids with PLBs of reduced sized and partially developed thylakoids; and III, plastids in which all PLBs had transformed into thylakoids.

Phylogenetic analysis

Amino acid sequences were obtained by BLAST searches of the Phytozome 13 database (Goodstein et al., 2012) (Table S4). Sequences were then aligned by the MAFFT multiple sequence alignment program (Katoh & Standley, 2013). Poor quality alignments were filtered out by Gblocks (Castresana, 2000) and only conserved sequences were retained. Phylogeny was inferred using IQ-TREE (Nguyen, Schmidt, von Haeseler, & Minh, 2015), and maximum likelihood tree was built. Bootstrap percentages at the branch points were estimated from 1,000 bootstrap replications. Finally, the phylogenetic tree was drawn by iTOL (Letunic & Bork, 2016) using the tree file obtained from IQ-TREE.

Statistical Analysis

Statistical calculations (mean, SEM, and *t* test) were performed using Microsoft Excel software. The statistical significance of differences between two experimental groups was assessed using a two-tailed Student's *t*-test. Differences between two datasets were considered significant at $P < 0.05$.

AlphaFold Prediction

Modelled the binding of the TTOP UBL with RPN6 using the AlphaFold2 machine learning algorithm (Jumper et al., 2021; Mirdita et al., 2021). Take TTOP-UBL and RPN6 as an example, in the Google_colab AlphaFold2_advanced(https://colab.research.google.com/github/sokrypton/ColabFold/blob/main/beta/AlphaFold2_advanced.ipynb#scrollTo=rowN0bVYLe9n webpage, we input the TTOP-UBL and RPN6 sequences in the Sequence column and run 24 recycles for refinement (TLELNIKTLDSRTYTFQVNKNETVLLFKEKIASETGVPVGQQRLIFRGRVLKD DHPLSEYHLENGHTLHLIVRQPAE:MVSYRATTETISLALEANSSEAITILYQVL

EDPSSSPEAIRIKEQAITNLCDRLTEEKRGEDLRKLLTKLRPFFSLIPKAKTAKIV
RGIIDAVAKIPGTTDLQITLCKEMVEWTRAEKRTFLRQRVEARLAALLMENKE
YVEALALLSTLVKEVRRLDDKLLLVDIDLLESKLHFSLRNLPKAKAALTAART
AANAIYVPPAQQGTIDLQSGILHAEEKDYKTGYSYFFEAFESFNALGDPRAVFS
LKYMLLCKIMVSQADDVAGIISSKAGLQYVGPDLDAMKAVADAHSKRSLKLF
ENALRDYKAQLEDDPIVHRHLSSLYDTLLEQNLCRLIEPFSRVEIAHIAELIGLP
LDHVEKKLSQMILDKKFAGTLDQGAGCLIIFEDPKADAIYSATLETIANMGKV
VDSLYVRSAKIMS). AlphaFold2 generated 5 models which were ranked by pLDDT (redicted Local Distance Difference Test) and pTMscore (post-translational modifications score) (Mariani, Biasini, Barbato, & Schwede, 2013; Tsaban et al., 2022). Higher pLDDT indicated higher prediction quality. But high pLDDT did not necessarily indicate a correct complex prediction, the inter-complex PAE (predicted alignment error) was used to rank complexes. Low inter PAE between chains indicates a confident prediction. The predictions of the interaction between TTOP UBL and RPNs, and the interaction between the C-terminal of TTOP with the transmembrane domains of TOC/TOM all followed the above method.

Accession Numbers

The Arabidopsis Genome Initiative locus identifiers for the genes mentioned in this article are as follows: *TTOP* (At5g42220), *Toc33* (At1g02280), *Toc34* (At5g05000), *Tom20-2* (At1g27390), *Tom20-3* (At3g27080), *Tom20-4* (At5g40930), *PAP2* (At1g13900), *CDC48A* (At3g09840), SP1 (At1g63900), *SP2* (At3g44160), *RPN6* (At1g29150), *RPN10* (At4g38630), *RPN12* (At1g64520), *RPN13* (At2g26590), *AtUba1* (At2g30110), *AtUbc8* (At5g41700), and *AtUb* (At4g02890).

Real-time quantitative PCR analysis

Total RNA was extracted using the total RNA isolation TRIzol™ Reagent (Thermo Fisher Scientific, USA) following the manufacturer's instructions from 8-day-old *pTA7002-GFP-TTOP* plants subjected to DEX or DMSO treatment for 1 (D1) or 2 days (D2), or untreated. 1 μg total RNA was used for first-strand cDNA synthesis with the HiScript III Enzyme Mix, RT Mix, and oligo$(dT)_{20}$VN (Vazyme, China). Transcript levels were determined by RT-qPCR with the SYBR green master mix (Applied Biosystems, USA) on the StepOnePlus Real-Time PCR System (Applied Biosystems, USA). RT-qPCR was performed in triplicates. The relative expression levels were calculated with the $2^{-\Delta\Delta Ct}$ method (Livak & Schmittgen, 2001). Primers used for RT-qPCR are listed in Supplementary Table 1.

Acknowledgements

This project was supported by the Science, Technology and Innovation Commission of Shenzhen Municipality (Basic Research Program 201708183000803), the Hong Kong Research Grants Council Area of Excellence Scheme (AoE/M-403/16), and the Innovation and Technology Fund (Funding Support to State Key Laboratory of Agrobiotechnology) of the Hong Kong Special Administrative Region, China. Any opinions, findings, conclusions or recommendations expressed in this publication do

not reflect the views of the Government of the Hong Kong Special Administrative Region or the Innovation and Technology Commission.

Author contributions

B.L.L. and M.Y. designed the study. S.L.L., J.Y.Z., and K.C.C. generated the majority of constructs and plant transgenic lines. S.C. carried out the *in vitro* ubiquitination experiments and AlphaFold2 prediction. Z.Z. carried out phylogenetic analysis. L.Y. carried out some BiFc experiments. M.Y. generated some constructs and plant lines and carried out all the remaining experiments. B.L.L. and M.Y. wrote the manuscript. All authors revised and approved the manuscript.

Competing interests: The authors declare no competing interests.

Data analysis: All data are presented as means with standard errors (mean ± SEM). The collected data were analyzed for statistical significance using analysis of variance (ANOVA) with Tukey's HSD, paired *t*-tests, or unpaired *t*-tests at $P < 0.001$, $P < 0.01$, and $P < 0.05$ by SPSS (version 22).

Data and materials availability: All data are available in the main text or the supplementary materials. Materials are available from the corresponding authors upon request.

References

Aoyama, T., and Chua, N.H. (1997). A glucocorticoid-mediated transcriptional induction system in transgenic plants. Plant Journal *11*, 605-612.

Bae, W., Lee, Y.J., Kim, D.H., Lee, J., Kim, S., Sohn, E.J., and Hwang, I. (2008). AKr2A-mediated import of chloroplast outer membrane proteins is essential for chloroplast biogenesis. Nat Cell Biol *10*, 220-U101.

Castresana, J. (2000). Selection of conserved blocks from multiple alignments for their use in phylogenetic analysis. Molecular Biology and Evolution *17*, 540-552. 10.1093/oxfordjournals.molbev.a026334.

Chen, X., Randles, L., Shi, K., Tarasov, Sergey G., Aihara, H., and Walters, Kylie J. (2016). Structures of Rpn1 T1:Rad23 and hRpn13:hPLIC2 reveal distinct binding mechanisms between substrate receptors and shuttle factors of the proteasome. Structure *24*, 1257-1270. 10.1016/j.str.2016.05.018.

Chio, U.S., Cho, H., and Shan, S.O. (2017). Mechanisms of tail-anchored membrane protein targeting and insertion. Annu Rev Cell Dev Biol *33*, 417-438. 10.1146/annurev-cellbio-100616-060839.

Clough, S.J., and Bent, A.F. (1998). Floral dip: a simplified method for Agrobacterium-mediated transformation of Arabidopsis thaliana. The Plant journal : for cell and molecular biology *16*, 735-743.

Collins, G.A., and Goldberg, A.L. (2020). Proteins containing ubiquitin-like (Ubl) domains not only bind to 26S proteasomes but also induce their activation. Proceedings of the National Academy of Sciences *117*, 4664-4674. doi:10.1073/pnas.1915534117.

Duncan, O., Murcha, M.W., and Whelan, J. (2013). Unique components of the plant mitochondrial protein import apparatus. Biochimica et Biophysica Acta (BBA) - Molecular Cell Research *1833*, 304-313. https://doi.org/10.1016/j.bbamcr.2012.02.015.

Earley, K.W., Haag, J.R., Pontes, O., Opper, K., Juehne, T., Song, K., and Pikaard, C.S. (2006). Gateway-compatible vectors for plant functional genomics and proteomics. The Plant Journal *45*, 616-629. 10.1111/j.1365-313X.2005.02617.x.

Eisele, M.R., Reed, R.G., Rudack, T., Schweitzer, A., Beck, F., Nagy, I., Pfeifer, G., Plitzko, J.M., Baumeister, W., Tomko, R.J., Jr., and Sakata, E. (2018). Expanded coverage of the 26S proteasome conformational landscape reveals mechanisms of peptidase gating. Cell Rep *24*, 1301-1315.e1305. 10.1016/j.celrep.2018.07.004.

Eubel, H., Braun, H.P., and Millar, A.H. (2005). Blue-native PAGE in plants: a tool in analysis of protein-protein interactions. Plant methods *1*, 11. 10.1186/1746-4811-1-11.

Fellerer, C., Schweiger, R., Schongruber, K., Soll, J., and Schwenkert, S. (2011). Cytosolic HSP90 cochaperones HOP and FKBP interact with freshly synthesized chloroplast preproteins of Arabidopsis. Molecular plant *4*, 1133-1145. 10.1093/mp/ssr037.

Fernández-Bautista, N., Fernández-Calvino, L., Muñoz, A., and Castellano, M.M. (2017). HOP3, a member of the HOP family in Arabidopsis, interacts with BiP and plays a major role in the ER stress response. Plant, cell & environment *40*, 1341-1355. https://doi.org/10.1111/pce.12927.

Gao, C., Yu, C.K., Qu, S., San, M.W., Li, K.Y., Lo, S.W., and Jiang, L. (2012). The Golgi-localized Arabidopsis endomembrane protein12 contains both endoplasmic reticulum export and Golgi retention signals at its C terminus. The Plant cell *24*, 2086-2104. 10.1105/tpc.112.096057.

Ghifari, A.S., Gill-Hille, M., and Murcha, M.W. (2018). Plant mitochondrial protein import: the ins and outs. Biochem J *475*, 2191-2208.

Goodstein, D.M., Shu, S.Q., Howson, R., Neupane, R., Hayes, R.D., Fazo, J., Mitros, T., Dirks, W., Hellsten, U., Putnam, N., and Rokhsar, D.S. (2012). Phytozome: a comparative platform for green plant

838 genomics. Nucleic Acids Research *40*, D1178-D1186. 10.1093/nar/gkr944.
839 Guna, A., and Hegde, R.S. (2018). Transmembrane domain recognition during membrane Protein
840 biogenesis and quality control. Current Biology *28*, R498-R511.
841 https://doi.org/10.1016/j.cub.2018.02.004.
842 Hessa, T., Sharma, A., Mariappan, M., Eshleman, H.D., Gutierrez, E., and Hegde, R.S. (2011). Protein
843 targeting and degradation are coupled for elimination of mislocalized proteins. Nature *475*, 394-397.
844 10.1038/nature10181.
845 Husnjak, K., Elsasser, S., Zhang, N., Chen, X., Randles, L., Shi, Y., Hofmann, K., Walters, K.J., Finley, D.,
846 and Dikic, I. (2008). Proteasome subunit Rpn13 is a novel ubiquitin receptor. Nature *453*, 481-488.
847 10.1038/nature06926.
848 Jefferson, R.A., Kavanagh, T.A., and Bevan, M.W. (1987). GUS fusions: beta-glucuronidase as a sensitive
849 and versatile gene fusion marker in higher plants. The EMBO journal *6*, 3901-3907.
850 Jumper, J., Evans, R., Pritzel, A., Green, T., Figurnov, M., Ronneberger, O., Tunyasuvunakool, K., Bates,
851 R., Zidek, A., Potapenko, A., et al. (2021). Highly accurate protein structure prediction with AlphaFold.
852 Nature *596*, 583-589. 10.1038/s41586-021-03819-2.
853 Katoh, K., and Standley, D.M. (2013). MAFFT Multiple Sequence Alignment Software Version 7:
854 Improvements in Performance and Usability. Molecular Biology and Evolution *30*, 772-780.
855 10.1093/molbev/mst010.
856 Kim, J., Na, Y.J., Park, S.J., Baek, S.H., and Kim, D.H. (2019). Biogenesis of chloroplast outer envelope
857 membrane proteins. Plant cell reports *38*, 783-792. 10.1007/s00299-019-02381-6.
858 Krysztofinska, E.M., Martínez-Lumbreras, S., Thapaliya, A., Evans, N.J., High, S., and Isaacson, R.L.
859 (2016). Structural and functional insights into the E3 ligase, RNF126. Sci Rep-Uk *6*, 26433.
860 10.1038/srep26433.
861 Law, Y.S., Zhang, R., Guan, X., Cheng, S., Sun, F., Duncan, O., Murcha, M., Whelan, J., and Lim, B.L.
862 (2015). Phosphorylation and dephosphorylation of the presequence of pMORF3 during import into
863 mitochondria from *Arabidopsis thaliana*. Plant Physiology *169*, 1-12. 10.1104/pp.15.01115.
864 Letunic, I., and Bork, P. (2016). Interactive tree of life (iTOL) v3: an online tool for the display and
865 annotation of phylogenetic and other trees. Nucleic Acids Research *44*, W242-W245.
866 10.1093/nar/gkw290.
867 Ling, Q., Broad, W., Trösch, R., Töpel, M., Demiral Sert, T., Lymperopoulos, P., Baldwin, A., and Jarvis,
868 R.P. (2019a). Ubiquitin-dependent chloroplast-associated protein degradation in plants. Science (New
869 York, N.Y.) *363*. 10.1126/science.aav4467.
870 Ling, Q., Huang, W., Baldwin, A., and Jarvis, P. (2012). Chloroplast biogenesis is regulated by direct
871 action of the ubiquitin-proteasome system. Science (New York, N.Y.) *338*, 655-659.
872 10.1126/science.1225053.
873 Ling, Q., and Jarvis, P. (2015). Regulation of Chloroplast Protein Import by the Ubiquitin E3 Ligase SP1
874 Is Important for Stress Tolerance in Plants. Curr Biol *25*, 2527-2534. 10.1016/j.cub.2015.08.015.
875 Ling, Q.H., Broad, W., Trosch, R., Topel, M., Sert, T.D., Lymperopoulos, P., Baldwin, A., and Jarvis, R.P.
876 (2019b). Ubiquitin-dependent chloroplast-associated protein degradation in plants. Science *363*,
877 aav4467.
878 Livak, K.J., and Schmittgen, T.D. (2001). Analysis of relative gene expression data using real-time
879 quantitative PCR and the 2(-Delta Delta C(T)) Method. Methods, 402–408. https://doi.org/10.1006/
880 meth.2001.1262.
881 Mariani, V., Biasini, M., Barbato, A., and Schwede, T. (2013). lDDT: a local superposition-free score for

882 comparing protein structures and models using distance difference tests. Bioinformatics (Oxford,
883 England) *29*, 2722-2728. 10.1093/bioinformatics/btt473.
884 Martensson, C.U., Priesnitz, C., Song, J., Ellenrieder, L., Doan, K.N., Boos, F., Floerchinger, A., Zufall, N.,
885 Oeljeklaus, S., Warscheid, B., and Becker, T. (2019). Mitochondrial protein translocation-associated
886 degradation. Nature *569*, 679-683. 10.1038/s41586-019-1227-y.
887 Mirdita, M., Ovchinnikov, S., and Steinegger, M. (2021). ColabFold - Making protein folding accessible
888 to all. bioRxiv, 2021.2008.2015.456425. 10.1101/2021.08.15.456425.
889 Mock, J.-Y., Chartron, J.W., Zaslaver, M.a., Xu, Y., Ye, Y., and Clemons, W.M. (2015). Bag6 complex
890 contains a minimal tail-anchor-targeting module and a mock BAG domain. Proceedings of the National
891 Academy of Sciences *112*, 106-111. doi:10.1073/pnas.1402745112.
892 Mullally, J.E., Chernova, T., and Wilkinson, K.D. (2006). Doa1 is a Cdc48 adapter that possesses a novel
893 ubiquitin binding domain. Mol Cell Biol *26*, 822-830. 10.1128/MCB.26.3.822-830.2006.
894 Nakai, M. (2018). New Perspectives on Chloroplast Protein Import. Plant and Cell Physiology *59*,
895 1111-1119. 10.1093/pcp/pcy083.
896 Nguyen, L.T., Schmidt, H.A., von Haeseler, A., and Minh, B.Q. (2015). IQ-TREE: A Fast and Effective
897 Stochastic Algorithm for Estimating Maximum-Likelihood Phylogenies. Molecular Biology and
898 Evolution *32*, 268-274. 10.1093/molbev/msu300.
899 Pan, R., Satkovich, J., and Hu, J. (2016). E3 ubiquitin ligase SP1 regulates peroxisome biogenesis in
900 Arabidopsis. Proc Natl Acad Sci U S A *113*, E7307-E7316. 10.1073/pnas.1613530113.
901 Pan, R.H., and Hu, J.P. (2018). The Arabidopsis E3 Ubiquitin Ligase SP1 Targets to Chloroplasts,
902 Peroxisomes, and Mitochondria. Plant Physiology *176*, 480-482.
903 Panigrahi, R., Whelan, J., and Vrielink, A. (2014). Exploring ligand recognition, selectivity and dynamics
904 of TPR domains of chloroplast Toc64 and mitochondria Om64 from *Arabidopsis thaliana*. Journal of
905 molecular recognition : JMR *27*, 402-414. 10.1002/jmr.2360.
906 Park, C.-J., Canlas, P.E., and Ronald, P.C. (2012). Establishment of glucocorticoid-mediated
907 transcriptional induction of the rice XA21 pattern recognition receptor. J Plant Biol *55*, 43-49.
908 10.1007/s12374-011-9188-1.
909 Schneider, C.A., Rasband, W.S., and Eliceiri, K.W. (2012). NIH Image to ImageJ: 25 years of image
910 analysis. Nature methods *9*, 671-675. 10.1038/nmeth.2089.
911 Schuberth, C., and Buchberger, A. (2005). Membrane-bound Ubx2 recruits Cdc48 to ubiquitin ligases
912 and their substrates to ensure efficient ER-associated protein degradation. Nat Cell Biol *7*, 999-1006.
913 10.1038/ncb1299.
914 Shao, S., Rodrigo-Brenni, M.C., Kivlen, M.H., and Hegde, R.S. (2017). Mechanistic basis for a molecular
915 triage reaction. Science *355*, 298-302. doi:10.1126/science.aah6130.
916 Shi, L.-X., and Theg, S.M. (2013). The chloroplast protein import system: From algae to trees.
917 Biochimica et Biophysica Acta (BBA) - Molecular Cell Research *1833*, 314-331.
918 https://doi.org/10.1016/j.bbamcr.2012.10.002.
919 Shi, Y., Chen, X., Elsasser, S., Stocks, B.B., Tian, G., Lee, B.-H., Shi, Y., Zhang, N., Poot, S.A.H.d., Tuebing,
920 F., et al. (2016). Rpn1 provides adjacent receptor sites for substrate binding and deubiquitination by
921 the proteasome. Science *351*, aad9421. doi:10.1126/science.aad9421.
922 Sommer, M., Rudolf, M., Tillmann, B., Tripp, J., Sommer, M.S., and Schleiff, E. (2013). Toc33 and
923 Toc64-III cooperate in precursor protein import into the chloroplasts of *Arabidopsis thaliana*. Plant,
924 cell & environment *36*, 970-983. 10.1111/pce.12030.
925 Sun, F., Carrie, C., Law, S., Murcha, M.W., Zhang, R., Law, Y.S., Suen, P.K., Whelan, J., and Lim, B.L.

(2012). AtPAP2 is a tail-anchored protein in the outer membrane of chloroplasts and mitochondria. Plant signaling & behavior *7*, 927-932. 10.4161/psb.20769.

Tsaban, T., Varga, J.K., Avraham, O., Ben-Aharon, Z., Khramushin, A., and Schueler-Furman, O. (2022). Harnessing protein folding neural networks for peptide–protein docking. Nature Communications *13*, 176. 10.1038/s41467-021-27838-9.

Tsutsui, H., and Higashiyama, T. (2017). pKAMA-ITACHI vectors for highly efficient CRISPR/Cas9-mediated gene knockout in *Arabidopsis thaliana*. Plant & cell physiology *58*, 46-56. 10.1093/pcp/pcw191.

VanderLinden, R.T., Hemmis, C.W., Yao, T., Robinson, H., and Hill, C.P. (2017). Structure and energetics of pairwise interactions between proteasome subunits RPN2, RPN13, and ubiquitin clarify a substrate recruitment mechanism. J Biol Chem *292*, 9493-9504. 10.1074/jbc.M117.785287.

Voon, C.P., Law, Y.S., Guan, X., Lim, S.L., Xu, Z., Chu, W.T., Zhang, R., Sun, F., Labs, M., Leister, D., et al. (2021). Modulating the activities of chloroplasts and mitochondria promotes ATP production and plant growth. Quantitative Plant Biology *2* (*e7*), 1-10. 10.1017/qpb.2021.7.

Waadt, R., Schmidt, L.K., Lohse, M., Hashimoto, K., Bock, R., and Kudla, J. (2008). Multicolor bimolecular fluorescence complementation reveals simultaneous formation of alternative CBL/CIPK complexes in planta. The Plant journal : for cell and molecular biology *56*, 505-516. 10.1111/j.1365-313X.2008.03612.x.

Wang, J., Tse, Y.C., Hinz, G., Robinson, D.G., and Jiang, L. (2012). Storage globulins pass through the Golgi apparatus and multivesicular bodies in the absence of dense vesicle formation during early stages of cotyledon development in mung bean. J Exp Bot *63*, 1367-1380. 10.1093/jxb/err366.

Wang, Q., Liu, Y., Soetandyo, N., Baek, K., Hegde, R., and Ye, Y. (2011). A ubiquitin ligase-associated chaperone holdase maintains polypeptides in soluble states for proteasome degradation. Mol Cell *42*, 758-770. 10.1016/j.molcel.2011.05.010.

Wu, X., Li, L., and Jiang, H. (2016). Doa1 targets ubiquitinated substrates for mitochondria-associated degradation. The Journal of cell biology *213*, 49-63. 10.1083/jcb.201510098.

Yoo, S.D., Cho, Y.H., and Sheen, J. (2007). Arabidopsis mesophyll protoplasts: a versatile cell system for transient gene expression analysis. Nat Protoc *2*, 1565-1572. 10.1038/nprot.2007.199.

Zhang, R., Guan, X., Law, Y.S., Sun, F., Chen, S., Wong, K.B., and Lim, B.L. (2016). AtPAP2 modulates the import of the small subunit of Rubisco into chloroplasts. Plant signaling & behavior *11*, e1239687.

Zhang, T., and Ye, Y. (2016). Doa1 is a MAD adaptor for Cdc48. The Journal of cell biology *213*, 7-9. 10.1083/jcb.201603078.

Zheng, J., Li, L., and Jiang, H. (2019). Molecular pathways of mitochondrial outer membrane protein degradation. Biochemical Society transactions *47*, 1437-1447. 10.1042/BST20190275.

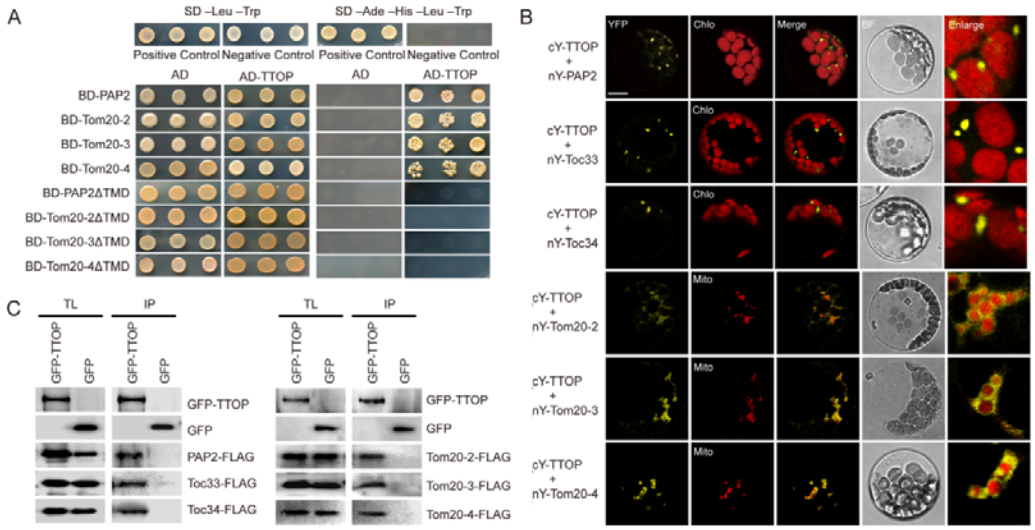

Figure 1. TTOP interacts with chloroplast and mitochondrial outer membrane tail-anchored proteins.

(A) Yeast two-hybrid analysis of the interaction between TTOP and tail-anchored (TA) proteins. Yeast from the Y2HGold strain were co-transformed with pairs of the indicated constructs encoding TTOP and full-length or TMD-truncated (ΔTMD) TA proteins. The TMD-truncated TA proteins include PAP2ΔTMD (a.a. 1-614 & 637-656), Tom20-2ΔTMD (a.a. 1-174 & 193-202), Tom20-3ΔTMD (a.a. 1-182 & 201-210), and Tom20-4ΔTMD (a.a. 1-161 & 179-187). Co-transformation of pGADT7-T and pGBKT7-53 constructs, or pGADT7-T and pGBKT7-lam constructs, into yeast was employed as the positive and negative controls, respectively. **(B)** Bimolecular fluorescence complementation (BiFC) analysis of the interaction between TTOP and TA proteins. Protoplasts were transiently co-transfected with the indicated pairs of constructs, which encode the fusion proteins carrying complementary N- or C-terminal YFP fragments (nY or cY), respectively. Reconstitution of YFP fluorescence in protoplasts was detected by confocal microscopy; representative images are shown. Chlo, chloroplast autofluorescence. Mito, mitochondria marked with MitoTracker. BF, brightfield. Scale bar, 10 μm. **(C)** Co-immunoprecipitation (co-IP) of TA proteins in **(B)** by TTOP from protoplast extracts. Protoplasts were transiently co-transfected with constructs encoding FLAG-tagged TA proteins and GFP-TTOP or GFP. Protoplast total lysis (TL) and immunoprecipitates (IP) eluted from GFP-Trap agarose were subjected to immunoblotting analysis with anti-GFP and anti-FLAG antibodies, respectively.

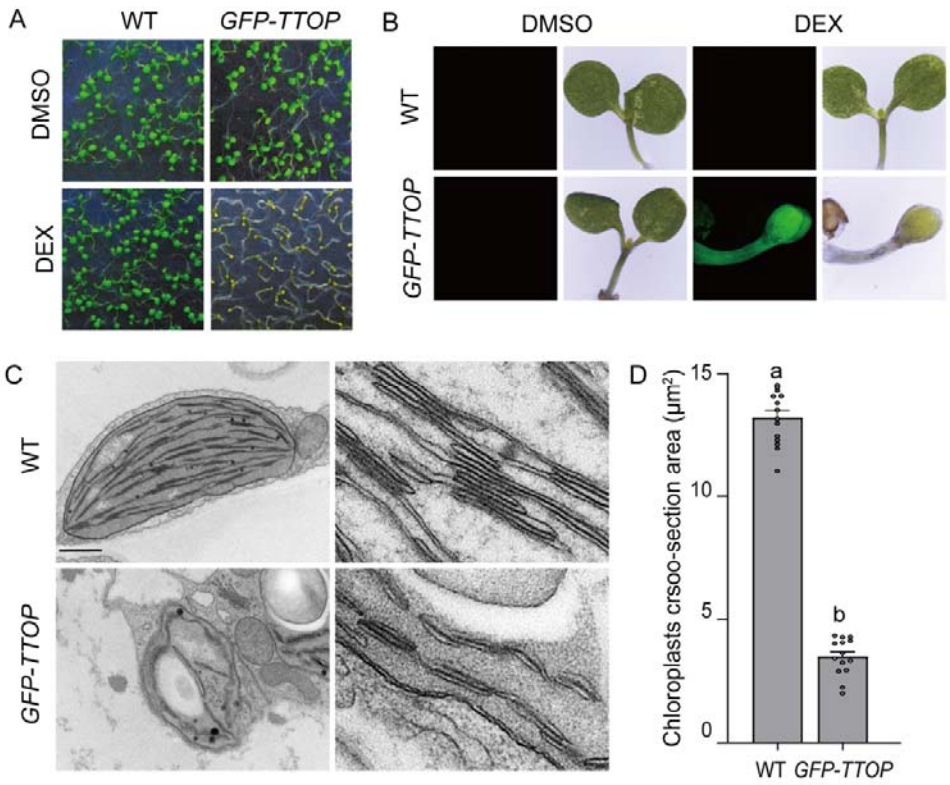

Figure 2. Overexpression of *TTOP* impairs chloroplast development.

(A and **B)** Col-0 **(**WT) and pTA7002-*GFP-TTOP* seedlings were germinated on half-strength MS medium containing 10 μM DEX or DMSO (mock control treatment lacking the inducer) for 7 days. Typical seedling phenotypes are shown in **(A)**. GFP fluorescence in seedlings was detected by CLSM; typical images are shown **(B)**. **(C)** TEM analysis of the ultrastructure of cotyledon chloroplasts in the DEX-treated seedlings in **(A)**. Left, representative TEM micrographs of chloroplasts; right, thylakoid development. (**D**) Micrographs were used to estimate the cross-sectional area (bar chart) occupied by chloroplasts with ImageJ software. Scale bar, 1.0 μm. Bars show means ± SEM (n = 20 chloroplasts). Different letters indicate significant differences as analyzed by Tukey's HSD test ($P < 0.05$).

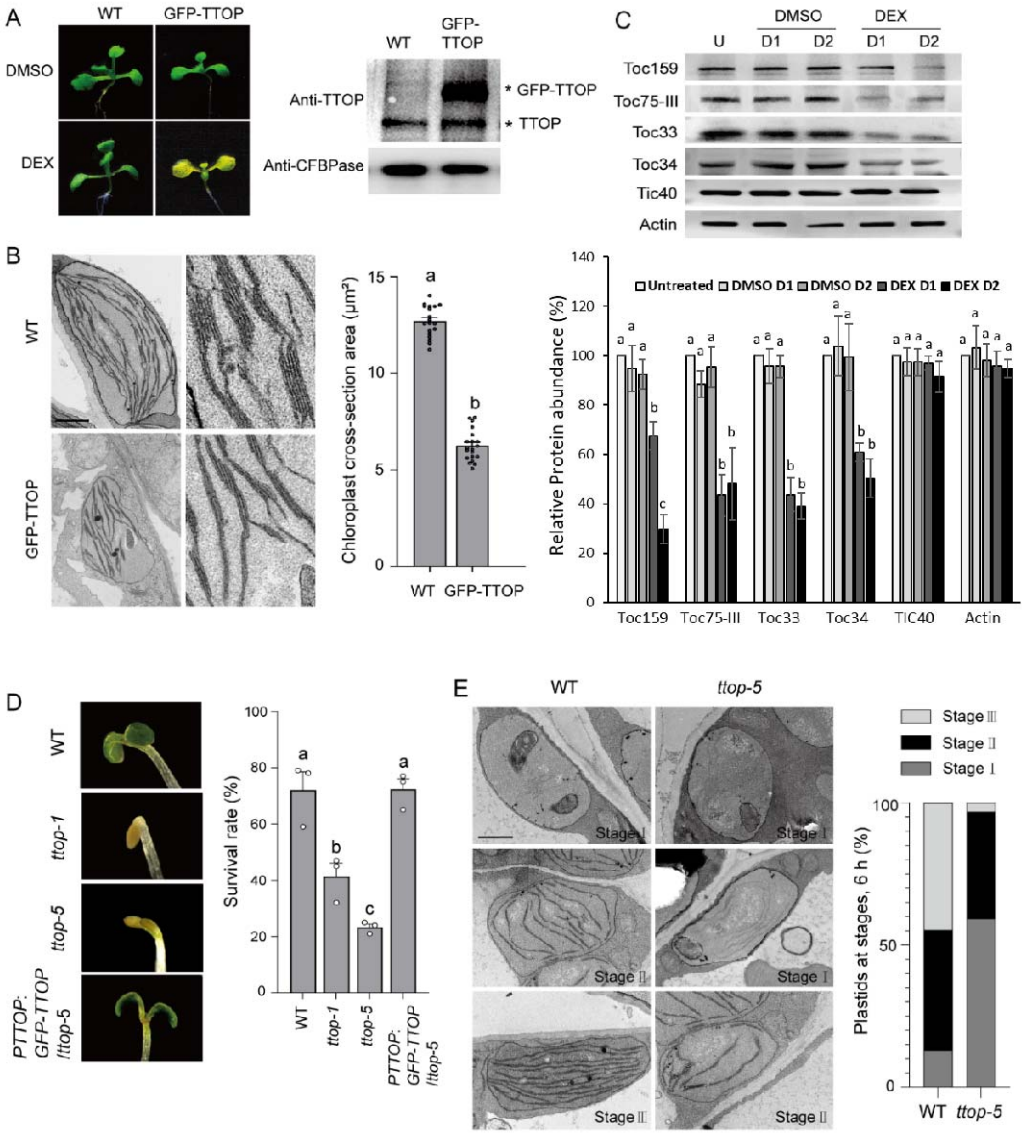

Figure 3. TTOP is essential for chloroplast biogenesis.

(A) Left, representative images of 5-day-old pTA7002-*GFP-TTOP* and wild-type Col-0 (WT) seedlings grown on half-strength MS medium after 3 days of growth on half-strength MS medium containing 10 µM DEX or DMSO. Right, DEX-induced accumulation of GFP-TTOP as revealed by immunoblotting with anti-TTOP antibodies. Anti-cFBPase was used as a loading control. **(B)** Transmission electron microscopy (TEM) analysis of the ultrastructure of chloroplasts in cotyledons of seedlings shown in **(A)**. Micrographs show chloroplasts (left) and thylakoid development (right). Scale bar, 1.0 µm. Bar chart shows estimates of chloroplast cross-sectional area determined from the micrographs using ImageJ software. **(C)** Immunoblotting analysis of TOC receptors in total leaf proteins from pTA7002-*GFP-TTOP* plants subjected to DEX or DMSO treatment for 1 (D1) or 2 days (D2), or untreated (U). Anti-actin was used as a loading control. Untreated samples = 100%. Band of untreated samples were normalized **(D)** Results of de-etiolation of *ttop-1*, *ttop-5*, *ttop-5 pTTOP:GFP-TTOP*, and WT seedlings, grown in the dark for 6 days, upon transfer into continuous light. After 2 days of illumination, cotyledon phenotypes

(left) and plant survival rates (right) were recorded. **(E)** Left, TEM analysis of the ultrastructure of cotyledon plastids in different genotypes after 0, 6, and 24 hours of illumination as in **(D)**. Right, proportions of plastids at each of three developmental stages estimated after 6 hours of illumination. Scale bar, 1.0 µm. Bars show means ± SEM (n = 20 chloroplasts in B, n = 3 experiments in C, $n \geq 30$ images in D, E). Different letters indicate significant differences as analyzed by Tukey's HSD test ($P < 0.05$).

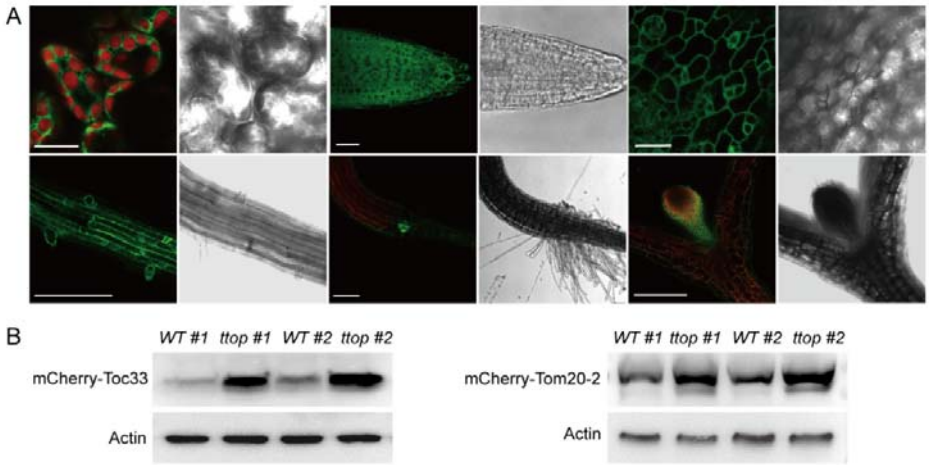

Figure 4. *In planta* expression patterns of TTOP.

(A) Analysis of tissue expression pattern and subcellular localization of TTOP in 6-day-old *ttop-5 pTTOP:GFP-TTOP* transgenic seedlings. Representative images of TTOP expression in different tissues are shown. TTOP accumulates in mesophyll cells, roots, and epidermis. TTOP has a cytosolic localization in different tissues. Red signal is chlorophyll autofluorescence. Brightfield images are shown for reference. Scale bar in the upper panels, 20 µm. Scale bar in the below panels, 200 µm. **(B)** Transgenic *ttop-5* mutant plants expressing mCherry-Toc33 or mCherry-Tom20-2 were crossed with WT plants to obtain WT plants expressing mCherry-Toc33 or mCherry-Tom20-2 for comparisons of mCherry-Toc33 or mCherry-Tom20-2 abundance between *ttop-5* and WT. Two individual homozygous lines for each *ttop* and WT genotype were tested by immunoblotting with anti-mCherry antibodies, which showed more mCherry-Toc33 and mCherry-Tom20-2 in the *ttop-5* mutant than the WT. Anti-actin was used as a loading control. Scale bar, 10 µm.

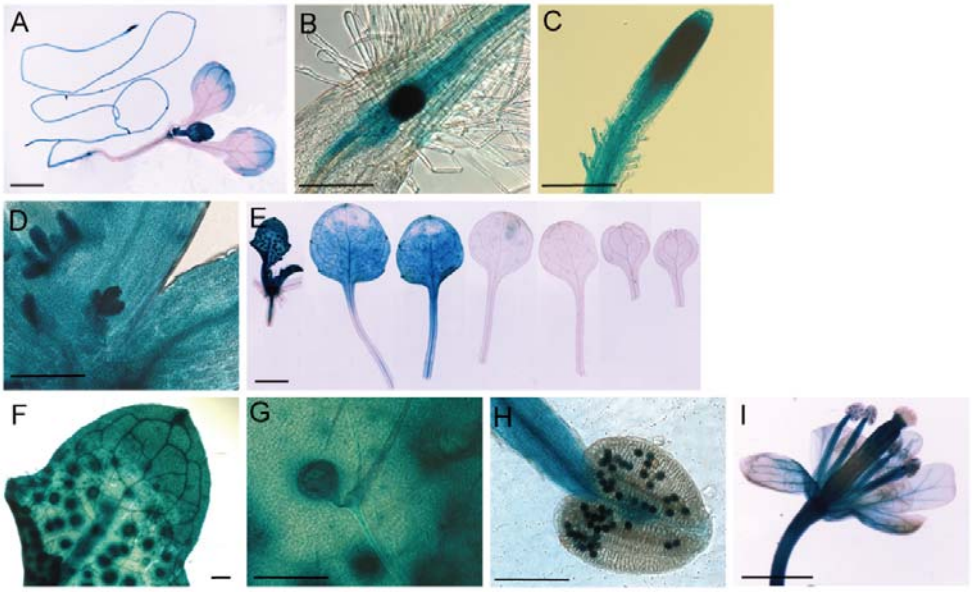

Figure 5. Expression patterns of *TTOP* at different developmental stages in *pTTOP:GUS* plants.

Ten-day-old seedlings **(A-D, F, G)** and 23-day-old plants **(E)** from *pTTOP:GUS* transgenic lines were used for GUS staining. Decreases in *TTOP* expression were observed in older tissues, particularly in leaves **(A, E)**, with high *TTOP* expression in newly grown leaves and no *TTOP* expression in fully grown leaves **(E;** left to right, youngest to oldest leaves**)**. High *TTOP* expression was also observed in meristematic regions, including the root-hypocotyl junction **(B)**, root meristem **(C)**, and shoot meristem **(D)**, and in other tissues such as trichome bases **(F** and **G)**, mature pollen **(H)**, and flowers **(I).** Scale bar in A, E, I, 2.0 mm. Scale bar in B, C, D, F, G, H, 200 µm.

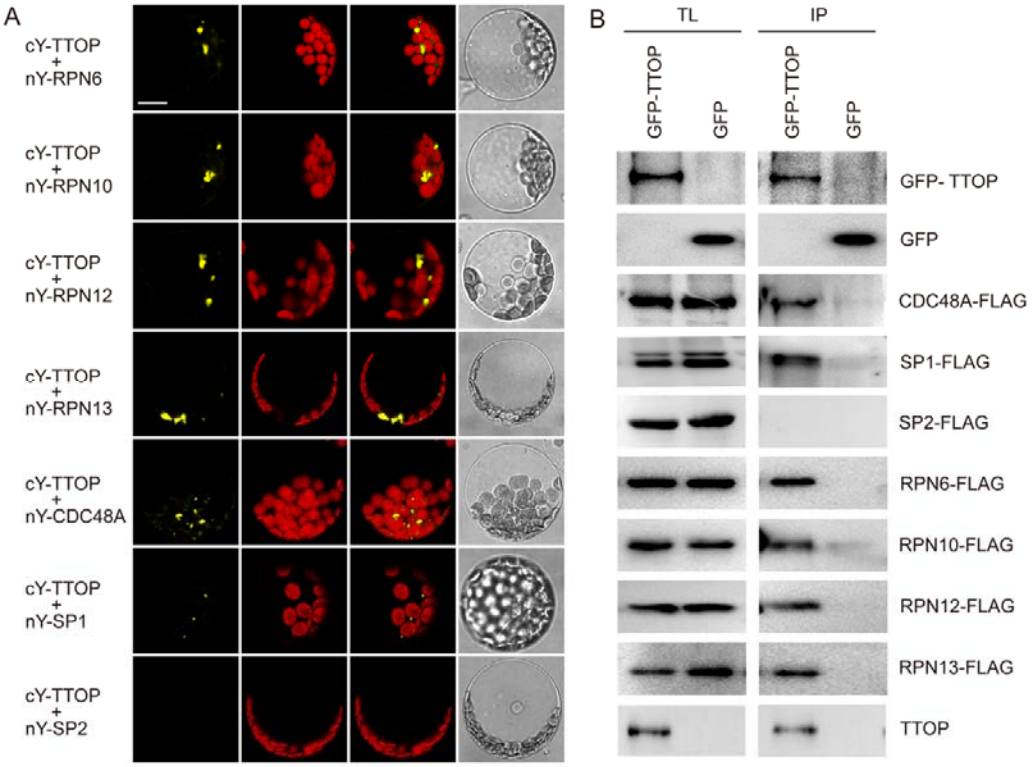

Figure 6. TTOP, chloroplast, and mitochondrial TA proteins, CDC48A, and 26S proteasome subunits form complexes *in vivo*.

(A) BiFC analysis of the interactions between TTOP and CDC48A, SP1, SP2, and 26S proteasome subunits. Protoplasts were co-transfected with the indicated pairs of constructs encoding fusion proteins with cY or nY. Reconstitution of YFP fluorescence in protoplasts was detected by confocal microscopy. Chlo, chloroplast autofluorescence. BF, brightfield. Scale bar, 10 µm. **(B)** Co-IP of CDC48A, SP1, or 26S subunits with TTOP from protoplast extracts. Protoplasts were co-transfected with constructs encoding GFP-TTOP or GFP and constructs encoding FLAG-tagged CDC48A, SP1, or 26S proteasome subunits. Protoplast extracts and elution proteins from GFP-Trap agarose were subjected to immunoblotting analysis with anti-GFP and anti-FLAG antibodies as described above.

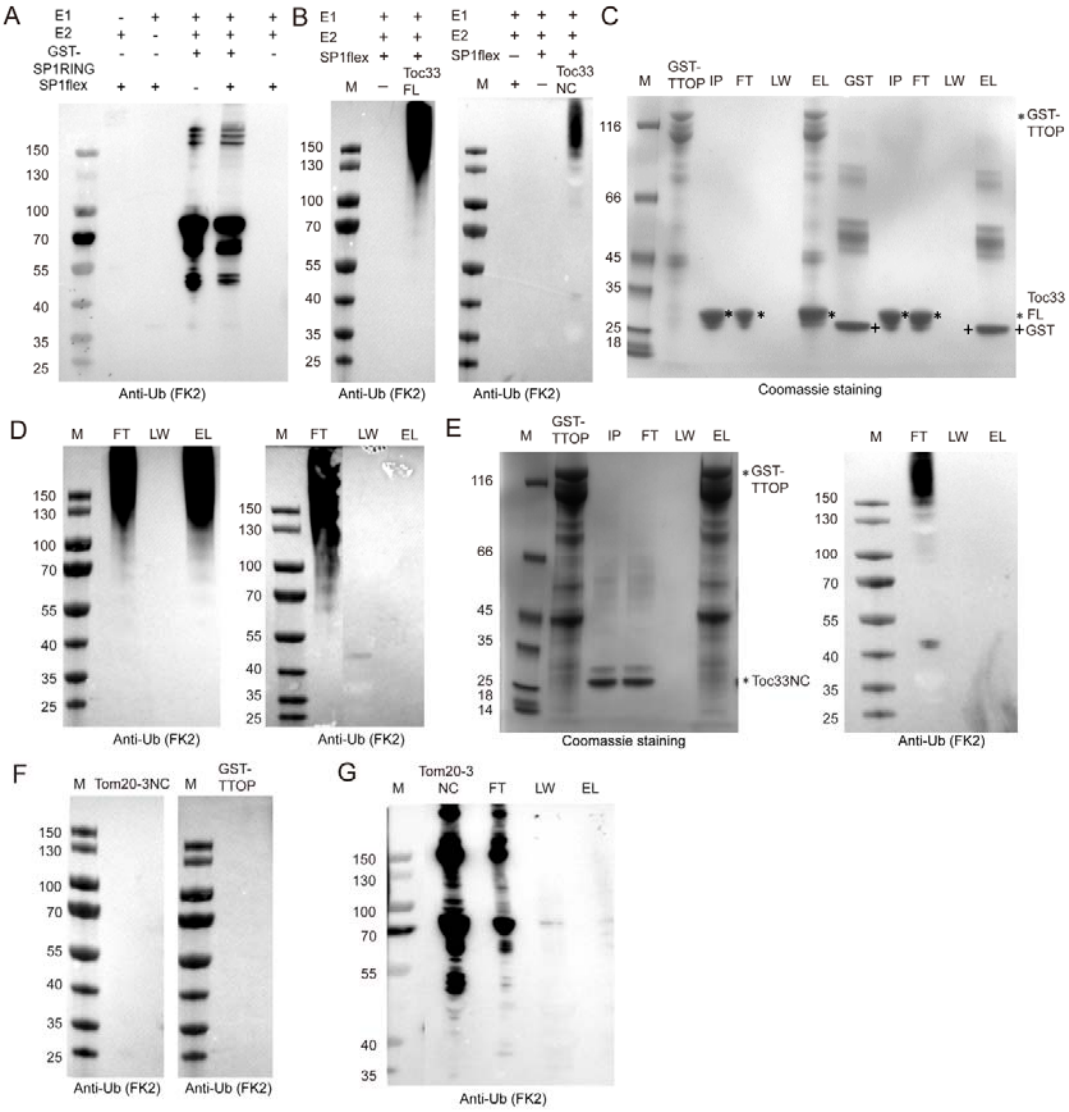

Figure 7. *In vitro* ubiquitination assays of tail-anchored receptors.

(A) Analysis of SP1 auto-ubiquitination activity *in vitro*. Recombinant SP1flex was purified and tested for self-ubiquitination activity. Western blotting was analyzed with anti-ubiquitin (FK2, MERCK). SP1flex cannot self-ubiquitinate (lane 6), but only GST-SP1RING (lane 4) and GST-SP1 RING plus SP1flex (lane 5) can self-ubiquitinate at the GST fusion protein. **(B)** *In vitro* ubiquitination of His-Toc33FL (a.a. 1-297) and His-Toc33NC (a.a. 1-266) by recombinant SP1flex. **(C)** GST-TTOP but not GST alone can pull down non-ubiquitinated His-Toc33FL. IP: input His-Toc33FL; FT: Flow through; LW; last washing fraction; EL: eluted proteins. (**D)** GST-TTOP (left panel) but not GST alone (right panel) can pull down ubiquitinated His-Toc33FL. (**E**) Neither non-ubiquitinated (left panel) nor ubiquitinated (right panel) His-Toc33NC was pulled down by GST-TTOP. **(F)** His-Tom20-3NC (left panel) and TTOP (right panel) were not ubiquitinated by recombinant SP1flex and UBC8 *in vitro*. (**G**) Ubiquitination of His-Tom20-3NC (a.a. 1-174) was facilitated by plant extracts (lane 1), but ubiquitinated His-Toc33NC cannot be pulled down by recombinant GST-TTOP (lane 4). Positions of molecular weight markers are indicated at left (sizes in kDa). M, protein marker.

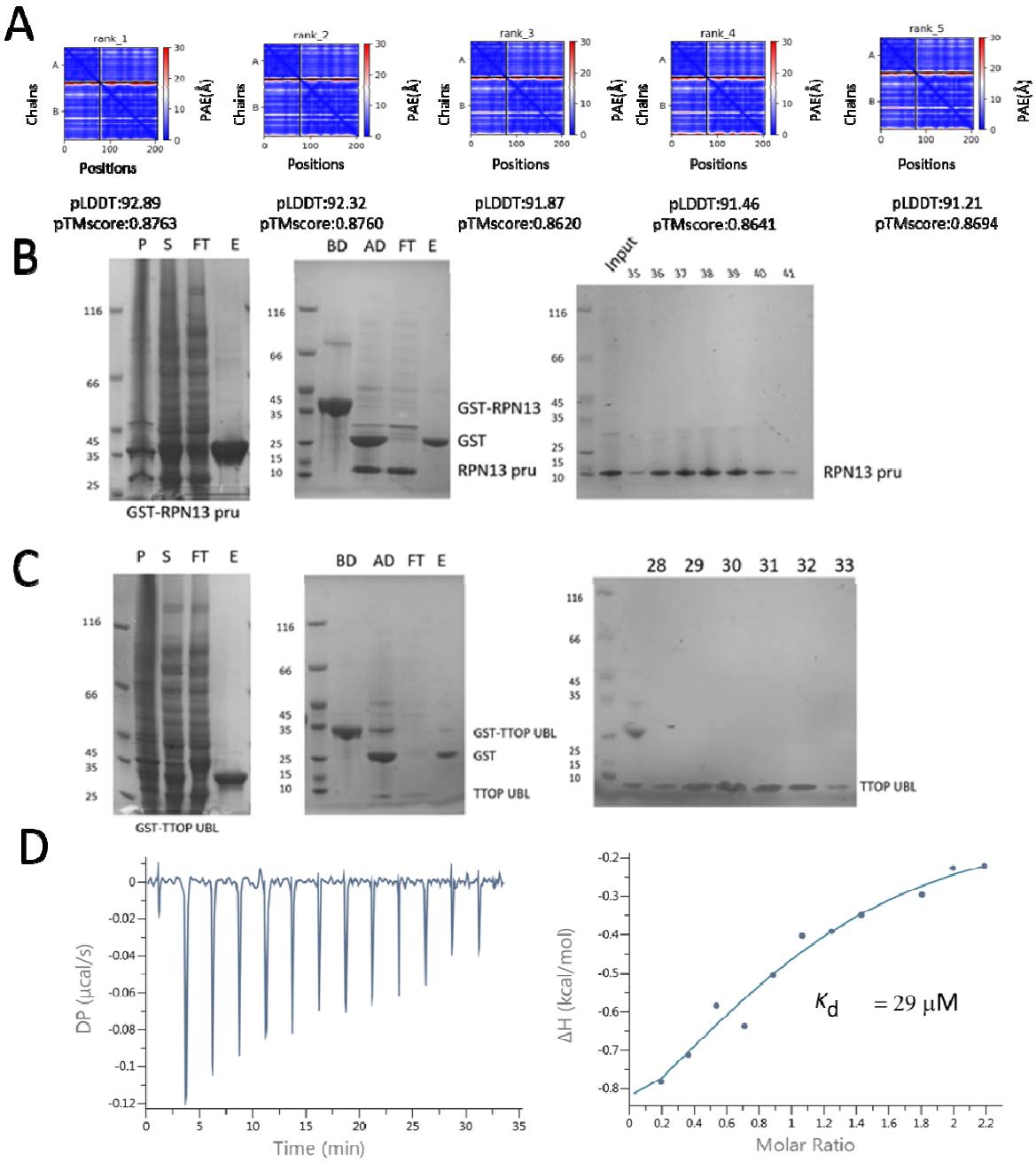

Figure 8. TTOP UBL domain could interact with RPN13 pru domain

By AlphaFold2 prediction, the high value of pLDDT and pTMscore and the low value of PAE showed that TTOP UBL could interact with the pru domain of RPN13. Recombinant TTOP UBL domain (B) and RPN13 pru domain (C) were purified by using GST fusion protein purification, on-column digestion and HiLoad 26/200 Superdex 200pg column. Isothermal titration calorimetry (ITC)-based measurement of the binding affinity between the UBL domain of TTOP and the pru domain of RPN13 at a 1:1 ratio is determined to be 29µM (D).

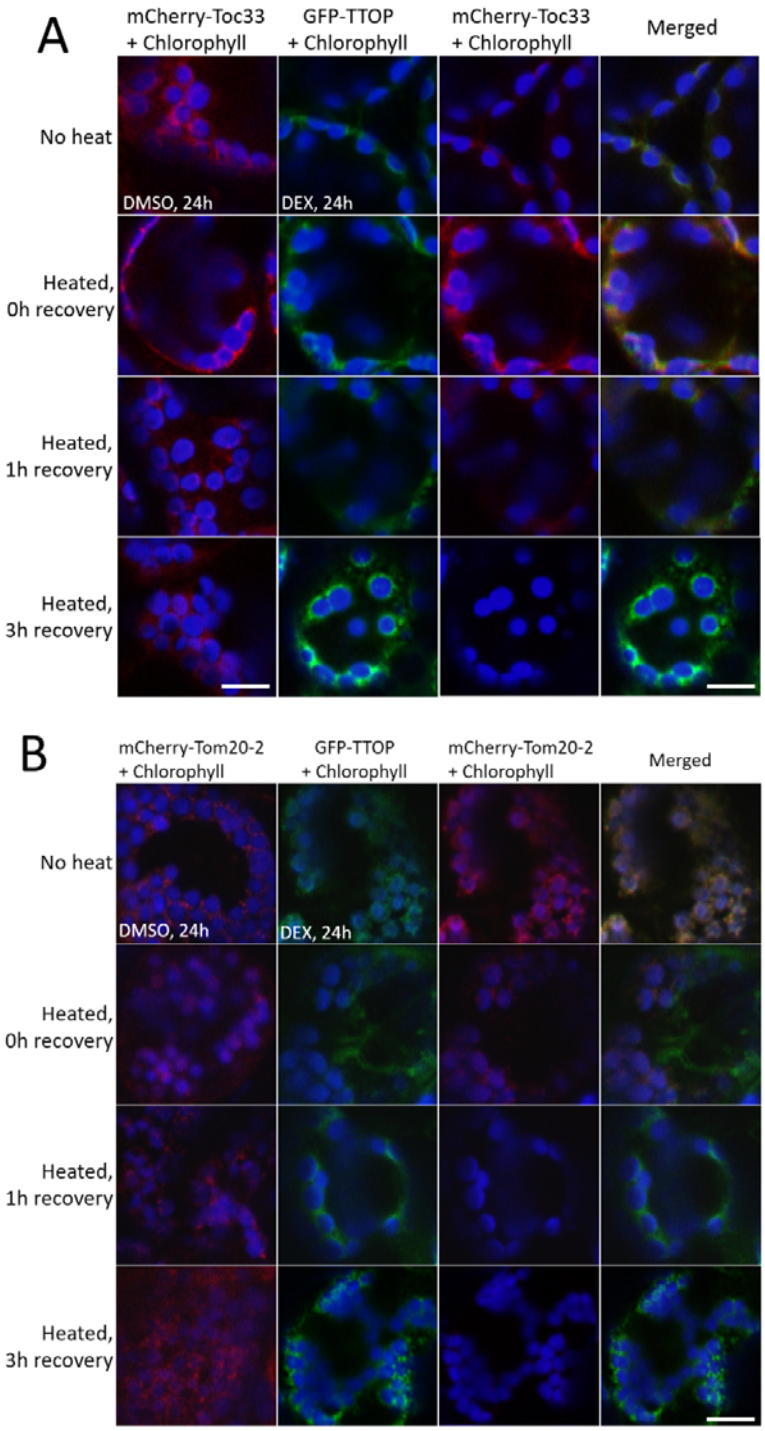

Figure 9. TTOP assists the degradation of Toc33 and Tom20-2 in planta.

The transgenic DEX-GFP-TTOP line was transformed with 35S: mCherry-Toc33 (A), and 35S: mCherry-Tom20-2 (B), respectively. 25μM DEX were sprayed to the seedlings at 8-day-old. Some seedlings were treated with DMSO as negative controls. After 24 h, seedlings were placed in 45°C incubator for 30 minutes (heated) or kept in R.T. (no heat). Heat-treated seedlings were allowed to recover in R.T. for 1 and 3 hours prior to the imaging. Green: GFP-PFP; Red: mCherry-Toc33; Blue: Chlorophyll auto-fluorescence. Bars = 20 μm.

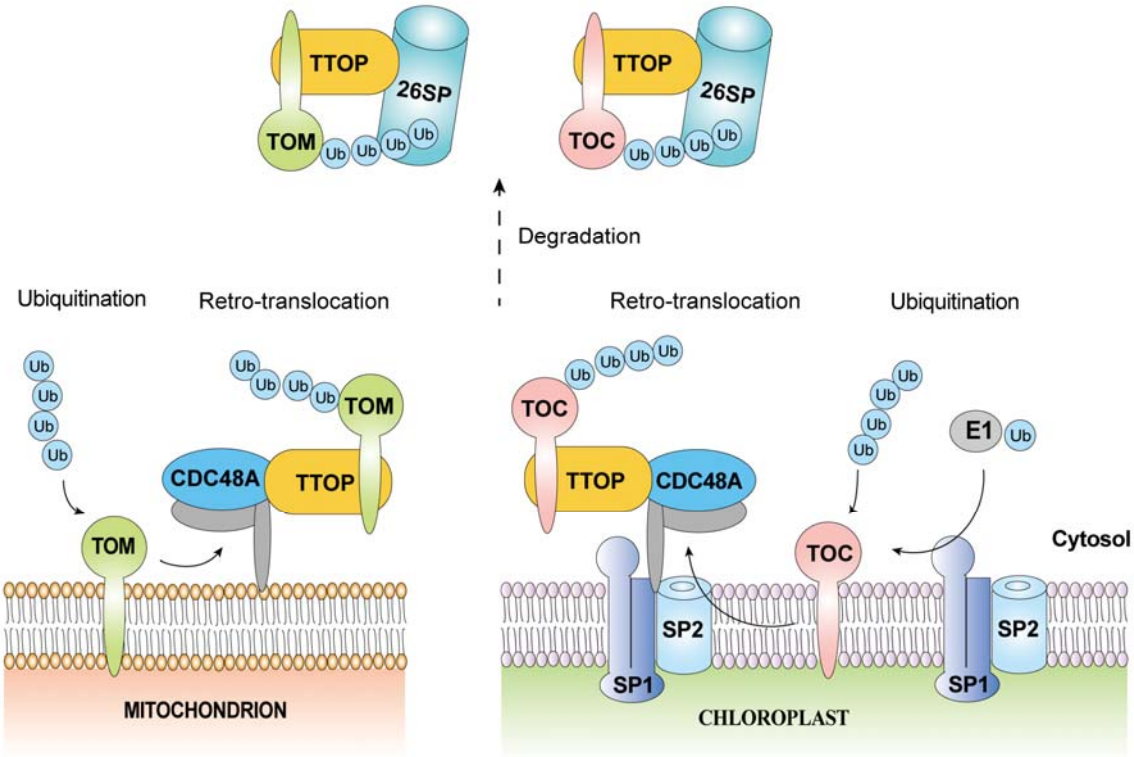

Figure 10. Proposed model for the role of TTOP in a converged pathway for the degradation of tail-anchored receptors of TOC and TOM translocases. In the CHLORAD proteolytic system, TOC components of the chloroplast protein import machinery are selectively removed by the SP1-SP2-CDC48A complex. After the TOC tail-anchored receptors are ubiquitinated by SP1, SP2 and CDC48A act as a conduit and a molecular motor, respectively, to mediate retrotranslocation of TOC complex out of the membrane. Similarly, tail-anchored receptors of TOM complexes are also ubiquitinated by an unknown E3 ubiquitin ligase and presumably pulled out from the outer envelope membrane (OEM) by CDC48A. Cytosolic TTOP then binds to the transmembrane domains (TMDs) of the retrotranslocated TOC/TOM receptors, masking the hydrophobic aggregation-prone TMDs and stabilizing ubquitinated TOC/TOM complexes in the cytosol. TTOP, via its interaction with RPN subunits of the 26S proteasome, then delivers the ubiquitinated receptors to the 26S proteasome for degradation. Association of TTOP with both CDC48A and RPN subunits of the 26S proteasome might allow efficient delivery of ubiquitinated receptors to the proteasome, thereby avoiding the risk of protein aggregation and enhancing degradation efficiency.

References

Aoyama, T., & Chua, N. H. (1997). A glucocorticoid-mediated transcriptional induction system in transgenic plants. *Plant Journal, 11*(3), 605-612. Retrieved from <Go to ISI>://WOS:A1997WT99100023

Bae, W., Lee, Y. J., Kim, D. H., Lee, J., Kim, S., Sohn, E. J., & Hwang, I. (2008). AKr2A-mediated import of chloroplast outer membrane proteins is essential for chloroplast biogenesis. *Nature Cell Biology, 10*(2), 220-U101. Retrieved from <Go to ISI>://WOS:000252897800018

Castresana, J. (2000). Selection of conserved blocks from multiple alignments for their use in phylogenetic analysis. *Molecular Biology and Evolution, 17*(4), 540-552. doi:10.1093/oxfordjournals.molbev.a026334

Chen, X., Randles, L., Shi, K., Tarasov, Sergey G., Aihara, H., & Walters, Kylie J. (2016). Structures of Rpn1 T1:Rad23 and hRpn13:hPLIC2 reveal distinct binding mechanisms between substrate receptors and shuttle factors of the proteasome. *Structure, 24*(8), 1257-1270. doi:10.1016/j.str.2016.05.018

Chio, U. S., Cho, H., & Shan, S. O. (2017). Mechanisms of tail-anchored membrane protein targeting and insertion. *Annu Rev Cell Dev Biol, 33*, 417-438. doi:10.1146/annurev-cellbio-100616-060839

Clough, S. J., & Bent, A. F. (1998). Floral dip: a simplified method for Agrobacterium-mediated transformation of Arabidopsis thaliana. *Plant J, 16*(6), 735-743.

Collins, G. A., & Goldberg, A. L. (2020). Proteins containing ubiquitin-like (Ubl) domains not only bind to 26S proteasomes but also induce their activation. *Proceedings of the National Academy of Sciences, 117*(9), 4664-4674. doi:doi:10.1073/pnas.1915534117

Duncan, O., Murcha, M. W., & Whelan, J. (2013). Unique components of the plant mitochondrial protein import apparatus. *Biochimica et Biophysica Acta (BBA) - Molecular Cell Research, 1833*(2), 304-313. doi:https://doi.org/10.1016/j.bbamcr.2012.02.015

Earley, K. W., Haag, J. R., Pontes, O., Opper, K., Juehne, T., Song, K., & Pikaard, C. S. (2006). Gateway-compatible vectors for plant functional genomics and proteomics. *The Plant Journal, 45*(4), 616-629. doi:10.1111/j.1365-313X.2005.02617.x

Eisele, M. R., Reed, R. G., Rudack, T., Schweitzer, A., Beck, F., Nagy, I., . . . Sakata, E. (2018). Expanded coverage of the 26S proteasome conformational landscape reveals mechanisms of peptidase gating. *Cell Reports, 24*(5), 1301-1315.e1305. doi:10.1016/j.celrep.2018.07.004

Eubel, H., Braun, H. P., & Millar, A. H. (2005). Blue-native PAGE in plants: a tool in analysis of protein-protein interactions. *Plant Methods, 1*(1), 11. doi:10.1186/1746-4811-1-11

Fellerer, C., Schweiger, R., Schongruber, K., Soll, J., & Schwenkert, S. (2011). Cytosolic HSP90 cochaperones HOP and FKBP interact with freshly synthesized chloroplast preproteins of Arabidopsis. *Mol Plant, 4*(6), 1133-1145. doi:10.1093/mp/ssr037

Fernández-Bautista, N., Fernández-Calvino, L., Muñoz, A., & Castellano, M. M. (2017). HOP3, a member of the HOP family in Arabidopsis, interacts with BiP and plays a major role in the ER stress response. *Plant Cell Environ, 40*(8), 1341-1355. doi:https://doi.org/10.1111/pce.12927

Gao, C., Yu, C. K., Qu, S., San, M. W., Li, K. Y., Lo, S. W., & Jiang, L. (2012). The Golgi-localized Arabidopsis endomembrane protein12 contains both endoplasmic reticulum export and Golgi retention signals at its C terminus. *Plant Cell, 24*(5), 2086-2104. doi:10.1105/tpc.112.096057

Ghifari, A. S., Gill-Hille, M., & Murcha, M. W. (2018). Plant mitochondrial protein import: the ins and outs. *Biochemical Journal, 475*, 2191-2208. Retrieved from <Go to

ISI>://WOS:000441394800005
Goodstein, D. M., Shu, S. Q., Howson, R., Neupane, R., Hayes, R. D., Fazo, J., . . . Rokhsar, D. S. (2012). Phytozome: a comparative platform for green plant genomics. *Nucleic Acids Research, 40*(D1), D1178-D1186. doi:10.1093/nar/gkr944
Guna, A., & Hegde, R. S. (2018). Transmembrane domain recognition during membrane Protein biogenesis and quality control. *Current Biology, 28*(8), R498-R511. doi:https://doi.org/10.1016/j.cub.2018.02.004
Hessa, T., Sharma, A., Mariappan, M., Eshleman, H. D., Gutierrez, E., & Hegde, R. S. (2011). Protein targeting and degradation are coupled for elimination of mislocalized proteins. *Nature, 475*(7356), 394-397. doi:10.1038/nature10181
Husnjak, K., Elsasser, S., Zhang, N., Chen, X., Randles, L., Shi, Y., . . . Dikic, I. (2008). Proteasome subunit Rpn13 is a novel ubiquitin receptor. *Nature, 453*(7194), 481-488. doi:10.1038/nature06926
Jefferson, R. A., Kavanagh, T. A., & Bevan, M. W. (1987). GUS fusions: beta-glucuronidase as a sensitive and versatile gene fusion marker in higher plants. *Embo j, 6*(13), 3901-3907.
Jumper, J., Evans, R., Pritzel, A., Green, T., Figurnov, M., Ronneberger, O., . . . Hassabis, D. (2021). Highly accurate protein structure prediction with AlphaFold. *Nature, 596*(7873), 583-589. doi:10.1038/s41586-021-03819-2
Katoh, K., & Standley, D. M. (2013). MAFFT Multiple Sequence Alignment Software Version 7: Improvements in Performance and Usability. *Molecular Biology and Evolution, 30*(4), 772-780. doi:10.1093/molbev/mst010
Kim, J., Na, Y. J., Park, S. J., Baek, S. H., & Kim, D. H. (2019). Biogenesis of chloroplast outer envelope membrane proteins. *Plant Cell Rep, 38*(7), 783-792. doi:10.1007/s00299-019-02381-6
Krysztofinska, E. M., Martínez-Lumbreras, S., Thapaliya, A., Evans, N. J., High, S., & Isaacson, R. L. (2016). Structural and functional insights into the E3 ligase, RNF126. *Scientific Reports, 6*(1), 26433. doi:10.1038/srep26433
Law, Y. S., Zhang, R., Guan, X., Cheng, S., Sun, F., Duncan, O., . . . Lim, B. L. (2015). Phosphorylation and dephosphorylation of the presequence of pMORF3 during import into mitochondria from *Arabidopsis thaliana*. *Plant physiology, 169,* 1-12. doi:10.1104/pp.15.01115
Letunic, I., & Bork, P. (2016). Interactive tree of life (iTOL) v3: an online tool for the display and annotation of phylogenetic and other trees. *Nucleic Acids Research, 44*(W1), W242-W245. doi:10.1093/nar/gkw290
Ling, Q., Broad, W., Trösch, R., Töpel, M., Demiral Sert, T., Lymperopoulos, P., . . . Jarvis, R. P. (2019). Ubiquitin-dependent chloroplast-associated protein degradation in plants. *Science, 363*(6429). doi:10.1126/science.aav4467
Ling, Q., Huang, W., Baldwin, A., & Jarvis, P. (2012). Chloroplast biogenesis is regulated by direct action of the ubiquitin-proteasome system. *Science, 338*(6107), 655-659. doi:10.1126/science.1225053
Ling, Q., & Jarvis, P. (2015). Regulation of Chloroplast Protein Import by the Ubiquitin E3 Ligase SP1 Is Important for Stress Tolerance in Plants. *Curr Biol, 25*(19), 2527-2534. doi:10.1016/j.cub.2015.08.015
Ling, Q. H., Broad, W., Trosch, R., Topel, M., Sert, T. D., Lymperopoulos, P., . . . Jarvis, R. P. (2019). Ubiquitin-dependent chloroplast-associated protein degradation in plants. *Science, 363*, aav4467. Retrieved from <Go to ISI>://WOS:000459387100035
Livak, K. J., & Schmittgen, T. D. (2001). Analysis of relative gene expression data using real-time

quantitative PCR and the 2(-Delta Delta C(T)) Method. *Methods*(25), 402–408. doi:https://doi.org/10.1006/
meth.2001.1262
Mariani, V., Biasini, M., Barbato, A., & Schwede, T. (2013). lDDT: a local superposition-free score for comparing protein structures and models using distance difference tests. *Bioinformatics (Oxford, England), 29*(21), 2722-2728. doi:10.1093/bioinformatics/btt473
Martensson, C. U., Priesnitz, C., Song, J., Ellenrieder, L., Doan, K. N., Boos, F., . . . Becker, T. (2019). Mitochondrial protein translocation-associated degradation. *Nature, 569*(7758), 679-683. doi:10.1038/s41586-019-1227-y
Mirdita, M., Ovchinnikov, S., & Steinegger, M. (2021). ColabFold - Making protein folding accessible to all. *bioRxiv*, 2021.2008.2015.456425. doi:10.1101/2021.08.15.456425
Mock, J.-Y., Chartron, J. W., Zaslaver, M. a., Xu, Y., Ye, Y., & Clemons, W. M. (2015). Bag6 complex contains a minimal tail-anchor-targeting module and a mock BAG domain. *Proceedings of the National Academy of Sciences, 112*(1), 106-111. doi:doi:10.1073/pnas.1402745112
Mullally, J. E., Chernova, T., & Wilkinson, K. D. (2006). Doa1 is a Cdc48 adapter that possesses a novel ubiquitin binding domain. *Mol Cell Biol, 26*(3), 822-830. doi:10.1128/MCB.26.3.822-830.2006
Nakai, M. (2018). New Perspectives on Chloroplast Protein Import. *Plant and Cell Physiology, 59*(6), 1111-1119. doi:10.1093/pcp/pcy083
Nguyen, L. T., Schmidt, H. A., von Haeseler, A., & Minh, B. Q. (2015). IQ-TREE: A Fast and Effective Stochastic Algorithm for Estimating Maximum-Likelihood Phylogenies. *Molecular Biology and Evolution, 32*(1), 268-274. doi:10.1093/molbev/msu300
Pan, R., Satkovich, J., & Hu, J. (2016). E3 ubiquitin ligase SP1 regulates peroxisome biogenesis in Arabidopsis. *Proc Natl Acad Sci U S A, 113*(46), E7307-E7316. doi:10.1073/pnas.1613530113
Pan, R. H., & Hu, J. P. (2018). The Arabidopsis E3 Ubiquitin Ligase SP1 Targets to Chloroplasts, Peroxisomes, and Mitochondria. *Plant Physiology, 176*(1), 480-482. Retrieved from <Go to ISI>://WOS:000419675300037
Panigrahi, R., Whelan, J., & Vrielink, A. (2014). Exploring ligand recognition, selectivity and dynamics of TPR domains of chloroplast Toc64 and mitochondria Om64 from *Arabidopsis thaliana*. *J Mol Recognit, 27*(6), 402-414. doi:10.1002/jmr.2360
Park, C.-J., Canlas, P. E., & Ronald, P. C. (2012). Establishment of glucocorticoid-mediated transcriptional induction of the rice XA21 pattern recognition receptor. *Journal of Plant Biology, 55*(1), 43-49. doi:10.1007/s12374-011-9188-1
Schneider, C. A., Rasband, W. S., & Eliceiri, K. W. (2012). NIH Image to ImageJ: 25 years of image analysis. *Nat Methods, 9*(7), 671-675. doi:10.1038/nmeth.2089
Schuberth, C., & Buchberger, A. (2005). Membrane-bound Ubx2 recruits Cdc48 to ubiquitin ligases and their substrates to ensure efficient ER-associated protein degradation. *Nature Cell Biology, 7*(10), 999-1006. doi:10.1038/ncb1299
Shao, S., Rodrigo-Brenni, M. C., Kivlen, M. H., & Hegde, R. S. (2017). Mechanistic basis for a molecular triage reaction. *Science, 355*(6322), 298-302. doi:doi:10.1126/science.aah6130
Shi, L.-X., & Theg, S. M. (2013). The chloroplast protein import system: From algae to trees. *Biochimica et Biophysica Acta (BBA) - Molecular Cell Research, 1833*(2), 314-331. doi:https://doi.org/10.1016/j.bbamcr.2012.10.002
Shi, Y., Chen, X., Elsasser, S., Stocks, B. B., Tian, G., Lee, B.-H., . . . Walters, K. J. (2016). Rpn1 provides adjacent receptor sites for substrate binding and deubiquitination by the proteasome.

Science, 351(6275), aad9421. doi:doi:10.1126/science.aad9421

Sommer, M., Rudolf, M., Tillmann, B., Tripp, J., Sommer, M. S., & Schleiff, E. (2013). Toc33 and Toc64-III cooperate in precursor protein import into the chloroplasts of *Arabidopsis thaliana*. *Plant Cell Environ, 36*(5), 970-983. doi:10.1111/pce.12030

Sun, F., Carrie, C., Law, S., Murcha, M. W., Zhang, R., Law, Y. S., . . . Lim, B. L. (2012). AtPAP2 is a tail-anchored protein in the outer membrane of chloroplasts and mitochondria. *Plant Signal Behav, 7*(8), 927-932. doi:10.4161/psb.20769

Tsaban, T., Varga, J. K., Avraham, O., Ben-Aharon, Z., Khramushin, A., & Schueler-Furman, O. (2022). Harnessing protein folding neural networks for peptide–protein docking. *Nature communications, 13*(1), 176. doi:10.1038/s41467-021-27838-9

Tsutsui, H., & Higashiyama, T. (2017). pKAMA-ITACHI vectors for highly efficient CRISPR/Cas9-mediated gene knockout in *Arabidopsis thaliana*. *Plant Cell Physiol, 58*(1), 46-56. doi:10.1093/pcp/pcw191

VanderLinden, R. T., Hemmis, C. W., Yao, T., Robinson, H., & Hill, C. P. (2017). Structure and energetics of pairwise interactions between proteasome subunits RPN2, RPN13, and ubiquitin clarify a substrate recruitment mechanism. *Journal of Biological Chemistry, 292*(23), 9493-9504. doi:10.1074/jbc.M117.785287

Voon, C. P., Law, Y. S., Guan, X., Lim, S. L., Xu, Z., Chu, W. T., . . . Lim, B. L. (2021). Modulating the activities of chloroplasts and mitochondria promotes ATP production and plant growth. *Quantitative Plant Biology, 2*, 1-10. doi:10.1017/qpb.2021.7

Waadt, R., Schmidt, L. K., Lohse, M., Hashimoto, K., Bock, R., & Kudla, J. (2008). Multicolor bimolecular fluorescence complementation reveals simultaneous formation of alternative CBL/CIPK complexes in planta. *Plant J, 56*(3), 505-516. doi:10.1111/j.1365-313X.2008.03612.x

Wang, J., Tse, Y. C., Hinz, G., Robinson, D. G., & Jiang, L. (2012). Storage globulins pass through the Golgi apparatus and multivesicular bodies in the absence of dense vesicle formation during early stages of cotyledon development in mung bean. *J Exp Bot, 63*(3), 1367-1380. doi:10.1093/jxb/err366

Wang, Q., Liu, Y., Soetandyo, N., Baek, K., Hegde, R., & Ye, Y. (2011). A ubiquitin ligase-associated chaperone holdase maintains polypeptides in soluble states for proteasome degradation. *Molecular Cell, 42*(6), 758-770. doi:10.1016/j.molcel.2011.05.010

Wu, X., Li, L., & Jiang, H. (2016). Doa1 targets ubiquitinated substrates for mitochondria-associated degradation. *J Cell Biol, 213*(1), 49-63. doi:10.1083/jcb.201510098

Yoo, S. D., Cho, Y. H., & Sheen, J. (2007). Arabidopsis mesophyll protoplasts: a versatile cell system for transient gene expression analysis. *Nat Protoc, 2*(7), 1565-1572. doi:10.1038/nprot.2007.199

Zhang, R., Guan, X., Law, Y. S., Sun, F., Chen, S., Wong, K. B., & Lim, B. L. (2016). AtPAP2 modulates the import of the small subunit of Rubisco into chloroplasts. *Plant Signal Behav, 11*(10), e1239687.

Zhang, T., & Ye, Y. (2016). Doa1 is a MAD adaptor for Cdc48. *J Cell Biol, 213*(1), 7-9. doi:10.1083/jcb.201603078

Zheng, J., Li, L., & Jiang, H. (2019). Molecular pathways of mitochondrial outer membrane protein degradation. *Biochem Soc Trans, 47*(5), 1437-1447. doi:10.1042/BST20190275

Supplementary Materials for

A converged ubiquitin-proteasome pathway for the degradation of TOC and TOM tail-anchored receptors

Meijing Yang*, Shuai Chen*, Shey-Li Lim, Jia Yi Zhong, Koon Chuen Chan, Kam-Bo Wong, Junqi Wang, and Boon Leong Lim†

***These authors contributed equally to this work.**

†Corresponding authors. E-mail: bllim@hku.hk

This PDF file includes:

Supplemental Figures 1-16

Table S1 to S3

Supplementary figures

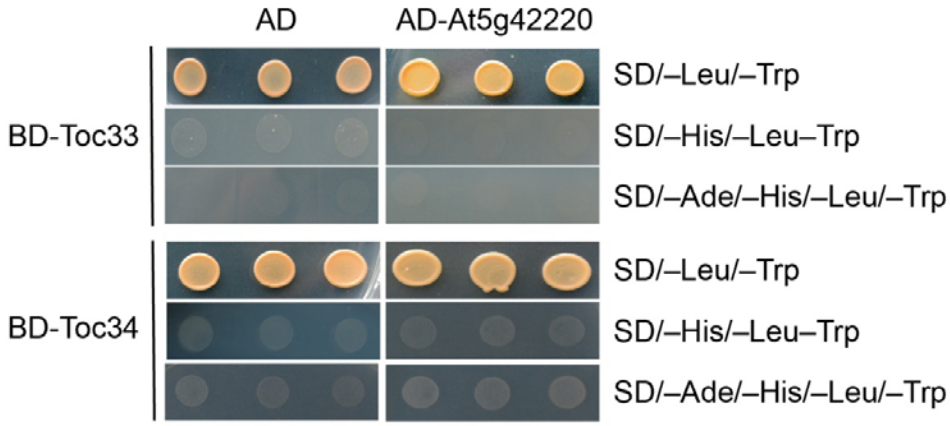

Fig. S1. Yeast two-hybrid analysis of the interaction between TTOP and Toc33/Toc34. Yeast was co-transformed with the indicated pairs of constructs. The growth of yeast on selective plates is shown. Growth of yeast on SD –Leu –Trp medium confirms the presence of the pair of vectors. Failure of yeast growth on SD –His –Leu –Trp and SD –Ade –His –Leu –Trp medium indicates the absence of protein–protein interaction between TTOP and Toc33/Toc34 in yeast cells.

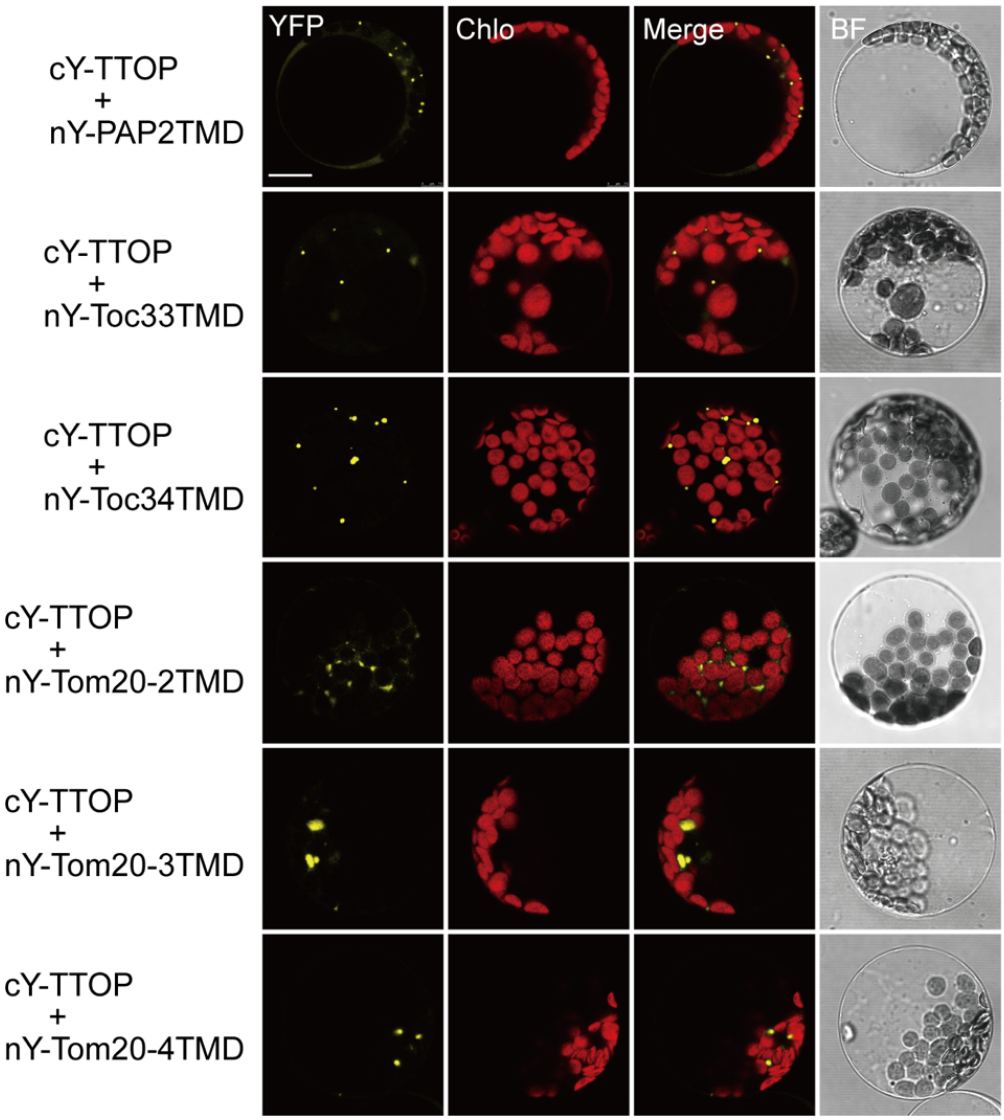

Fig. S2. BiFC analysis of the interaction between TTOP and the TMD motifs of TA proteins. Protoplasts were co-transfected with the indicated pairs of constructs, which encode the fusion proteins carrying nY or cY, respectively. The TMD motifs include PAP2TMD (a.a. 615-636), Toc33TMD (a.a. 267-282), Toc34TMD (a.a. 269-287), Tom20-2TMD (a.a. 175-192), Tom20-3TMD (a.a. 183-200) and Tom20-4TMD (a.a. 162-178). Reconstitution of YFP fluorescence in protoplasts was detected by CLSM, and representative confocal images are shown. Chlo, chloroplast auto-fluorescence. BF, brightfield. Scale bar, 10 μm.

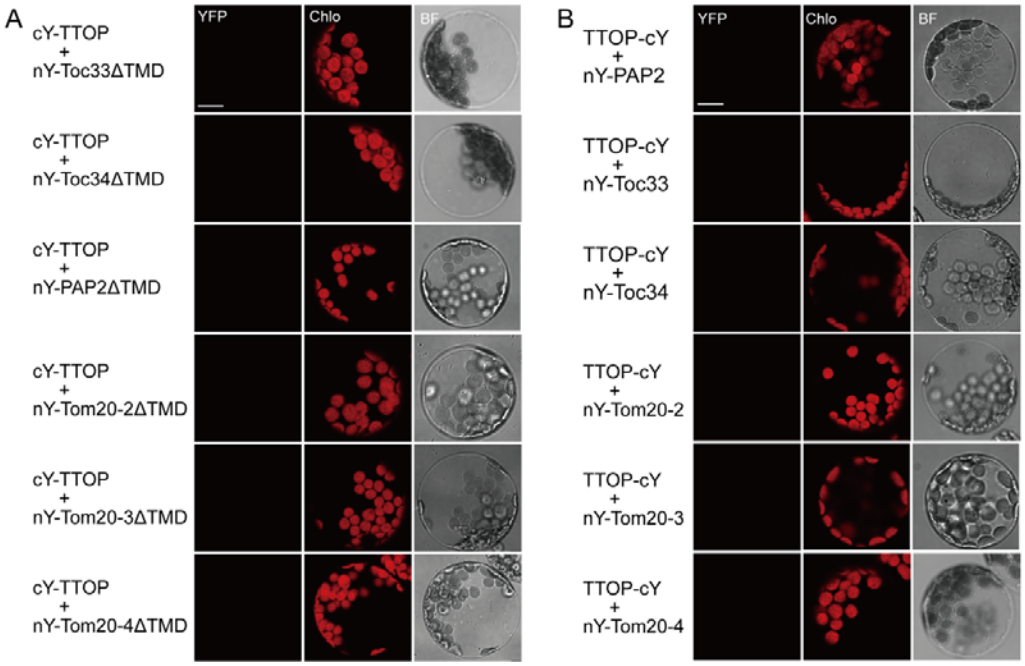

Fig. S3. No interaction is detected between TTOP and TA proteins without TMD motifs. Protoplasts were co-transfected with the indicated pairs of constructs encoding the fusion proteins carrying nY or cY, respectively. The TMD-truncated TA proteins include Toc33ΔTMD (a.a. 1-266 & 283-297), Toc34ΔTMD (a.a. 1-268 & 288-313), PAP2ΔTMD (a.a. 1-614 & 637-656), Tom20-2ΔTMD (a.a. 1-174 & 193-202), Tom20-3ΔTMD (a.a. 1-182 & 201-210), and Tom20-4ΔTMD (a.a. 1-161 & 179-187). Reconstitution of YFP fluorescence in protoplasts was analyzed by CLSM, and representative confocal images are shown. No interaction was detected when the TMD motifs of the TA proteins were truncated **(A)** or when cY was fused to the C terminus of TTOP **(B)**. Chlo, chloroplast auto-fluorescence. BF, brightfield. Scale bar, 10 µm.

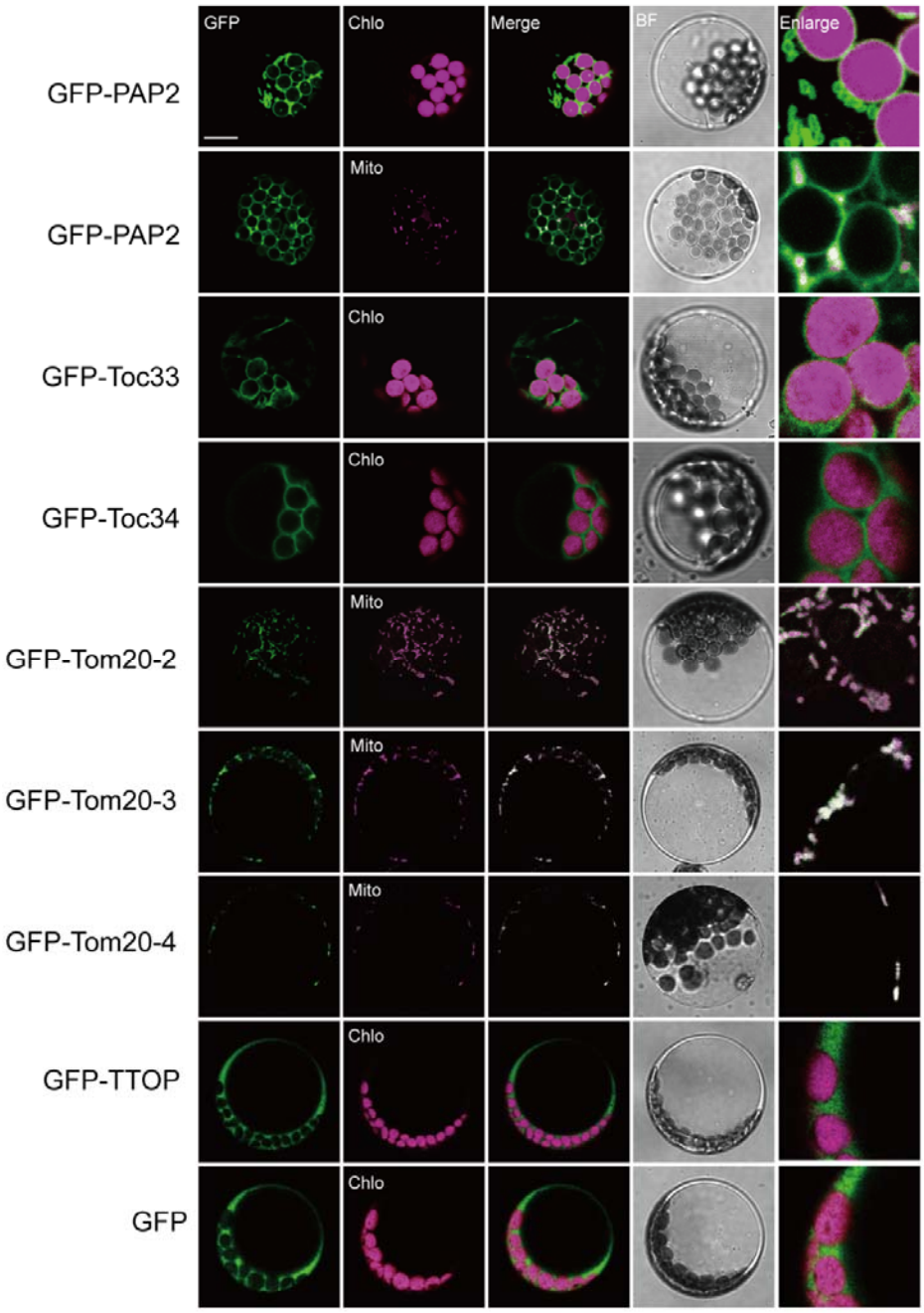

Fig. S4. Subcellular localization of TTOP and chloroplast and mitochondrial outer membrane TA proteins in protoplasts.

Protoplasts were transfected with the indicated constructs encoding fusion proteins carrying a GFP protein at their N terminus. The GFP fluorescence in protoplasts was analyzed by CLSM, and representative confocal images are shown. A construct encoding free GFP was also transfected in protoplasts as a positive control for GFP fluorescence and as a negative control for organellar localization. Chlo, chloroplast auto-fluorescence; Mito, mitochondria marked with MitoTracker. BF, brightfield. Scale bar, 10 μm.

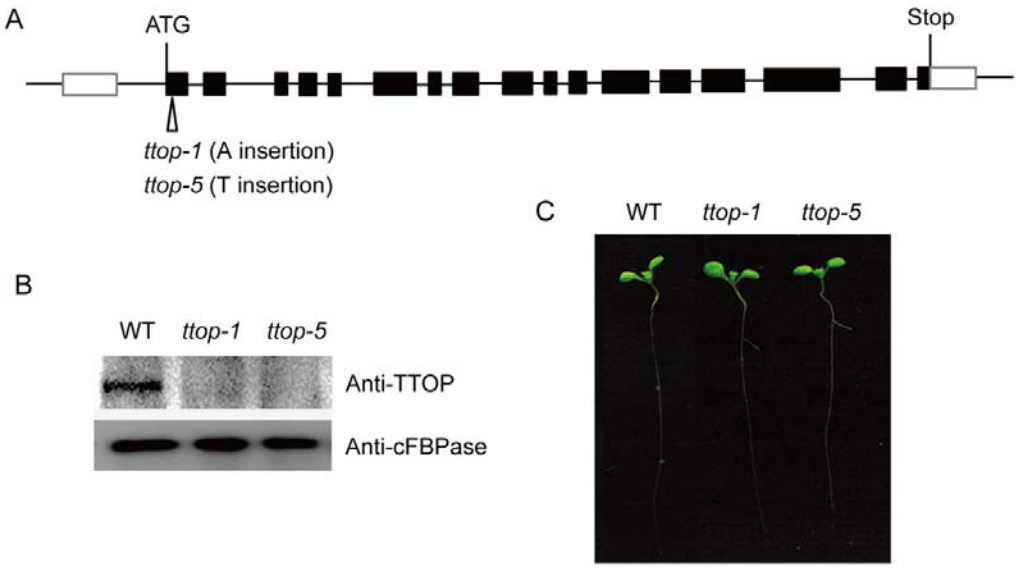

Fig. S5. Identification and growth phenotype of *ttop* mutant seedlings.
(A) Schematic representation of the *TTOP* (At5g42220) locus, annotated with the positions of the *ttop-1* and *ttop-5* mutations. ttop-1 and ttop-5 has a single-base insertion of an A or T in the 43 bp of the first TTOP exon, respectively. Black boxes, exons; white boxes, untranslated regions; black lines, introns. **(B)** Immunoblotting analysis of TTOP abundance in the wild-type Col-0 (WT) and *ttop1-1* and *ttop1-5* seedlings with the rabbit anti-TTOP antibody developed in this study. Anti-cFBPase was used as a loading control. **(C)** Representative growth phenotypes of 8-day-old WT, *ttop1-1*, and *ttop1-5* seedlings grow under normal conditions.

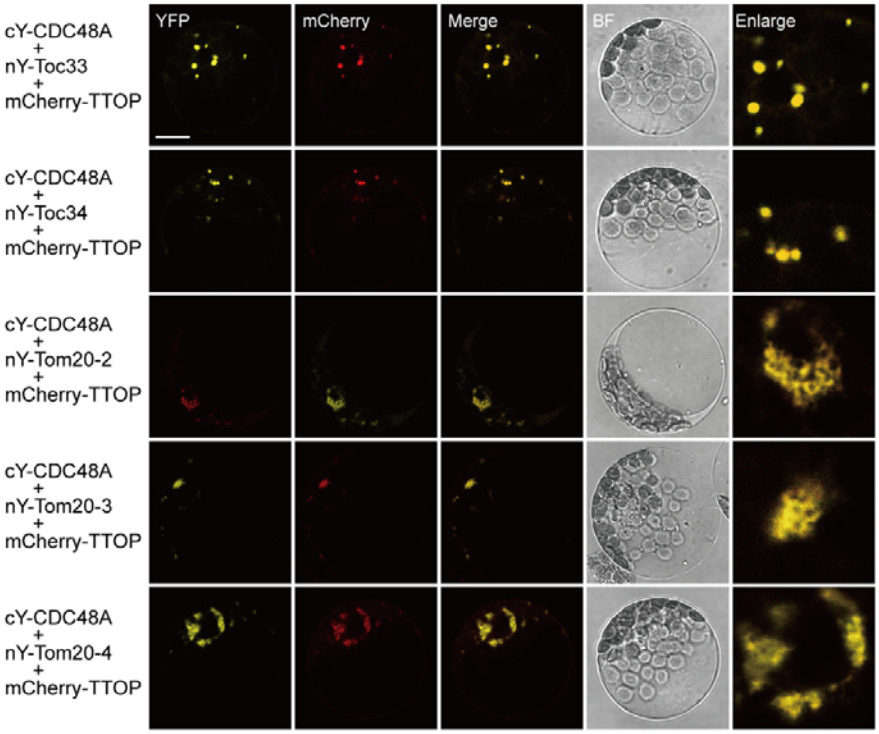

Fig. S6. Co-localization of TTOP, CDC48A, and chloroplast or mitochondrial outer membrane TA receptors in protoplasts.

Protoplasts were co-transfected with constructs encoding TTOP fused to mCherry at its N terminus or encoding CDC48A and TA proteins fused to nY or cY at their N termini. YFP and mCherry fluorescence in protoplasts was analyzed by CLSM; representative confocal images are shown. Overlap of YFP and mCherry signals is shown in protoplasts, indicating the co-localization of TTOP and CDC48A with TA proteins. BF, brightfield. Scale bar, 10 μm.

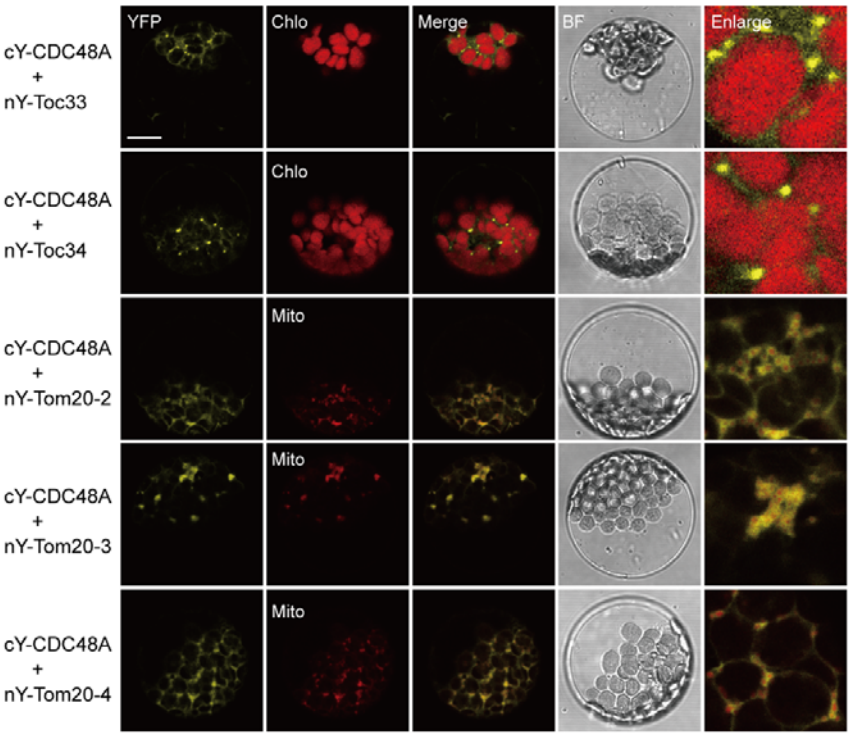

Fig. S7. BiFC analysis of the interaction between CDC48A and the TA receptor proteins. Protoplasts were co-transfected with the indicated pairs of constructs encoding CDC48A or TA proteins carrying nY or cY in their respective N termini. Reconstitution of YFP fluorescence in protoplasts was detected by CLSM, and the representative confocal images are shown. Chlo, chloroplast auto-fluorescence; Mito, mitochondria marked with MitoTracker. BF, brightfield. Scale bar, 10 μm.

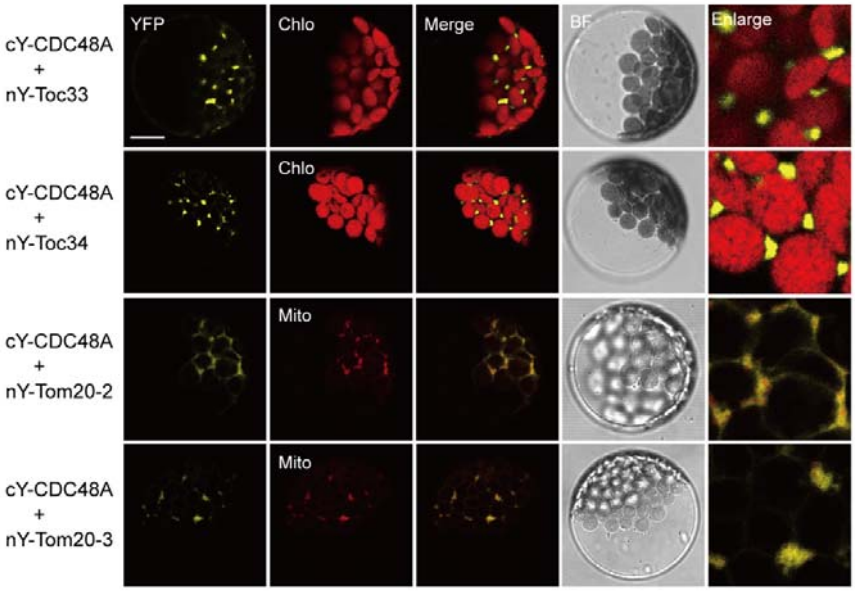

Fig. S8. BiFC analysis of the interaction between CDC48A and TA proteins in the absence of TTOP.

Protoplasts were prepared from the *ttop1-5* mutant and were co-transfected with the indicated pairs of constructs encoding CDC48A or TA proteins carrying nY or cY in their respective N termini. Reconstitution of YFP fluorescence in protoplasts was detected by CLSM; representative confocal images are shown. Chlo, chloroplast auto-fluorescence; Mito, mitochondria marked with MitoTracker. BF, brightfield. Scale bar, 10 μm.

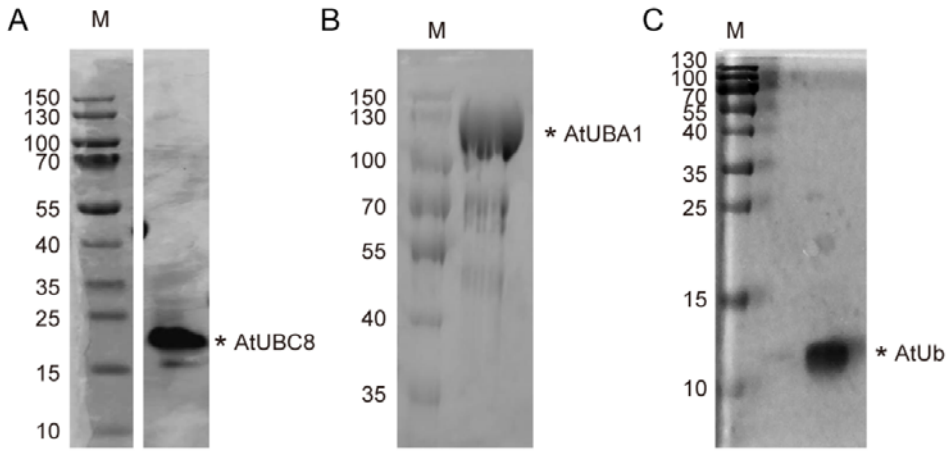

Fig. S9. Purification of recombinant AtUBC8, AtUBA1, and AtUb.
SDS-PAGE analysis of purified AtUBC8 **(A)**, AtUBA1 **(B)** and AtUb (**C)** proteins after removal of GST-tag and purification by gel-filtration. Positions of molecular weight markers are indicated at left (sizes in kDa).

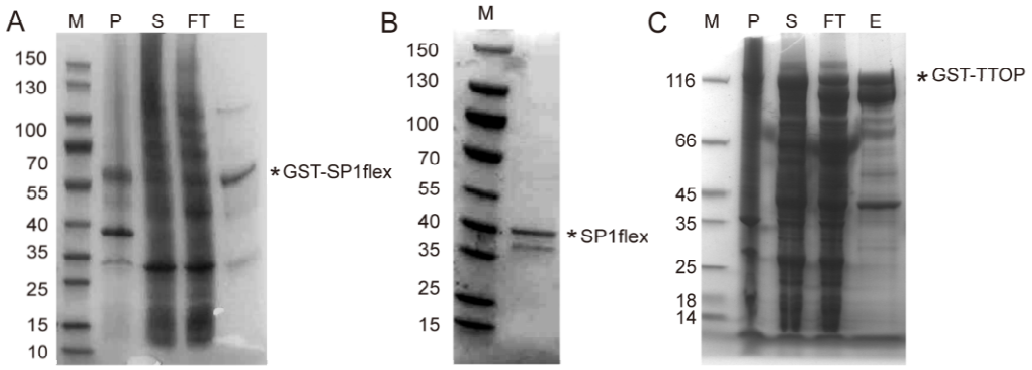

Fig. S10. Purification of recombinant SP1flex and TTOP.

(A) SDS-PAGE analysis of GST-SP1flex protein purified using a GST column. **(B)** SP1flex purified by gel filtration after PreScission Protease digestion of GST-SP1flex. **(C)** SDS-PAGE analysis of GST-TTOP protein purified using a GST column. Positions of molecular weight markers are indicated to the left (sizes in kDa). M, protein marker; P, pellet; S, supernatant; FT, flow-through; E, eluent. BD, before protease digestion. AD, after protease digestion. GF, gel filtration.

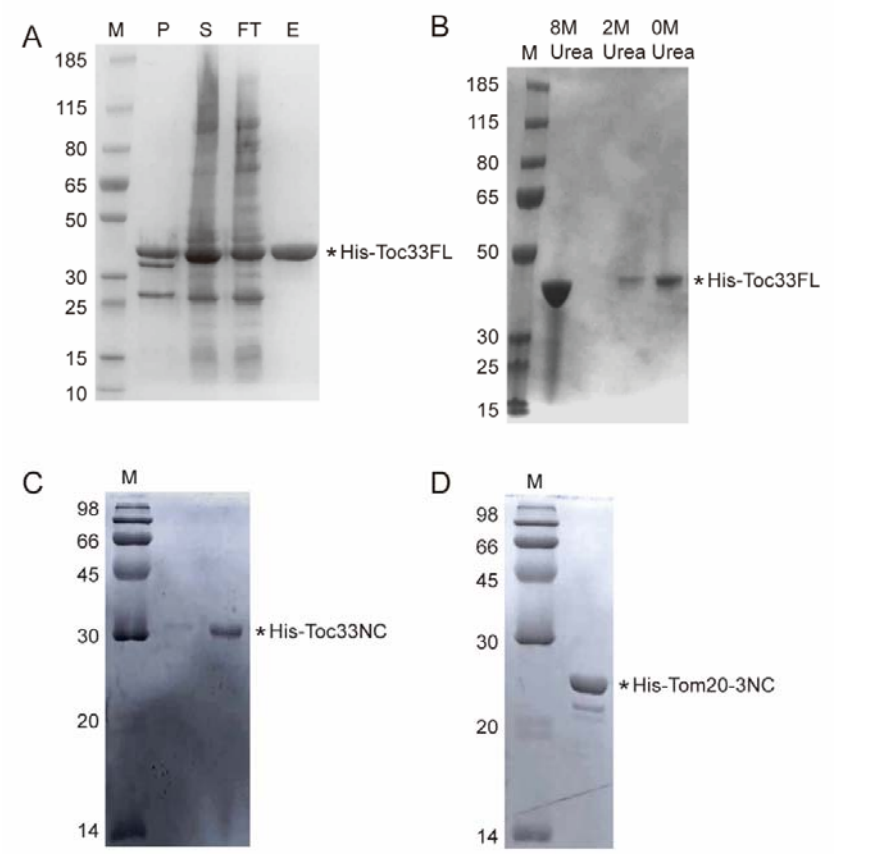

Fig. S11. Purification of recombinant Toc33FL, Toc33NC, and Tom20-3NC.
(A) SDS-PAGE analysis of unfolded His-Toc33FL purified using a Ni column. **(B)** Refolding of His-Toc33FL protein upon removal of urea by dialysis. **(C** and **D)** SDS-PAGE analysis of purified His-Toc33NC **(C)** and His-Tom20-3NC **(D)** proteins using a Ni column. Positions of molecular weight markers are indicated at left (sizes in kDa). M, protein marker; P, pellet; S, supernatant; FT, flow-through; E, eluent.

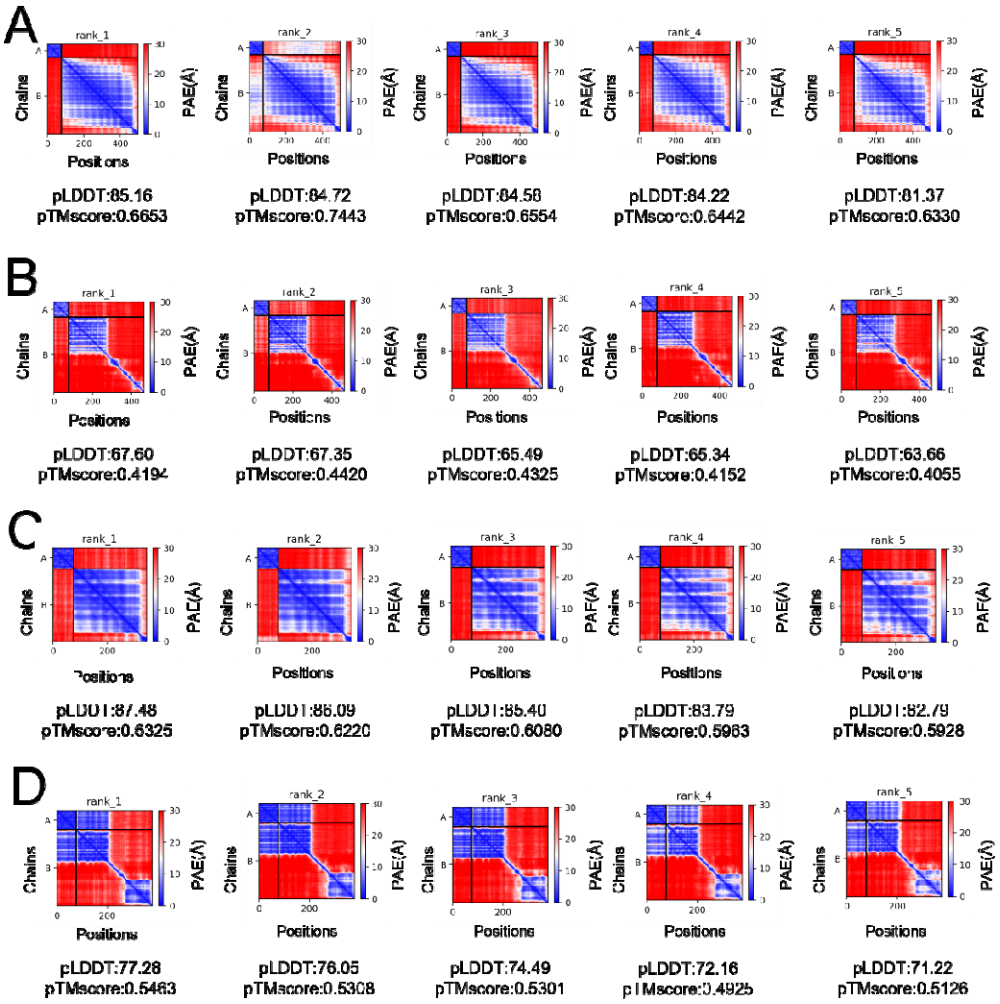

Fig. S12. Prediction of TTOP interacting domain to RPN subunits by Alphafold

By Alphafold2 prediction, the UBL domain of TTOP could not interact with RPN6 (A), RPN10 (B), nor RPN12 (C). It is predicted that the UBL domain of TTOP could interact with RPN13 (D).

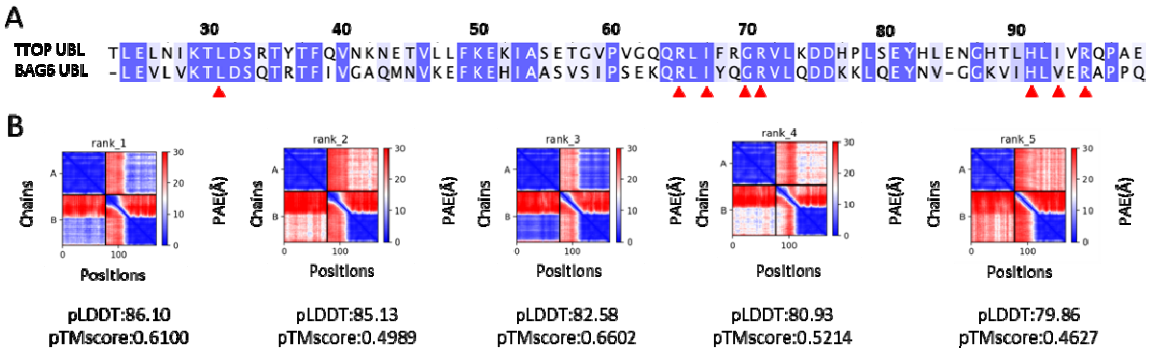

Fig. S13. Prediction of TTOP UBL domain and SP1 RING interaction.

Amino acid sequence alignment between the TTOP UBL and human BAG6 UBL domains. TTOP UBL contains the conserved RNF126_NZF interacting residues (Red triangle) (A). By AlphaFold2 prediction, the UBL domain of TTOP could interact with SP1 RING domain, especially rank_1 and rank_3 give much lower PAE values (B).

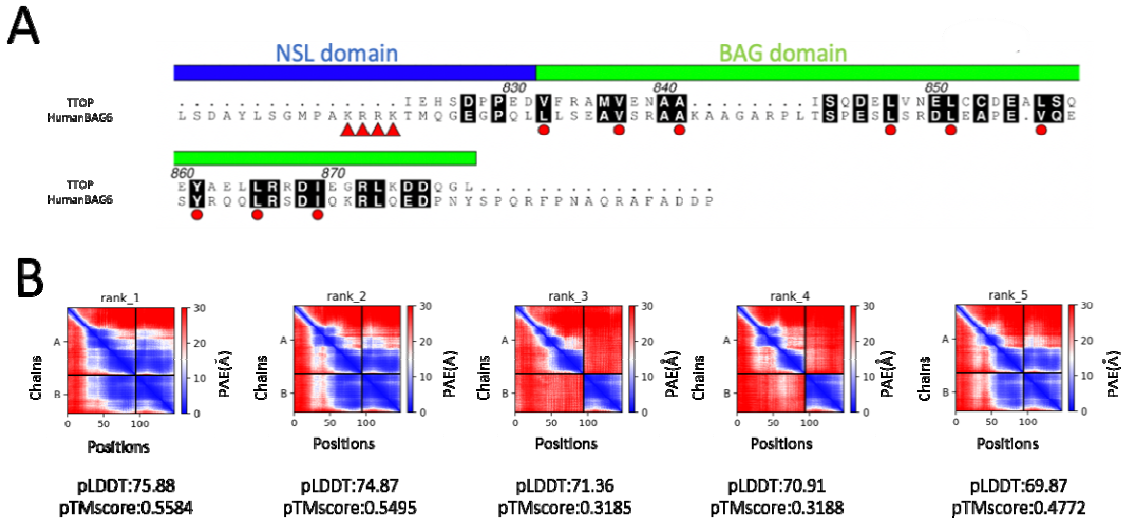

Fig. S14. TTOP C-terminus contains a BAG domain

Amino acid sequence alignment between the C-termini of TTOP and human BAG6. TTOP C-terminus does not contain the TRC35 interaction residues (Red triangle) in the NSL domain of BAG6 but contains a BAG domain. Especially, the TTOP C-terminal contains the conserved Ubl4A interaction residues (Red circle) (A). By AlphaFold2 prediction, the low PAE value predicted that the C-terminal of TTOP could interact with human Ubl4A (B).

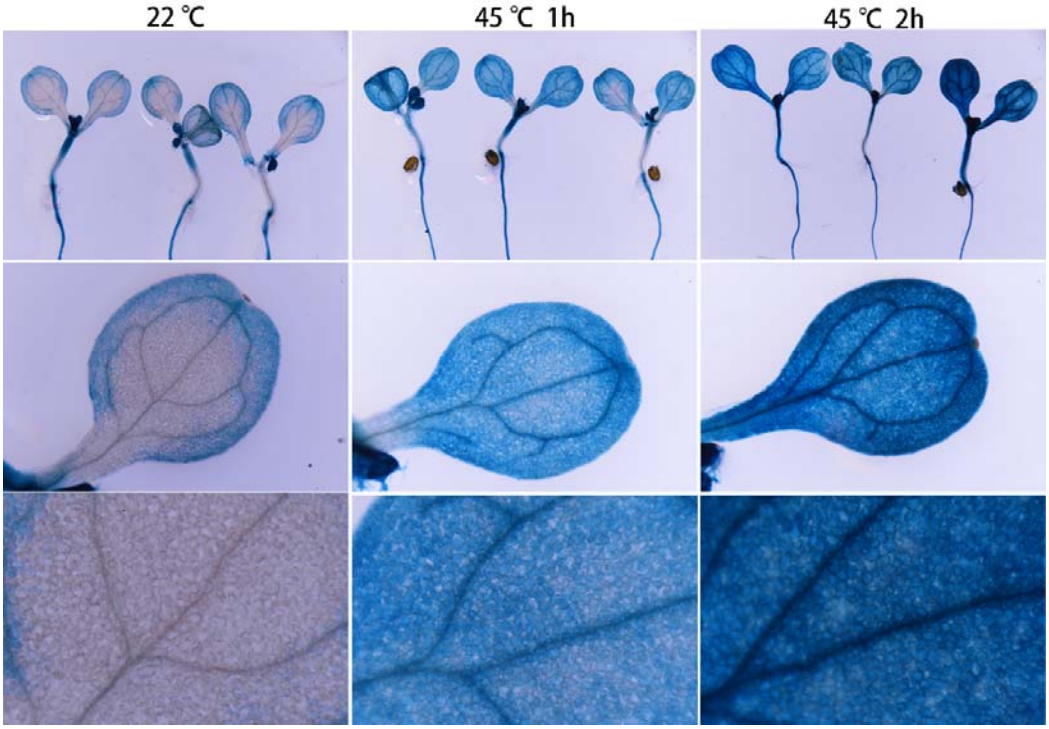

Fig. S15. Heat treatment induces TTOP mRNA transcription.

Ten-day-old *pTTOP:GUS* seedlings were used for GUS staining. For heat treatment, the seedlings were placed in 45°C incubator for 1 or 2h before GUS staining. Scale bar in A, E, I, 2.0 mm. Scale bar in B, C, D, F, G, H, 200 μm.

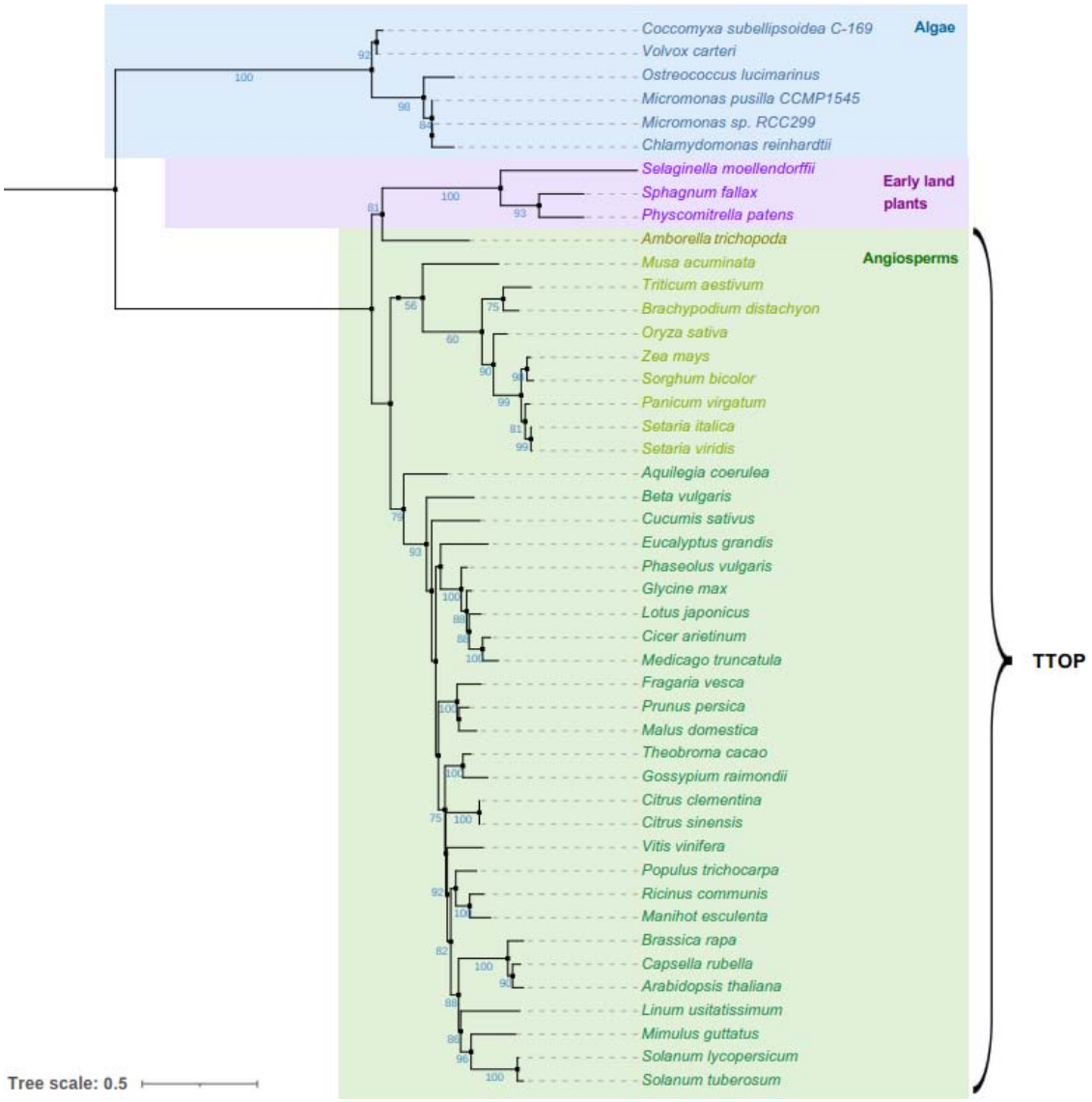

Fig. S16. Phylogenetic tree of TTOP

Phylogenetic analysis of TTOP was conducted using the maximum likelihood method. Percent support values from 1,000 bootstrap samples and scale bar are shown.

Table S1. PCR primers for vector construction.

Primer name	Primer sequence (5′ to 3′)	Application
TTOP-CDS-1F	CCAGGCCTACTAGTGGATCCATGGAAGATCAACCCATTAA	Cloning *TTOP* CDS into pBI221 vector carrying *nY* or *eGFP* or *mCherry*
TTOP-CDS-1R	ACCCGGGAGCGGTACCTTATAGACCTTGATCATCTTTTAG	
TTOP-CDS-2F	TGGGCATCGATACGGGATGGAAGATCAACCCATTAA	Cloning *TTOP* CDS into pGADT7 vector
TTOP-CDS-2R	CAGCTCGAGCTCGATGTTATAGACCTTGATCATCTTTTAG	
Myc-TTOP-CDS-F	AGAACACGGGGGACTCTAGAATGGAGCAAAAGTTGATTTCTGAGGAGGATCTTATGGAAGATCAACCCATTAA	Cloning *TTOP* CDS with Myc tag in the N terminus into pBI221 vector
GFP-TTOP CDS-1F	TAGTCGACTCTAGCCTCGAGATGGTGAGCAAGGGCGA	Cloning *TTOP* CDS as GFP fusion in the N terminus into pTA7002 vector
GFP-TTOP CDS-1R	GTCGATCCTCTAGCCTCGAGTTATAGACCTTGATCATCTTTT	
mCherry-TTOP CDS-F	TAGTCGACTCTAGCCTCGAGATGTTGAGCAAGGGCGAG	Cloning *TTOP* CDS with *mCherry* fusion in the N terminus into pTA7002 vector
mCherry-TTOP CDS-R	GTCGATCCTCTAGCCTCGAGTTATAGACCTTGATCATCTTTT	
GFP-TTOP CDS-2F	ACTCTAGAGGATCCCCGGGATGGTGAGCAAGGGCGA	Cloning *TTOP* CDS with GFP *fusion* in the N terminus into pBI121 vector to replace *GUS*
GFP-TTOP CDS-2R	ATCGGGGAAATTCGAGCTCTTATAGACCTTGATCATCTTTT	
TTOP Pro-F	GACCATGATTACGCCAAGCTTCTTATTTACAATGGCTGCCACTGG	Cloning *TTOP* promoter into pBI121 vector carrying *GUS* to replace *35S* promoter
TTOP Pro-R	AGGGACTGACCACCCGGGGAACCCTAAAGTATTAAAATT	
PAP2-CDS-1F	CCAGGCCTACTAGTGGATCCATGATCGTTAATTTCTCTTT	Cloning *PAP2* CDS into pBI221 vector carrying *nY* or *eGFP* in the N terminus
PAP2-CDS-1R	ACCCGGGAGCGGTACCTTATGTCTCCTCGTTCTTG	
PAP2-CDS-2F	TATGGCCATGGAGGCCGAATTCATGATCGTTAATTTCTCTTT	Cloning *PAP2* CDS into pGBKT7 vector
PAP2-CDS-2R	TTATGCGGCCGCTGCAGGTTATGTCTCCTCGTTCTTG	
PAP2-CDS-3F	TTGCTCCGTGGATCCGGTACCATGATCGTTAATTTCTCTTT	Cloning *PAP2* CDS into HBT vector carrying *FLAG* tag in the C terminus
PAP2-CDS-3R	CTTGTAGTCAGAAGGCCTCCCGGGTGTCTCCTCGTTCTTGACTGG	

1426 **Table S1 (continued). PCR primers for vector construction.**

PAP2-ΔTMD-1R	ACCCGGGAGCGGTACCTTATGTCTCCTCGTTCTTGACTGGGATCCAACGGTTTCCAGACGAAGATTTCTTTCCCCGGGTAGCATTAGATTCTGATTTTCCC	Cloning TMD-truncated *PAP2* CDS into pBI221 vector carrying *nY* in the N terminus
PAP2-ΔTMD-2R	TTATGCGGCCGCTGCAGGTTATGTCTCCTCGTTCTTGACTGGGATCCAACGGTTTCCAGACGAAGATTTCTTTCCCCGGGTAGCATTAGATTCTGATTTTCCC	Cloning TMD-truncated *PAP2* CDS into in pGBKT7 vector
PAP2-TMD-F	GATCCTTGTGGTATGCCAAAGGAGCAGGCTTGATGGTTGTGGGTGTGCTTTTAGGGTTCATTATCGGGTTTTTTTAAGGTAC	Cloning TMD of *PAP2* into in pBI221 vector carrying *nY* in the N terminus
PAP2-TMD-R	CTTAAAAAAACCCGATAATGAACCCTAAAAGCACACCCACAACCATCAAGCCTGCTCCTTTGGCATACCACAAG	
Toc33-CDS-1F	CCAGGCCTACTAGTGGATCCATGGGGTCTCTCGTTCG	Cloning *Toc33* CDS into pBI221 vector carrying *nY* or *eGFP* in the N terminus
Toc33-CDS-1R	ACCCGGGAGCGGTACCTTAAAGTGGCTTTCCACTTG	
Toc33-CDS-2F	TATGGCCATGGAGGCCGAATTCATGGGGTCTCTCGTTCG	Cloning *Toc33* CDS into pGBKT7 vector
Toc33-CDS-2R	TTATGCGGCCGCTGCAGTTAAAGTGGCTTTCCACTTG	
Toc33-CDS-3F	TTGCTCCGTGGATCCGGTACCATGGGGTCTCTCGTTCG	Cloning *Toc33* CDS into HBT vector carrying *FLAG* tag in the C terminus
Toc33-CDS-3R	CTTGTAGTCAGAAGGCCTCCCGGGAAGTGGCTTTCCACTTGTC	
Toc33-ΔTMD-R	ACCCGGGAGCGGTACCTTAAAGTGGCTTTCCACTTGTCTTGATATCATTTCTGATTGCTCCTTG TTTCTTTCCTTTATCATCAGAG	Cloning TMD-truncated *Toc33* CDS into pBI221 vector carrying *nY* in the N terminus
Toc33-TMD-F	GATCCCTCATCCCTCTTATCATAGGCGCTCAGTATTTGATCGTTAAGATGATTTAAGGTAC	Cloning TMD of *Toc33* into in pBI221 vector carrying *nY* in the N terminus
Toc33-TMD-R	CTTAAATCATCTTAACGATCAAATACTGAGCGCCTATGATAAGAGGGATGAGG	
mCherry-Toc33-CDS-F	GAGGATCCCCGGGTACCATGGTGAGCAAGGGCGA	Cloning *Toc33* CDS fused to *mCherry* in the N terminus into pBI121 vector
mCherry-Toc33-CDS-R	GGGGAAATTCGAGCTCTTAAAGTGGCTTTCCACTTG	
Toc34-CDS-1F	CCAGGCCTACTAGTGGATCCATGGCAGCTTTGCAAAC	Cloning *Toc34* CDS into pBI221 vector carrying *nY* or *eGFP* in the N terminus
Toc34-CDS-1R	ACCCGGGAGCGGTACCTCAAGACCTTCGACTTG	

Table S1 (continued). PCR primers for vector construction.

Primer name	Primer sequence (5′ to 3′)	Application
Toc34-CDS-2F	TATGGCCATGGAGGCCGAATTCATGGCAGCTTTGCAAAC	Cloning *Toc34* CDS into pGBKT7 vector
Toc34-CDS-2R	TTATGCGGCCGCTGCAGTCAAGACCTTCGACTTGC	
Toc34-CDS-3F	TTGCTCCGTGGATCCGGTACCATGGCAGCTTTGCAAAC	Cloning *Toc34* CDS into HBT vector carrying *FLAG* tag in the C terminus
Toc34-CDS-3R	CTTGTAGTCAGAAGGCCTCCCGGGAGACCTTCGACTTGCTA	
Toc34-ΔTMD -R	ACCCGGGAGCGGTACCTCAAGACCTTCGACTTGCTAAACCGGAGTCTCGCAGCTCCCACGCCGGTTTACTCTCTCTCGAAACATCGGACTTGATTGCTTTTTTTCCTCTTTCGTTTGGG	Cloning TMD-truncated *Toc34* CDS into pBI221 vector carrying *nY* in the N terminus
Toc34-TMD -F	GATCCCTGATTCCTTTAATGTTTGCATTCCAATACTTGCTGGTGATGAAGCCATTGGTTCGATAAGGTAC	Cloning TMD of *Toc34* into in pBI221 vector carrying *nY* in the N terminus
Toc34-TMD -R	CTTATCGAACCAATGGCTTCATCACCAGCAAGTATTGGAATGCAAACATTAAAGGAATCAGG	
Tom20-2-CDS-1F	CCAGGCCTACTAGTGGATCCATGGAGTTCTCTACCGC	Cloning *Tom20-2* CDS into pBI221 vector carrying *nY* or *eGFP* in the N terminus
Tom20-2-CDS-1R	ACCCGGGAGCGGTACCTTATCTGGCAGGAGGTG	
Tom20-2-CDS-2F	TATGGCCATGGAGGCCGAATTCATGGAGTTCTCTACCGC	Cloning *Tom20-2* CDS into pGBKT7 vector
Tom20-2-CDS-2R	TTATGCGGCCGCTGCAGTTATCTGGCAGGAGGTG	
Tom20-2-CDS-3F	TTGCTCCGTGGATCCGGTACCATGGAGTTCTCTACCGC	Cloning *Tom20-2* CDS into HBT vector carrying *FLAG* tag in the C terminus
Tom20-2-CDS-3R	CTTGTAGTCAGAAGGCCTCCCGGGTCTGGCAGGAGGTGGAGGGCCAAG	
Tom20-2-ΔTMD -1R	ACCCGGGAGCGGTACCTTATCTGGCAGGAGGTGGAGGGCCAAGGGATTTATCATAAGTGAATTCAGTGTTCCTC	Cloning TMD-truncated *Tom20-2* CDS into pBI221 vector carrying *nY* in the N terminus
Tom20-2-ΔTMD -2R	TTATGCGGCCGCTGCAGGTTATCTGGCAGGAGGTGGAGGGCCAAGGGATTTATCATAAGTGAATTCAGTGTTCCTC	Cloning TMD-truncated *Tom20-2* CDS into pGBKT7 vector
Tom20-2-TMD-F	GATCCGTATGCGGTTGGATAATTCTCGCTTGTGGGATTGTTGCTTGGGTTGGCATGGCATAAGGTAC	Cloning TMD of *Tom20-2* into in pBI221 vector carrying *nY* in the N terminus
Tom20-2-TMD-R	CTTATGCCATGCCAACCCAAGCAACAATCCCACAAGCGAGAATTATCCAACCGCATACG	

Table S1 (continued). PCR primers for vector construction.

Primer name	Primer sequence (5′ to 3′)	Application
mCherry-Tom20-2-CDS-F	GAGGATCCCCGGGTACCATGGTGAGCAAGGGCGA	Cloning *Tom20-2* CDS fused to *mCherry* in the N terminus into pBI121 vector
mCherry-Tom20-2-CDS-R	GGGGAAATTCGAGCTCTTATCTGGCAGGAGGTG	
Tom20-3-CDS-1F	CCAGGCCTACTAGTGGATCCATGGATACGGAAACTGAGTT	Cloning *Tom20-3* CDS into pBI221 vector carrying *nY* or *eGFP* in the N terminus
Tom20-3-CDS-1R	ACCCGGGAGCGGTACCTTAACGAGGAGGAGAGACA	
Tom20-3-CDS-2F	TATGGCCATGGAGGCCGAATTCATGGATACGGAAACTGAGTT	Cloning *Tom20-3* CDS into pGBKT7 vector
Tom20-3-CDS-2R	TTATGCGGCCGCTGCAGTTAACGAGGAGGAGAGACA	
Tom20-3-CDS-3F	TTGCTCCGTGGATCCGGTACCATGGATACGGAAACTGAGTT	Cloning *Tom20-3* CDS into HBT vector carrying *FLAG* tag in the C terminus
Tom20-3-CDS-3R	CTTGTAGTCAGAAGGCCTCCCGGGACGAGGAGGAGAGACA	
Tom20-3-ΔTMD -1R	ACCCGGGAGCGGTACCTTAACGAGGAGGAGAGACAGGCACATTAGCTTTATCATACTTGGCATCACTACTT	Cloning TMD-truncated *Tom20-3* CDS into pBI221 vector carrying *nY* in the N terminus
Tom20-3-ΔTMD -2R	TTATGCGGCCGCTGCAGGTTAACGAGGAGGAGAGACAGGCACATTAGCTTTATCATACTTGGCATCACTACTT	Cloning TMD-truncated *Tom20-3* CDS into pGBKT7 vector
Tom20-3-TMD -F	GATCCGCTATGGGTTGGGTGATTCTAGCCATTGGTGTTGTTGCTTGGATCAGTTTCGCGTAAGGTAC	Cloning TMD of *Tom20-3* into in pBI221 vector carrying *nY* in the N terminus
Tom20-3-TMD -R	CTTACGCGAAACTGATCCAAGCAACAACACCAATGGCTAGAATCACCCAACCCATAGCG	
Tom20-4-CDS-1F	CCAGGCCTACTAGTGGATCCATGGATATGCAGAATGAAA	Cloning *Tom20-4* CDS into pBI221 vector carrying *nY* or *eGFP* in the N terminus
Tom20-4-CDS-1R	ACCCGGGAGCGGTACCTTACTGCCTTGACACCG	
Tom20-4-CDS-2F	TATGGCCATGGAGGCCGAATTCATGGATATGCAGAATGAAAACG	Cloning *Tom20-4* CDS into pGBKT7 vector
Tom20-4-CDS-2R	TTATGCGGCCGCTGCAGTTACTGCCTTGACACCG	
Tom20-4-CDS-3F	TTGCTCCGTGGATCCGGTACCATGGATATGCAGAATGAAA	Cloning *Tom20-4* CDS into HBT vector carrying *FLAG* tag in the C terminus
Tom20-4-CDS-3R	CTTGTAGTCAGAAGGCCTCCCGGGCTGCCTTGACACCGGCGT	
Tom20-4-ΔTMD -1R	ACCCGGGAGCGGTACCTTACTGCCTTGACACCGGCGTCTGAGAATTATCATACTTGAACTCACTGGTC	Cloning TMD-truncated *Tom20-4* CDS into pBI221 vector carrying *nY* in the N terminus

Table S1 (continued). PCR primers for vector construction.

Primer name	Primer sequence (5′ to 3′)	Application
Tom20-4-ΔTMD -2R	TTATGCGGCCGCTGCAGGTTACTGCCTTGACACCGGCGTCTGAGAATTATCATACTTGAACTCACTGGTC	Cloning TMD-truncated *Tom20-4* CDS into pGBKT7 vector
Tom20-4-TMD-F	GATCCGTGTTCGGATGGGTCATCTTAGCCAGTTACGTTGTTGCGTGGATCAGTTTTGCCTAAGGTAC	Cloning TMD of *Tom20-4* into in pBI221 vector carrying *nY* in the N terminus
Tom20-4-TMD-R	CTTAGGCAAAACTGATCCACGCAACAACGTAACTGGCTAAGATGACCCATCCGAACACG	
SP1-CDS-1F	CCAGGCCTACTAGTGGATCCATGATTCCTTGGGGTGGAGTTAC	Cloning *SP1* CDS into pBI221 vector carrying *nY* in the N terminus
SP1-CDS-1R	ACCCGGGAGCGGTACCTCAGTGACGATATGTCTTAACCGCC	
SP1-CDS-2F	TTGCTCCGTGGATCCGGTACCATGATTCCTTGGGGTGGAGTT	Cloning *SP1* CDS into HBT vector carrying *FLAG* tag in the C terminus
SP1-CDS-2R	CTTGTAGTCAGAAGGCCTCCCGGGGTGACGATATGTCTTAACCGC	
SP2-CDS-1F	CCAGGCCTACTAGTGGATCCATGGGAGCTCAGAAGAGTA	Cloning *SP2* CDS into pBI221 vector carrying *nY* in the N terminus
SP2-CDS-1R	ACCCGGGAGCGGTACCCTATGTTGATGAAGCAAGATTGGTG	

Table S1 (continued). PCR primers for vector construction.

Primer name	Primer sequence (5′ to 3′)	Application
RPN6-CDS-1F	CCAGGCCTACTAGTGGATCCATGGTTTCCTATCGTGCTACCACAG	Cloning *RPN6* CDS into pBI221 vector carrying *nY* in the N terminus
RPN6-CDS-1R	ACCCGGGAGCGGTACCTCAGGACATGATTTTGGCAGACCGG	
RPN6-CDS-2F	TTGCTCCGTGGATCCGGTACCATGGTTTCCTATCGTGCTACCACAG	Cloning *RPN6* CDS into HBT vector carrying *FLAG* tag in the C terminus
RPN6-CDS-2R	CTTGTAGTCAGAAGGCCTCCCGGGGGACATGATTTTGGCAGACCG	
HA-RPN6-CDS-F	AGAACACGGGGGACTCTAGAATGTACCCATACGATGTTCCAGATTACGCTATGGTTTCCTATCGTGCTACCACAG	Cloning *RPN6* CDS fused to *HA* tag in N terminus into pBI221 vector
RPN10-CDS-1F	CCAGGCCTACTAGTGGATCCATGGTTCTCGAGGCGACTATG	Cloning *RPN10* CDS into pBI221 vector carrying *nY* in the N terminus
RPN10-CDS-1R	ACCCGGGAGCGGTACCTCACTTCTTCTCATCCTCGCC	
RPN10-CDS-2F	TTGCTCCGTGGATCCGGTACCATGGTTCTCGAGGCGACTATG	Cloning *RPN10* CDS into HBT vector carrying *FLAG* tag in the C terminus
RPN10-CDS-2R	CTTGTAGTCAGAAGGCCTCCCGGGCTTCTTCTCATCCTCGCC	
HA-RPN10-CDS-F	AGAACACGGGGGACTCTAGAATGTACCCATACGATGTTCCAGATTACGCTATGGTTCTCGAGGCGACTATG	Cloning *RPN10* CDS fused to *HA* tag in N terminus into pBI221 vector
RPN12-CDS-1F	CCAGGCCTACTAGTGGATCCATGGATCCGCAGCTAACTGAAG	Cloning *RPN12* CDS into pBI221 vector carrying *nY* in the N terminus
RPN12-CDS-1R	ACCCGGGAGCGGTACCTTACACGATACGCTCCAGCTCTC	
RPN12-CDS-2F	TTGCTCCGTGGATCCGGTACCATGGATCCGCAGCTAACTGAAG	Cloning *RPN12* CDS into HBT vector carrying *FLAG* tag in the C terminus
RPN12-CDS-2R	CTTGTAGTCAGAAGGCCTCCCGGGCACGATACGCTCCAGCTCT	
RPN13-CDS-1F	CCAGGCCTACTAGTGGATCCATGAGTTCAAGCGAAGCGTTTC	Cloning *RPN13* CDS into pBI221 vector carrying *nY* in the N terminus
RPN13-CDS-1R	ACCCGGGAGCGGTACCTTAACTCTCATCCATCGCATCCC	
RPN13-CDS-2F	TTGCTCCGTGGATCCGGTACCATGAGTTCAAGCGAAGCGTTTC	Cloning *RPN13* CDS into HBT vector carrying *FLAG* tag in the C terminus
RPN13-CDS-2R	CTTGTAGTCAGAAGGCCTCCCGGGACTCTCATCCATCGCATCCCTTG	
CDC48A-CDS-1F	CCAGGCCTACTAGTGGATCCATGTCTACCCCAGCTGAATCTT	Cloning *CDC48A* CDS into pBI221 vector carrying *nY* or *cY* in the N terminus
CDC48A-CDS-1R	ACCCGGGAGCGGTACCCTAATTGTAGAGATCATCATCGTCCCC	
6×His-CDC48A-CDS-F	AGAACACGGGGGACTCTAGAATGCATCATCATCATCATCATATGTCTACCCCAGCTGAATCTT	Cloning *CDC48A* CDS fused with *6×His* tag in N terminus into pBI221 vector
TTOPsgRNA-F	ATTGCTCTAGTAGCACCAATGCGT	Cloning sgRNA of *TTOP* into pKI1.1R vector
TTOPsgRNA-R	AAACACGCATTGGTGCTACTAGAG	

Table S1 (continued). PCR primers for vector construction.

Primer name	Primer sequence (5′ to 3′)	Application
TTOP-pGEX-F	TCTGTTCCAGGGGCCCCTGGGATCCATGGAAGATCAACCCATTAA	Cloning *TTOP* CDS into pGEX-GST vector
TTOP-pGEX-R	TCAGTCAGTCACGATGCGGCCGCTTATAGACCTTGATCATCTTTTAG	
Toc33NC-pET-F	TGGATCGCATATGGGGCCCGGGATGGGGTCTCTCGTTCG	Cloning C-terminally truncated *Toc33* CDS into pET507a-His vector
Toc33NC- pET-R	GGATCTGATCAGGTACCCTCGAGTTAGTCTACATGAATTGCTTTCCTC	
Toc33FL-pET-F	TGGATCGCATATGGGGCCCGGGATGGGGTCTCTCGTTCG	Cloning full-length *Toc33* CDS into pET507a-His vector
Toc33FL-pET-R	GGATCTGATCAGGTACCCTCGAGTTAAAGTGGCTTTCCACTTG	
Tom20-3NC-pET-F	TGGATCGCATATGGGGCCCGGGATGGATACGGAAACTGAGTT	Cloning the C-terminally truncated *Tom20-3* CDS into pET507a-His vector
Tom20-3NC-pET-R	GGATCTGATCAGGTACCCTCGAGTTAAGCATCATACTTGGCAT	

The nucleotides underlined do not correspond to the target gene, but to the linker sequences.

Table S. qRT-PCR primers.

Primer name	Primer sequence (5′ to 3′)
Toc33-F	TTGGATGTGTATAGAGTCGATGAGC
Toc33-R	CGTAGGAAAGTTCATCGGGAGGGGA
Toc34-F	ATCCAGCAGTTCCCACCTGCTACTC
Toc34-R	CTTTCCAACACCACCTTTCCCCATT
Toc159-F	ATCCCCGCCTCTCCCTTACTTGTTG
Toc159-R	GCTGGTCATACTCATCATCTTCCCC
Toc75-F	AGTTGCGGGAAGTAGAACAAGGGGC
Toc75-R	GACAGAGTACGGACCACCGAGGACA
PAP2-F	GCCTATTGCCTCGACAGTTCC
PAP2-R	CACACCACATTCGCCACCAC
Tic40-F	CACCTTTTCCGTTTCCATTTCC
Tic40-R	GTCTCTACTTTTGTCGCTGTCAC

1 **Table S2. Protein and nucleotide sequences of coding-optimized used in this study**

Constructs	Protein sequence	Nucleotide sequence
AtUba1 (72-1080)	EIDEDLHSRQLAV	GAGATTGACGAAGATCTGCACAGCCGTCAACTGGCGGTT
	YGRETMRRLFASNVLIS	TACGGTCGTGAAACCATGCGTCGTCTGTTCGCGAGCAACGTG
	GMHGLGAEIAKNLILAG	CTGATCAGCGGCATGCATGGTCTGGGCGCGGAAATCGCGAAA
	VKSVTLHDERVVELWDL	AACCTGATTCTGGCGGGTGTGAAGAGCGTTACCCTGCACGAC
	SSNFVFSEDDVGKNRAD	GAGCGTGTGGTTGAACTGTGGGATCTGAGCAGCAACTTCGTG
	ASVQKLQDLNNAVVVSS	TTTAGCGAGGACGATGTTGGCAAAAACCGTGCGGACGCGAGC
	LTKSLNKEDLSGFQVVV	GTTCAGAAGCTGCAAGATCTGAACAACGCGGTGGTTGTGAGC
	FSDISMERAIEFDDYCH	AGCCTGACCAAAAGCCTGAACAAGGAAGACCTGAGCGGTTTC
	SHQPPIAFVKADVRGLF	CAGGTTGTGGTTTTTAGCGATATCAGCATGGAGCGTGCGATT
	GSVFCDFGPEFAVLDVD	GAGTTCGACGATTACTGCCACAGCCACCAACCGCCGATCGCG
	GEEPHTGIIASISNENQ	TTCGTGAAGGCGGACGTTCGTGGTCTGTTTGGCAGCGTGTTC
	AFISCVDDERLEFEDGD	TGCGATTTTGGTCCGGAGTTCGCGGTGCTGGACGTTGATGGC
	LVVFSEVEGMTELNDGK	GAGGAACCGCACACCGGCATCATTGCGAGCATCAGCAACGAG
	PRKIKSTRPYSFTLDED	AACCAGGCGTTTATTAGCTGCGTTGACGATGAACGTCTGGAG
	TTNYGTYVKGGIVTQVK	TTCGAAGACGGTGATCTGGTGGTTTTTAGCGAGGTGGAGGGT
	QPKLLNFKPLREALKDP	ATGACCGAGCTGAACGACGGCAAACCGCGTAAGATCAAAAGC
	GDFLFSDFSKFDRPPLL	ACCCGTCCGTATAGCTTCACCCTGGACGAAGATACCACCAAC
	HLAFQALDHFKAEAGRF	TACGGCACCTATGTTAAGGGTGGCATTGTGACCCAGGTTAAA
	PVAGSEEDAQKLISIAT	CAACCGAAGCTGCTGAACTTTAAGCCGCTGCGTGAGGCGCTG
	AINTGQGDLKVENVDQK	AAGGACCCGGGTGATTTCCTGTTTAGCGACTTCAGCAAATTT
	LLRHFSFGAKAVLNPMA	GATCGTCCGCCGCTGCTGCACCTGGCGTTCCAGGCGCTGGAC
	AMFGGIVGQEVVKACSG	CACTTTAAAGCGGAAGCGGGTCGTTTCCCGGTGGCGGGCAGC
	KFHPLFQFFYFDSVESL	GAGGAAGATGCGCAAAAGCTGATCAGCATTGCGACCGCGATC
	PSEPVDSSDFAPRNSRY	AACACCGGTCAGGGCGACCTGAAAGTGGAGAACGTTGATCAA
	DAQISVFGAKFQKKLED	AAGCTGCTGCGTCACTTCAGCTTTGGCGCGAAGGCGGTTCTG
	AKVFTVGSGALGCEFLK	AACCCGATGGCGGCGATGTTTGGTGGCATTGTGGGTCAGGAA
	NLALMGVSCGSQGKLTV	GTGGTTAAAGCGTGCAGCGGCAAGTTCCACCCGCTGTTTCAA
	TDDDIIEKSNLSRQFLF	TTCTTTTACTTCGACAGCGTTGAGAGCCTGCCGAGCGAACCG
	RDWNIGQAKSTVAASAA	GTGGACAGCAGCGATTTTGCGCCGCGTAACAGCCGTTATGAC
	AVINPRFNIEALQNRVG	GCGCAGATCAGCGTTTTCGGTGCGAAATTTCAAAAGAAACTG
	AETENVFDDAFWENLTV	GAGGATGCGAAGGTGTTCACCGTTGGTAGCGGCGCGCTGGGT
	VVNALDNVNARLYVDSR	TGCGAATTTCTGAAAAACCTGGCGCTGATGGGCGTTAGCTGC
	CLYFQKPLLESGTLGTK	GGTAGCCAGGGCAAACTGACCGTGACCGACGATGACATCATT
	CNTQSVIPHLTENYGAS	GAGAAGAGCAACCTGAGCCGTCAGTTCCTGTTTCGTGACTGG
	RDPPEKQAPMCTVHSFP	AACATCGGCCAAGCGAAGAGCACCGTGGCGGCGAGCGCGGCG
	HNIDHCLTWARSEFEGL	GCGGTTATCAACCCGCGTTTCAACATTGAGGCGCTGCAAAAC
	LEKTPAEVNAYLSSPVE	CGTGTGGGTGCGGAAACCGAAAACGTTTTCGATGACGCGTTT
	YTNSMMSAGDAQARDTL	TGGGAAAACCTGACCGTGGTTGTGAACGCGCTGGACAACGTG
	ERIVECLEKEKCETFQD	AACGCGCGTCTGTACGTTGATAGCCGTTGCCTGTATTTTCAG
	CLTWARLRFEDYFVNRV	AAACCGCTGCTGGAAAGCGGCACCCTGGGCACCAAGTGCAAC
	KQLIYTFPEDAATSTGA	ACCCAAAGCGTTATCCCGCACCTGACCGAGAACTACGGTGCG
	PFWSAPKRFPRPLQYSS	AGCCGTGACCCGCCGGAAAAACAGGCGCCGATGTGCACCGTG
	SDPSLLNFITATAILRA	CACAGCTTCCCGCACAACATTGATCACTGCCTGACCTGGGCG
	ETFGIPIPEWTKNPKEA	CGTAGCGAGTTTGAAGGCCTGCTGGAGAAGACCCCGGCGGAA
	AEAVDRVIVPDFEPRQD	GTTAACGCGTACCTGAGCAGCCCGGTGGAGTATACCAACAGC
	AKIVTDEKATTLTTASV	ATGATGAGCGCGGGTGATGCGCAGGCGCGTGATACCCTGGAG
	DDAAVIDDLIAKIDQCR	CGTATCGTGGAATGCCTGGAGAAGGAAAAATGCGAAACCTTT
	HNLSPDFRMKPIQFEKD	CAAGATTGTTTAACCTGGGCGCGTCTGCGTTTCGAAGATTAC
	DDTNYHMDVIAGLANMR	TTTGTGAACCGTGTTAAACAACTGATTTATACCTTTCCGGAA
	ARNYSIPEVDKLKAKFI	GATGCGGCGACCAGCACCGGTGCGCCGTTCTGGAGCGCGCCG
	AGRIIPAIATSTAMATG	AAGCGTTTTCCGCGTCCGCTGCAGTACAGCAGCAGCGACCCG
	LVCLELYKVLDGGHKVE	AGCCTGCTGAACTTCATCACCGCGACCGCGATTCTGCGTGCG

	AYRNTFANLALPLFSMA EPLPPKVVKHRDMAWTV WDRWVLKGNPTLREVLQ WLEDKGLSAYSISCGSC LLFNSMFTRHKERMDKK VVDLARDVAKVELPPYR NHLDVVVACEDEDDNDV DIPLVSIYFR	GAAACCTTTGGTATCCCGATTCCGGAATGGACCAAAAACCCG AAAGAGGCGGCGGAAGCGGTTGACCGTGTGATCGTTCCGGAT TTCGAGCCGCGTCAAGACGCGAAAATTGTGACCGATGAAAAA GCGACCACCCTGACCACCGCGAGCGTGGATGATGCGGCGGTT ATCGATGACCTGATCGCGAAAATTGACCAGTGCCGTCACAAC CTGAGCCCGGATTTCCGTATGAAACCGATTCAATTTGAGAAG GATGACGATACCAACTACCACATGGACGTTATCGCGGGTCTG GCGAACATGCGTGCGCGTAACTATAGCATTCCGGAAGTGGAT AAGCTGAAAGCGAAGTTCATCGCGGGTCGTATCATTCCGGCG ATTGCGACCAGCACCGCGATGGCGACCGGCCTGGTGTGCCTG GAGCTGTACAAAGTTCTGGACGGTGGCCACAAGGTGGAAGCG TATCGTAACACCTTCGCGAACCTGGCGCTGCCGCTGTTTAGC ATGGCGGAGCCGCTGCCGCCGAAAGTTGTGAAGCACCGTGAC ATGGCGTGGACCGTGTGGGATCGTTGGGTTCTGAAAGGTAAC CCGACCCTGCGTGAGGTTCTGCAGTGGCTGGAAGACAAGGGT CTGAGCGCGTACAGCATCAGCTGCGGCAGCTGCCTGCTGTTC AACAGCATGTTTACCCGTCACAAAGAGCGTATGGATAAGAAA GTTGTGGACCTGGCGCGTGATGTGGCGAAGGTTGAACTGCCG CCGTACCGTAACCACCTGGACGTTGTGGTTGCGTGCGAGGAT GAAGACGATAACGACGTGGATATCCCGCTGGTTAGCATTTAT TTCCGT
AtUbc8 (1-149)	MASKRILKELKDL QKDPPTSCIFAGPVAED MFHWQATIMGPAESPYS GGVFLVTIHFPPDYPFK PPKVAFRTKVFHPNINS NGSICLDILKEQWSPAL TISKVLLSICSLLTDPN PDDPLVPEIAHMYKTDR AKYEATARNWTQKYAMG	ATGGCGAGCAAGCGTATCCTGAAGGAGCTGAAAGACCTG CAGAAAGATCCGCCGACCAGCTGCATTTTTGCGGGTCCGGTG GCGGAGGACATGTTCCACTGGCAAGCGACCATTATGGGTCCG GCGGAAAGCCCGTACAGCGGTGGCGTGTTCCTGGTTACCATT CACTTTCCGCCGGACTATCCGTTCAAGCCGCCGAAAGTGGCG TTCCGTACCAAGGTTTTTCACCCGAACATCAACAGCAACGGT AGCATCTGCCTGGATATTCTGAAGGAACAGTGGAGCCCGGCG CTGACCATCAGCAAAGTGCTGCTGAGCATTTGCAGCCTGCTG ACCGACCCGAACCCGGACGATCCGCTGGTTCCGGAGATTGCG CACATGTACAAGACCGATCGTGCGAAATATGAAGCGACCGCG CGTAACTGGACCCAAAAATACGCGATGGGC
AtUb (1-76)	MQIFVKTLTGKTI TLEVESSDTIDNVKAKI QDKEGIPPDQQRLIFAG KQLEDGRTLADYNIQKE STLHLVLRLRGG	ATGCAGATTTTTGTGAAGACCCTGACCGGCAAGACCATT ACCCTGGAAGTTGAAAGCAGCGACACCATTGATAACGTGAAA GCGAAAATCCAGGACAAAGAGGGTATCCCGCCGGATCAGCAA CGTCTGATCTTCGCGGGTAAACAACTGGAAGACGGCCGTACC CTGGCGGATTACAACATTCAAAAGGAGAGCACCCTGCATCTG GTTCTGCGTCTGCGTGGCGGT
SP1flex (The RING motif in SP1RING is shown in bold)	GRSSGRDAEVLKT VTRVNQLKELAQLLELD SKILPFIVAVSGRVGSE TPIKCEHSGIRGVIVEE TAEQHFLKHNETGSWVQ DSALMLSMSKEVPWFLD DGTSRVHVMGARGATGF ALTVGSEVFEESGRSLV RGTLDYLQGLKMLGVKR IERVLPTGIPLTIVGEA VKDDIGEFRIQKPDRGP FYVSPKSLDQLISNLGK WGGGGSGGGGSHVIDSV LERRRR**RQLQKRVLDAA** **AKRAELESEGSNGARES** **ISDSTKKEDAVPDLCVI** **CLEQEYNAVFVPCGMCC** **CTACSSHLTSCPLCRRR** **IDLAVKTYRH**	GGGAGGTCAAGTGGAAGAGATGCTGAAGTACTTAAGACGGTC ACCCGTGTAAATCAGTTAAAAGAGTTGGCACAGTTGCTGGAG TTAGACAGCAAGATCCTGCCATTTATCGTGGCCGTGAGCGGC CGTGTCGGCTCTGAGACCCCGATTAAATGCGAGCACAGTGGT ATTCGTGGCGTGATTGTTGAAGAGACTGCGGAACAGCATTTT TTAAAGCACAACGAAACGGGTAGCTGGGTTCAGGATAGTGCG TTGATGCTGAGCATGAGCAAGGAAGTGCCTTGGTTCCTGGAC GACGGCACGAGCCGTGTGCATGTTATGGGTGCTCGTGGTGCG ACCGGTTTCGCCTTGACCGTGGGTTCCGAGGTTTTTGAAGAA AGCGGCCGTAGCTTGGTTCGCGGCACCCTGGACTATCTGCAA GGTCTGAAGATGCTGGGTGTTAAGCGCATCGAGCGCGTCTTG CCGACCGGCATCCCGCTGACCATTGTCGGTGAAGCAGTCAAG GATGATATTGGTGAATTTCGTATCCAGAAGCCGGACCGCGGA CCGTTCTACGTTTCCCCGAAATCCCTGGACCAGCTGATCAGC AACCTGGGTAAATGGGGTGGCGGCGGTTCCGGCGGTGGCGGG TCGCACGTGATCGACTCAGTTCTAGAGCGTCGCCGTC**GTAGA** **CAACTGCAAAAACGTGTGCTCGACGCTGCGGCTAAACGCGCA** **GAACTGGAGTCTGAGGGCTCCAACGGCGCGAGAGAAAGCATT** **TCAGATAGCACCAAAAAAGAGGATGCGGTTCCGGATCTGTGT** **GTTATTTGCCTGGAGCAAGAATACAATGCAGTATTCGTGCCG**

		TGCGGTATGTGCTGCTGCACCGCGTGTAGCAGCCACCTGACTTCTTGTCCGCTCTGCCGTCGCCGTATCGATCTGGCGGTGAAGACCTATCGTCAT
RPN13 pru (9-122)	VMQEIMLEFRAGKMSLQGTRVVPDARKGLVRIARGDEGLIHFQWLDRNQNTVEDDQIVFPDEALFEKVNQSSDRVYILKFNSDDRKLFFWMQEPRAEGDAELCSSVNQYLNQPL	gtaatgcaagaaataatgctagagtttagggcgggtaaaatgagcctgcagggtacgcgtgtagttccggatgcgcgtaagggcttggttcgtattgcgcgtggtgatgaaggccttatccacttttcagtggctggatcgcaaccaaaacaccgtggaagatgatcagattgtctttccggacgaggctctgtttgaaaaggtgaaccaatcgtccgaccgcgtgtatatcctgaaattcaacagcgacgaccgcaagctgttcttctggatgcaggagccacgtgcagagggcgacgccgagctgtgcagctctgttaatcagtacttgaatcaaccgctg
TTOP UBL (23-99)	TLELNIKTLDSRTYTFQVNKNETVLLFKEKIASETGVPVGQQRLIFRGRVLKDDHPLSEYHLENGHTLHLIVRQPAE	actctagaattgaatataaaaacattagattcccgcacctatacctttcaggtcaataagaacgaaactgtgttgctgttcaaagaaaagatcgcgagcgagacgggtgttccggttggccaacaacgtctgattttccgcggtcgtgtgctgaaagatgaccacccgctgagcgagtaccatttggagaacggccacaccctgcatcttatcgtgcgtcagccggcagaa

Table S3. PCR primers used for genotype identification.

Primer name	Primer sequence (5′ to 3′)	Application
TTOPpro-128F	CTGGAAATGTGTGTGGTAAAGG	For cloning of cDNA of TTOP to identify the TTOP knock-out mutant
TTOPgeno-519R	GCTTCCTCTACGGTGTAAGACTCA	
LB-TTOP	ATTTTGCCGATTTCGGAAC	LB, LP, and RP are used for PCR to identify the T-DNA
SALK_128909-LP	AGCTGAAGTCCCGCTATCTTC	
SALK_128909-RP	TATCCTATGTGAATGCAGGGC	
SALK_151742-LP	GCTTGACTTGTTGCAGGAAAC	
SALK_151742-RP	TTGCCTAGGTTGTGAATGACC	